REDUCTION OF DIESEL ENGINE PARTICULATE MATTERS USING RETROFIT CEO2 DIESEL OXIDATIVE CATALYST AND PARTIAL FLOW DIESEL PARTICULATE FILTER SYSTEM

Hai Liu

A THESIS REPORT SUBMITTED IN PARTIAL FULFILLMENT
OF THE REQUIREMENTS FOR THE DEGREE OF
MASTER OF ENGINEERING IN AUTOMOTIVE ENGINEERING
SCHOOL OF ENGINEERING
KING MONGKUT'S INSTITUTE OF TECHNOLOGY LADKRABANG
YEAR 2023
KMITL-2023-EN-M-

THESIS TITLE	REDUCTION OF DIESEL ENGINE PARTICULATE MATTERS USING RETROFIT CEO2 DIESEL OXIDATIVE CATALYST AND PARTIAL FLOW DIESEL PARTICULATE FILTER SYSTEM
STUDENT NAME	Mr. HAI LIU
STUDENT ID	63601186
DEGREE	Master of Engineering
PROGRAM	Automotive and Advanced Transportation Engineering (International Program)
ADVISOR	Assoc.Prof. Dr. Chinda Charoenphonphanich
CO-ADVISOR	Prof. Dr. Katsunori Hanamura
CO-ADVISOR	Dr. Sompong Srimanosaowapak

ABSTRACT

Meeting regulatory requirements for low emissions from internal combustion engines has become increasingly difficult with traditional purification technology alone. As a result, the most widely used diesel engine exhaust after-treatment technologies are DOC (Diesel Oxidation Catalyst) and DPF (Diesel Particulate Filter) due to their significant reduction of NOx, HC, CO, and PM in exhaust gas. This study specifically utilized CeO2 as the DOC catalyst and a partial-flow DPF installed after the DOC.

After comparison of the pressure drop and filtration efficiency by using GT Power software, this study recommended a cell density of 200-300 CPSI, a channel length of 150-230mm, and a hydraulic diameter of 120-240mm for the DPF of a 3L diesel engine. During this research 2 aftertreatment samples were applied based on the simulation results and experience.

In-cylinder pressure sensors and crank angle encoders were used to monitor engine performance during experiments conducted at varying engine loads and RPMs. Engine testing results showed that the CeO2 DOC and DPF systems effectively reduced NOx by around 300 ppm and particulate matter by around 65%. CO and HC were also substantially reduced at the same time. DOC and DPF systems have no significant effect on combustion pressure, fuel consumption, SFC, SEC, and thermal efficiency owing to the particulate filter causes a pressure drop of 0.2-

2.3kPa. However, without DPF system, the IET is 4-6% higher than BTE; While with DPF system, ITE is 5-11% higher than BTE owing to the DPF system cause the friction loss increase between 1-6%; the friction loss increases with engine rpm increasing due to more revolution cause more friction work. Combustion trend to start earlier when engine load increasing or engine rpm decreasing.

Vehicle tests at the pollution control department revealed that the DOC and DPF systems reduced PN by 4.8E+13/km, PM by 20.9mg/km, NOx by 182mg/km. Comparisons between Catalytic DPF and Non-Cat DPF showed that applying CeO2 DPF resulted in a 3mg/km reduction in PM. The study also investigated the pressure drop and filtration efficiency of a 3-litre diesel engine, revealing that a partial-flow DPF had around 50% lower back pressure than full-flow DPF at the same geometric conditions, but with an average filtration efficiency of around 30% less. Some research methods and conclusions in this paper can also provide a certain reference for other types of DPFs.

Keywords: P-DPF, DOC, CeO2, Emissions, Combustion Characteristic, Emissions, Diesel Engine, Back Pressure, CPSI, Channel length, Hydraulic Diameter.

ACKNOWLEDGEMENT

Foremost, I would like to extend my deep appreciation to the King Mongkut's Institute of Technology Ladkrabang for awarding me the scholarship. I am truly grateful for this opportunity.

I would also like to express my heartfelt gratitude to my academic advisor, Assoc. Prof. Dr. Chinda Charoenphonphanich of King Mongkut's Institute of Technology Ladkrabang, co-advisor Dr. Sompong Srimanosaowapak of National Science and Technology Development Agency, and co-advisor Prof. Dr. Katsunori Hanamura of Tokyo Institute of Technology, for their valuable guidance and support throughout my research.

I am immensely grateful to Assoc. Prof. Dr. Preechar Karin from King Mongkut's Institute of Technology Ladkrabang, who played a pivotal role in guiding and supervising me throughout the research and provided me with invaluable suggestions and insights to overcome all obstacles and challenges.

I would also like to express my gratitude to all the members of the automotive laboratory at KMITL for their support, and for providing me with the necessary facilities and experimental devices to carry out this research.

Finally, I would like to convey my deepest appreciation to everyone who has contributed and inspired me along the way. Without their help, this thesis would not have been possible.

Sincerely

Hai Liu

TABLE OF CONTENTS

LIST OF TABLES

LIST OF FIGURES

CHAPTER 1

INTRODUCTION

1.1 Research background

Over the past few years, the diesel engine has gained widespread usage in a variety of vehicles and equipment such as passenger cars, trucks, buses, heavy machinery used in construction, and generators used in buildings and industrial plants. This is due to its high thermal efficiency, engine performance, and durability in various applications. However, the diesel engine's combustion process is non-homogeneous since the fuel is directly injected into the combustion chamber, resulting in the emission of high levels of particulate matter (PMs) or soot. Incomplete combustion is the root cause of these pollutants, which consist mainly of carbon in solid form mixed with other components such as minor ash of metals from additive lubricants and unburned hydrocarbon fuels that condense on the surface of carbon soot in a liquid phase. It is crucial to eliminate these harmful emissions from diesel engine exhaust to safeguard the environment and human health. As a result, regulations governing vehicle emissions have become increasingly stringent [1,2,3]. Simultaneous generation of NOx, HC, CO, and SOF occurs during non-homogeneous combustion. To address this, diesel engine after-treatment systems use a combination of purification technologies, including diesel vehicle oxidation catalytic (DOC) technology, which is a crucial component [4]. Traditional three-way catalytic technology is insufficient for effective purification, but the addition of a catalyst to the DOC can convert toxic exhaust gases into environmentally friendly gases. Typically, Pt, Pd, and Ce are used as catalysts for DOC, but CeO2 was chosen for the DOC in this article due to its low-temperature performance and sulfur resistance.

Removing carbon particulate matter from diesel exhaust gas is a relevant and challenging topic in automotive catalysis and engineering. As global emission standards become more stringent, the use of intensive engine development and optimization programs alone may not be sufficient to meet the required reduction of emissions [5]. To address this, particle filter DPF technology is used to capture and oxidize exhaust particles. Diesel particulate filters are

commonly used in vehicles to reduce the amount of particulate matter emitted by diesel engines. A well-functioning DPF undergoes soot accumulation and periodic filter regeneration through soot oxidation [6,7,8].

After-treatment technology is designed to trap and disperse polluting soot particles into CO2, which is then automatically managed by an electronic engine control system. This technology is commonly used in developed countries with enforced pollution control laws such as Euro 5 and above, including European countries, Japan, and America. However, some Asian countries have lower standards, such as Euro 3 for trucks and large buses and Euro 4 for passenger cars. While it may not be necessary to install post-combustion technology at this time, it is expected that a more stringent pollution control law equivalent to Euro 5 will be implemented soon to address pollution problems in large cities. Protecting the environment and human health necessitates starting with diesel engine exhaust gas, and therefore the regulation of automobile exhaust emissions is becoming increasingly strict [9,10,11].

The issue of diesel aircraft exhaust particulate emission control has become a major concern in reducing automobile emission pollutants. Among the various aftertreatment devices available for controlling diesel particulate emissions, particle capture collectors are widely recognized as highly effective, especially in the realm of small and medium displacement diesel cars and light commercial vehicles. Compared to other after-treatment purification devices, particulate filters offer clear advantages. However, traditional thermal regeneration processes for particulate traps require external heat sources and complex control systems, which increases fuel consumption and costs for diesel vehicles. The use of on-board power supplies as external heat sources also places high demands on batteries. In contrast, catalytic particulate filters do not require external heat sources or control systems, but their performance is highly dependent on the sulfur content of diesel fuel. Since the implementation of new fuel standards in the world, which regulate the sulfur content in diesel, replacing traditional particulate filters with a new type of catalytic particulate filter is of great significance in promoting energy-saving and reducing emissions in diesel vehicles.

Each year, global energy consumption continues to rise, with transportation relying heavily on petroleum as its primary energy source. According to the World Energy Statistics 2018 report, approximately half of oil consumption is attributed to roads, a figure that rose to 18% over a span of 45 years from 1973 to 2018 [12]. In Thailand, natural gas and diesel fuels accounted for nearly 40% of petroleum consumption in 2019, as reported by [13]. The Ministry of Alternative Energy Development and Efficiency's 2020 report stated that diesel product demand increased from 22.626 billion liters in 2016 to 23.92 billion liters in 2020, representing a growth rate of 5.7% over four years [14]. In an investigation by C. ChooChuay et al. [15], vehicle exhaust, biomass combustion, sea salt spray, power plants, and industrial pollutants contributed 43.7%, 24.0%, 10.5%, 6.48%, and 4.46% to PM2.5 in Bangkok, respectively. Furthermore, diesel vehicles emit approximately ten times more PM2.5 than gasoline vehicles [16,17].

One major drawback of diesel internal combustion engines is their emissions, including hydrocarbons (HC), carbon monoxide (CO), carbon dioxide (CO_2), nitrogen oxides (NO_x), and particulate matter (PMs) resulting from incomplete combustion [18].

1.2 Composition and Hazards of Particulate Emissions from Diesel Engine

Diesel engines emit particulate matter consisting of aggregates of microscopic spheres, predominantly composed of carbon, and structured as flocculation or chain formations as shown in **Figure 1.1** [19]. When the exhaust gas temperature is low, organic soluble components (SOF) such as unburned hydrocarbons, oxygen-containing organic compounds, and polycyclic aromatic hydrocarbons (PAH) adsorb onto the particles. These organic substances can be volatilized at a specific temperature or dissolved in certain organic solutions. However, when the temperature of the exhaust gas exceeds 500°C, particulate emissions exist primarily in the form of carbon microsphere aggregates. The SOF content in the particles decreases gradually as engine load and speed increase [20].

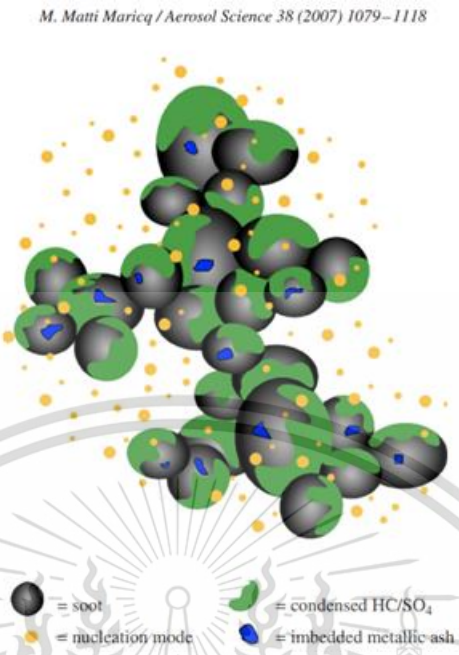

Figure 1.1 Composition of particulate matters

The formation mechanism of diesel particulate emissions is believed to occur in two stages: agglomeration and growth. In the agglomeration stage, ultrafine particle nuclei with a particle size of 0.01-0.05um form from oxidation intermediate products or pyrolysis products in the later stage of diesel combustion. Fuel molecules undergo nucleation, polymerization, and condensation to form 0.05-0.15um accumulated particles through pyrolysis and dehydrogenation in the high-temperature anoxic-rich region or the low-temperature region. During the growth stage, the particles stick to certain substances in the exhaust gas and undergo a dehydrogenation reaction to increase their mass, or they grow by collisions to form floc or chain aggregates. Diesel engine particulate emissions have a particle size distribution mainly between 0.01-1um, with most of the mass concentrated in particles with a size of 0.1-1um, and the number of particles mainly concentrated in particles with a size of 0.01-0.1um [21].

When diesel engine particles enter the atmosphere, particles with a size of 5um or more are deposited in the respiratory tract after inhalation, absorbed by the mucus, and discharged with sputum, which is less harmful to the human body due to their low number. However, smaller particles can penetrate deep into the lungs, with more than half of the particles with a size of 0.01~0.1um deposited in the lung cavity, causing mechanical overload of the lungs, damaging the

self-purification mechanism of various channels, and leading to cancer through mutagenesis [22]. Diesel engine particles and aerosols can also float in the air for an extended period, refracting light, darkening the sky, and reducing visibility. Additionally, the particle surface can adsorb various harmful gases and other pollutants.

1.3 Diesel Vehicle Emission Regulations for Particulate Emission Limits

Due to the increasing severity of automobile pollution, countries worldwide are placing greater emphasis on controlling this form of pollution. Consequently, they are enacting increasingly strict emission regulations. Currently, the United States, Europe, and Japan have established three major emission regulation systems globally. In fact, emission regulations have become a crucial factor for vehicle and engine manufacturers when developing new products and determining technical routes.

1.3.1 European Diesel Vehicle Emission Standard

In 1991, Europe started to develop European emission standards, which were then put into effect in 1992. The present-day European emission standards are referred to as Euro VI emission standards, which were first implemented in 2014. This year, Europe is scheduled to implement even more stringent European emission standards. The limits for diesel vehicle emissions are determined by vehicle weight classification, while diesel passenger cars and heavy-duty diesel vehicles adhere to a single standard. **Tables 1-1 and 1-2** display the emission standard limits for diesel passenger cars and light commercial diesel vehicles respectively.

Table 1-1 European emission standards for diesel passenger cars

Stages	Implementation year	Testing cycle	CO Limit (g/km)	NOx Limit (g/km)	PM Limit (g/km)
Euro Ⅰ	1992	ECE+EUDC	2.72	-	0.14
Euro Ⅱ	1996		1.0	-	0.08
Euro Ⅲ	2000		0.64	0.5	0.05
Euro Ⅳ	2005		0.5	0.25	0.025
Euro Ⅴ	2009		0.5	0.18	0.005
Euro Ⅵ	2014		0.5	0.08	0.005

Table 1-2 European emission standards for light commercial vehicles 1,305–1,760 kg

Stages	Implementation year	Testing cycle	CO Limit (g/km)	NOx Limit (g/km)	PM Limit (g/km)
Euro Ⅰ	1993	ECE+EUDC	5.17	-	0.19
Euro Ⅱ	1998		1.25	-	0.12
Euro Ⅲ	2001		0.8	0.65	0.07
Euro Ⅳ	2006		0.63	0.33	0.04
Euro Ⅴ	2010		0.63	0.235	0.005
Euro Ⅵ	2015		0.63	0.105	0.0045

1.3.2 Japanese Diesel Vehicle Emission Standard

During the late 1980s, Japan established the initial emission standards for on-road light-duty vehicles and heavy-duty engines. Nevertheless, these standards remained relatively lenient throughout the 1990s.

However, in 2003, the Ministry of the Environment (MOE) finalized highly stringent emission regulations for both light and heavy-duty vehicles, set to take effect in 2005. At the time, the heavy-duty vehicle regulations (NOx = 2 g/kWh, PM = 0.027 g/kWh) were considered the world's most stringent diesel emission standards. Subsequently, in 2009, these limits were further tightened to meet the requirements of US 2010 and Euro V standards, and as of 2016, they are as stringent as US 2010 and Euro VI standards.

1.3.3 American Diesel Vehicle Emission Standard

The implementation of emission regulations and controls on diesel engines was pioneered by the United States, who have the most extensive range of controls and the strictest standards. The U.S. federal government first developed regulations to limit the smoke levels produced by heavy-duty diesel vehicles and passenger vehicles operating under different conditions in 1970 [23]. Currently, the Tier2 standards have been enforced on light-duty vehicles since 2004. For vehicles manufactured in Model Year 2007 and beyond, emission standards have been introduced at later stages, which require reductions in NOx and PM emissions from 10.7g/(bph·hr) and 0.6g/(bph·hr) to 0.2g/(bph·hr) and 0.01g/(bph·hr) respectively.

1.4 Research Status of Diesel Engine Particulate Emission Control Technology

There are three distinct technologies used for controlling diesel particulate emissions based on their generation mechanism and emission characteristics: fuel pre-treatment, in-engine purification technology, and post-treatment purification technology.

1.4.1 Pre-treatment Technology

Pre-treatment of fuel mainly has 4 technology methods in recent years, including gas to liquid (GTL), biodiesel, hydrodesulfurization (HDS), and hydrodenitrogenation (HDN).

1) Gas to Liquid (GTL)

   GTL method use natural gas, which rarely has nitrogen and sulfur. GTL is a refining technique used to transform natural gas or other gaseous hydrocarbons into longer-chain hydrocarbons such as gasoline or diesel, resulting in a synthetic liquid fuel. There are two main approaches to this process: (i) direct partial combustion of methane to methanol, and (ii) Fischer-Tropsch-like processes that convert carbon monoxide and hydrogen into hydrocarbons. The second strategy involves various methods to convert the hydrogen-carbon monoxide mixture into a liquid. While direct partial combustion has been observed in nature, it has not been commercially reproduced. Technologies that rely on partial combustion have mainly been implemented in areas where natural gas prices are low [24][25]. The primary incentive for utilizing GTL is to create a liquid fuel that is more convenient to transport than methane. Methane must be cooled below its critical temperature of -82.3°C in order to liquefy under pressure, requiring the use of cryogenic equipment and LNG tankers for transportation. Methanol, on the other hand, is a flammable liquid that is simple to handle, but has only half the energy density of gasoline [26].

2) Biodiesels

   Biodiesels are produced from plants, it can absorb CO2 during the growing process, which are carbon neutral. Biodiesel has some O2 inside, it's good for soot, HC, and CO reduction due to a better combustion.

3) Hydrodesulfurization (HDS), and hydrodenitrogenation (HDN)

Hydrodesulfurization (HDS) and hydrodenitrogenation (HDN) are the two standard methods used in the industry for removing sulfur and nitrogen-based compounds from crude oil [27,28]. HDS is a highly efficient process, but it requires high temperatures (>350°C) and pressures (up to 6 MPa) and consumes significant amounts of hydrogen [29,30,31]. During HDS, the sulfur and nitrogen-containing compounds in the fuels are converted to hydrogen sulfide and ammonia, respectively, through catalytic reduction with H2 [32]. However, the presence of nitrogen compounds (NCs) can seriously affect the catalyst and cause corrosion of refinery equipment due to their high reactivity [32,33,34]. Therefore, it is important to remove NCs before fuel sulfur treatment or use alternative processes like deep desulfurization and denitrification to remove both NCs and sulfur compounds (SCs) simultaneously. This can help reduce the environmental impact by decreasing NOx and SOx emissions. Oxidative desulfurization (ODS) and oxidation nitrogen removal (ODN) processes have emerged as promising research areas in recent years as they can efficiently remove the most challenging sulfur and nitrogen contents present in fuels [35,36,37]. These techniques involve a combination of oxidation catalysis and liquid-liquid extraction steps [33,34]. The efficiency of the combined ODS/ODN process depends on the catalyst's performance and the ability to extract the solvent. Therefore, it offers an alternative solution to HDS/HDN, especially for removing NCs, which can cause severe problems in the HDS process.

1.4.2 Diesel Engine Internal Purification Technology

The term "diesel engine internal evolution technology" pertains to the enhancement of the internal combustion process of diesel engines. This is achieved through the use of fuel additives or the improvement of fuel quality. Additionally, it involves optimizing the exhaust gas combustion process by enhancing the intake system and fuel injection system, among other methods, in order to reduce diesel emissions. Currently, there are various types of diesel engine internal purification technologies, which include the following:

1) Fuel additive

From a functional perspective, diesel fuel additives can be classified into two types. The first type comprises soluble metal or metal salt additives that produce metal oxides upon combustion, which act as catalysts in decreasing diesel particle oxidation ignition temperature. This leads to increased oxidation rates of particles and reduced emissions. A study by Wang Tianyou et al. [38] found that the use of such additives increased the time for regeneration of the DPF to 23.5 hours from 19.5 hours under low exhaust temperature conditions. In high exhaust temperature conditions, the regeneration time was reduced by more than 50%, and regeneration efficiency was improved. The second type of diesel fuel additive is oxygenated fuel additives, which consist mainly of alcohols, acetates, and acids. When combusted in the right proportion with diesel, these additives enrich the oxygen content and exhibit excellent vaporization performance and low calorific value, resulting in reduced diesel engine particulate emissions. According to research by Liu Mingan and Sun Yuedong [39,40], adding 10% dimethyl ester significantly reduced particle emissions from diesel engines. When using less than 20% of ethanol, methylal, and carbonic acid, as well as dimethyl ester, the smoke level of the diesel engine decreased by 45% without a significant decrease in power performance.

2) Diesel injection system

Improving the injection system of a diesel engine can lead to a better fuel mixture quality and a decrease in diesel engine emissions. The fuel distribution within the combustion chamber can be made more uniform with an optimized fuel injector, allowing the fuel to evaporate promptly and create a mixed gas that effectively reduces particulate emissions. Precise fuel injection timing enhances the organization of air movement in the combustion chamber, resulting in more thorough fuel and air mixing, more complete combustion, and a reduction in particle emissions. Increasing fuel injection pressure produces finer fuel droplets that mix more evenly with air, which can inhibit particle generation. Additionally, a quick oil cut-off, appropriate combustion rate control, and effective injection pressure increase can all contribute significantly to reducing particulate emissions [41,42].

3) Electronic control system

In the 1970s, the electronic control system for diesel engines was developed. This system comprises various sensors, an electronic control unit (ECU), and actuators, and operates as a digital high-frequency control system. Compared to traditional mechanical control systems, the electronic control system provides significant advantages in real-time and precise control. As a result, it has rapidly developed and become widely used for diesel engines. The application of electronic control systems for meeting diesel engine emission requirements is now one of the main technical approaches for internal purification. It offers several functions, including fault self-diagnosis, failure protection, and improved low-temperature starting performance. The system can also effectively reduce particulate and nitrogen oxide emissions. Starting from the Euro III emission standard, only the electronic control system can enable emission reduction technologies such as variable flow, exhaust gas recirculation (EGR), and turbocharging. In the future, zero-emission vehicles will be possible with this technology [43,44].

4) Supercharging and intake intercooler

The use of turbocharging technology allows for an increase in intake pressure without modifying the engine's displacement. This results in a larger intake of air, which increases the amount of oxygen available during combustion and effectively reduces particle generation. However, the process of supercharging also raises the temperature and density of the air, necessitating intermediate cooling before entering the cylinder. Currently, most diesel engines use air-cooled intercoolers. By optimizing the selection of supercharger parameters and intercooler temperature, the air-fuel ratio and excess air ratio can be increased, leading to more complete combustion and a reduction in particle generation. Additionally, this approach can help to lower the emission level of NOx [45].

5) Combustion chamber structure

The emission of diesel engines can be affected by the structure of the combustion chamber. A well-designed combustion chamber can minimize the occurrence of high temperature and oxygen-deficient areas during combustion, while also increasing the intensity of the intake air flow. According to research by Zhao Changpu et al [46]. the main

area where particles are produced is the region with an in-cylinder temperature of 1500-2400K, and a combustion chamber with a too small constriction can lead to a significant increase in particle generation. Jiao Yunjing et al [47]. found that a combustion chamber with a diameter-to-depth ratio that is too small can hinder the mixing of oil and gas, leading to local hypoxia and increased particle generation. Experimental studies have demonstrated that the concentration of particulate emissions decreases as the intensity of the intake vortex increases. Furthermore, the use of multi-valve technology to increase the total flow area of the intake and exhaust valves can promote thorough combustion and form an intake air flow that is suitable for the speed of the diesel engine, ultimately increasing the air flow intensity and reducing particulate emissions [48,49].

6) Homogeneous charge compression ignition – HCCI

Advanced combustion technology is a technical solution for effectively decreasing particulate emissions produced by diesel engines. Homogeneous charge combustion technology (HCCI) has been the subject of numerous studies both domestically and internationally. Scholars have conducted various investigations into the impact of HCCI on emissions [50-54], and their findings indicate that HCCI can rapidly and uniformly ignite a homogeneous mixture at multiple points within the cylinder, resulting in low combustion temperatures, few generated particles, and an indistinct flame front. Consequently, HCCI differs from other in-engine technologies and when used in combination with other technologies, can significantly reduce particulate emissions. Experiments conducted by Kalghatgi et al. on a heavy-duty diesel engine with a compression ratio of 14, operating at 1200rpm and under various injection timings, showed that particle emissions ranged from only 0.18 to 0.27g/(kg-f) [55,56].

1.4.3 Diesel Engine Post-Treatment Technology

Despite the use of various in-engine purification technologies, the particulate emission level of diesel engines can only meet Euro III emission standards at best. As emission standards become stricter, separate in-engine purification technology is no longer sufficient. This is due to several reasons:

Firstly, advanced combustion technologies like HCCI have minimized the production of particulates in diesel engines. Prior to the development of these technologies, it was challenging to reduce the generation of particles in the cylinder using different methods to optimize gas injection and oil-air mixing effects.

Secondly, electronic control technology and high-pressure common rail injection technology are the most effective in reducing the generation of particles in the diesel engine cylinder. However, as fuel injection timing is more precisely controlled and injection pressure is increased, the mass of particulates in diesel engines decreases, but the concentration of particulates may not be evident and may even increase. Moreover, the harm caused by these particles is more significant [57].

Thirdly, the reduction of particulate emissions through fuel additives or improving fuel quality has hit a bottleneck stage. Developing better fuel additives or higher-quality oil products to reduce particulate emissions is not significant, and the process is complicated and costly. Diesel engine post-treatment purification technology has emerged as a viable solution to meet more stringent emission standards. The technology includes filter bag capture, electrostatic capture, cyclone separation, cleaning and filtration, plasma purification, and particulate filter technology.

This research will mainly focus on the diesel particulate filter (DPF) technology. And it's the most effective technology for treating diesel exhaust particulate, which has been widely adopted in diesel vehicles in the world. There are two types of DPFs: partial flow DPF and wall flow DPF. The partial flow type uses metal fiber mesh as the filter material, but only a portion of the exhaust gas is filtered through it. In contrast, the wall flow DPF uses a porous media filter material that filters all exhaust gas through the filter wall. Both types of DPFs are installed on the exhaust pipe of diesel engines to effectively filter particles in the exhaust gas. However, to ensure the DPF operates smoothly and prevent a decrease in power performance or engine damage from excessive exhaust resistance, the captured particles must be oxidized and regenerated.

1.5 Objective and Scope of Work

Reducing diesel particulate emissions is essential for complying with Euro IV and higher emission standards. After-treatment purification devices, such as catalytic passive regeneration

technology, are now more effective due to advancements in refining technology, which have reduced sulfur content in diesel. Catalytic passive regeneration technology is a low-cost and straightforward method that doesn't require external heat sources or regeneration. The DPF, supported by this strategy, is a promising post-treatment purification device, particularly for diesel cars and light commercial vehicles that have strict requirements on layout space and cost. In this study, the CeO2 catalyst and partial flow DPF are examined for their efficacy in reducing HC, CO, NOx, PM, and DOC emissions. The study also investigates the impact of the post-treatment system on engine performance, as well as the optimal size of the DPF for a 3L diesel engine. The study draws on the Thai National Research Council Fund Project, "398/2563 - Diesel Engine's Particulate Matters Reduction".

1.5.1 Objective

1) Evaluate the impact of DOC and DPF system on engine operation and performance.
2) Investigate the impact of CeO2 on particle emission reduction.

1.5.2 Scope of Work

The main contents of this research, as indicated in **Figure 1.1**, it includes three main line consists of DPF simulation, engine test, and chassis test:

1) Calculate and test the pressure drop for DPF, comparing the results with simulation, using software to design a DPF for a 3-litre engine based on DPF pressure drop and filtration efficiency.
2) Evaluate the impact of CeO2 DOC and partial flow DPFs based on engine performance and combustion of ISUZU 4JJ1-TC at 1000, 1500, and 2000 rpm under 20%-50% engine load.
3) Investigate the effect of CeO2 DOC and partial flow DPFs based on Toyota Hilux Tiger 2.5-litre diesel vehicle with new European driving cycle (NEDC).

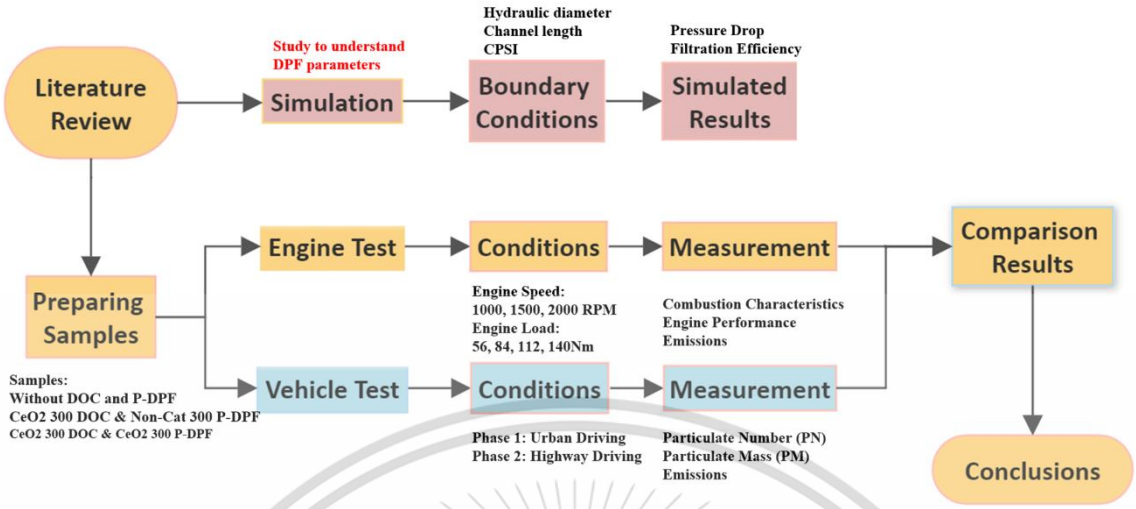

Figure 1.2 Main workflow chart of this topic

CHAPTER 2

Diesel Engine and Aftertreatment System

2.1 Diesel Engine

In 1897, Rudolf Diesel discovered the diesel engine, which is a form of internal combustion engine commonly known as a compression combustion engine. The compressed-combustion engine operates on the principle of injecting fuel directly into the combustion chamber at top dead center (TDC) while the piston moves upward during compression. This results in an increase in pressure in the combustion chamber, causing the fuel to spontaneously combust at high pressure and temperature.

2.1.1 Diesel Engine Cycles

The 4 strokes consist of, intake, compression, power, and exhaust as show in **Figure 2.1** In the intake stroke, the piston moves downward from the top dead center (TDC) to the bottom dead center (BDC) while the intake valve opens and the exhaust valve closes. As the piston moves down, it draws in fresh air into the combustion chamber. During the compression stroke, both the intake and exhaust valves remain closed. The piston moves upward from BDC to TDC, resulting in an increase in pressure and temperature within the cylinder due to compression. In the power stroke, the fuel is injected into the combustion chamber towards the end of the compression stroke, and the resulting combustion generates energy that is converted into mechanical energy through the piston to the crankshaft. In the exhaust stroke, the exhaust valve opens while the intake valve remains closed after the completion of the power stroke at BDC. As the piston moves upward, the exhaust air is pushed out of the combustion chamber.

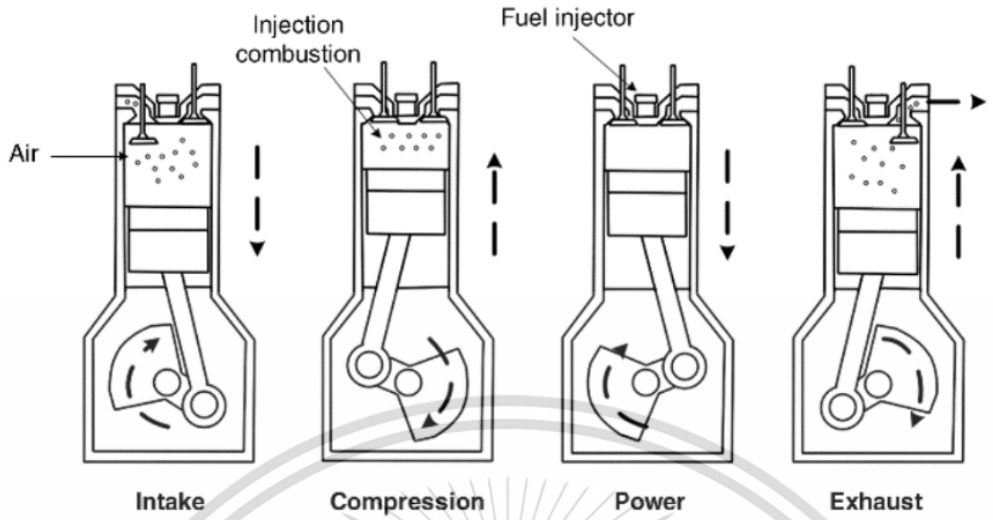

Figure 2.1 Diesel engine cycles [58]

2.1.2 Diesel Combustion Phases

Combustion occurs when fuel and air rapidly undergo a chemical reaction, resulting in the creation of heat and light. Diesel fuel is injected into the combustion chamber at a high pressure, and the combustion process in a compression ignition (CI) engine occurs in four stages.

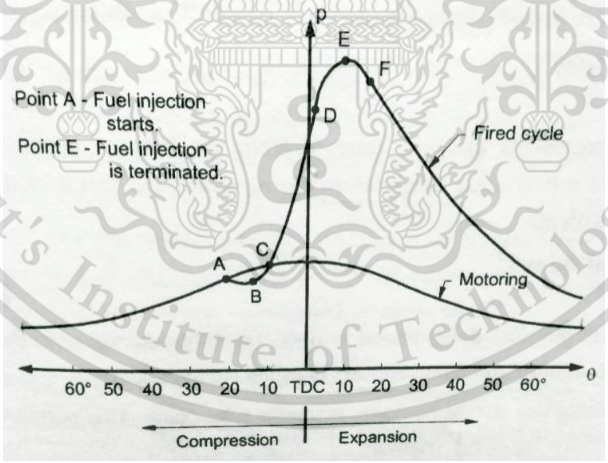

Figure 2.2 crank angle diagram of diesel engine [59]

The first stage is the ignition delay period, during which fuel is injected into the combustion chamber in the form of a jet. The fuel breaks down through atomization and vaporization, and the fuel gains heat from the compressed hot air around it. The pressure in the cylinder drops as a result of this process, which is visible in curve AB on **Figure 2.2**. The mixture in the combustion

chamber undergoes a pre-combustion reaction during this period, causing the pressure in the cylinder to slowly increase until the fuel catches fire, as seen at point C.

The second stage is the uncontrolled combustion period, which occurs when the air and fuel mixture spontaneously ignites at the spontaneous combustion temperature. Unlike in spark ignition (SI) engines, the mixture in CI engines is not uniform, resulting in flames appearing in multiple locations where the mixture concentration is high. Fuel that accumulated during the delay begins to burn rapidly, resulting in an increase in pressure and temperature in the cylinder. This period is referred to as the uncontrolled combustion period and is represented by curve CD.

The third stage is the controlled combustion period, which occurs when the fuel accumulated during the ignition delay has burned completely. The in-cylinder mixture's temperature and pressure are high, allowing new fuel ejected from the nozzle to burn rapidly due to the presence of enough oxygen in the combustion chamber. The fuel injection rate can be used to control the pressure increase in the cylinder during this combustion period.

The fourth stage is the post-combustion period, during which the combustion chamber reaches its maximum pressure at point E. Combustion of the fuel in the combustion chamber continues during the expansion stroke due to the recombination of dissociated gas and unburned fuel. This stage is referred to as post-combustion.

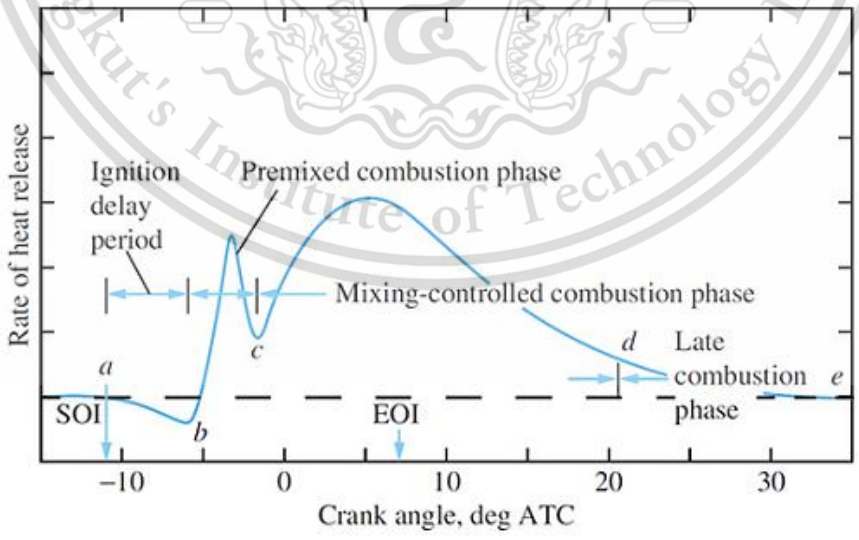

Figure 2.3 Phases of the diesel combustion process on heat release rate diagram [60]

The heat release rate diagram in **Figure 2.3** illustrates the various stages of the diesel combustion process from injection to the end of combustion. The ignition delay, marked as point (a-b), denotes the time between the start of fuel injection and the onset of combustion. The premixed combustion phase, marked as point (b-c), is characterized by a negative heat release rate curve due to the brief vaporization and heat absorption of the fuel mixed with air during the ignition delay period. The addition of ready-to-burn fuel to the combustion mixture results in a sharp increase in the heat release rate.

Point (c-d) represents the mixing-controlled combustion phase where the fuel and air premixed during the ignition delay have been consumed and released some energy. The heat release rate is now controlled by the availability of the mixture for burning, which involves processes such as fuel atomization, vaporization, mixture formation, and chemical reaction in the spray. The diffusion flame's burning rate is primarily influenced by the fuel and air mixing process during this phase.

Finally, point (d-e) marks the late combustion phase where the heat release rate continues but at a lower rate. This is because a small portion of the fuel may remain unburned, and a fraction of the fuel energy may be trapped in soot and combustion products that are still being released. During this phase, cylinder charge mixing promotes more complete combustion and less dissociated gases. The kinetics of the final burnout processes become slower as the temperature of the cylinder gases falls during expansion.

2.2 Aftertreatment System

2.2.1 Diesel Oxidative Catalyst (DOC)

The catalytic DPF features a front-end installation of the DOC, which utilizes flow-through porous media materials like cordierite, silicon carbide, and metal foam as its carrier. To achieve the necessary catalytic activity, noble metal catalysts such as Pt and Rh are coated onto the carrier. The traditional impregnation method is suitable for ceramic material carriers like cordierite, whereas metal materials require special coating processes. As illustrated in **Figure 2.4**, the DOC's primary function is to convert NO in diesel engine exhaust into NO2, a highly oxidizing compound

that can be used to oxidize the captured particles downstream, as well as purify HC, CO, and SOF in diesel engine exhaust.

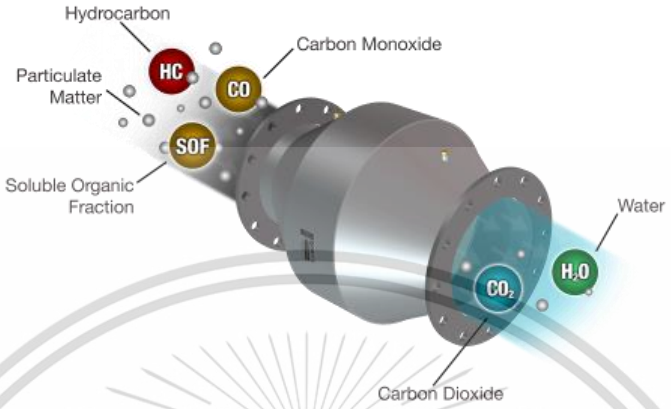

Figure 2.4 Working principal diagram of DOC [61]

$$2NO + O_2 \rightleftharpoons 2NO_2 \quad \textbf{(2.1)}$$

$$CO + 1/2\ O_2 \rightarrow CO_2 \quad \textbf{(2.2)}$$

$$4HC + 5O_2 \rightarrow 4CO_2 + 2H_2O \quad \textbf{(2.3)}$$

$$[SOF] + O_2 \rightarrow CO_2 + H2O \quad \textbf{(2.4)}$$

2.2.2 Diesel Particulate Filter (DPF)

The DPF is typically positioned downstream of the DOC. Its primary function is to capture particles in diesel engine exhaust by allowing them to accumulate on the filter wall of the carrier or on the metal fiber. The primary component of a diesel particulate filter (DPF) is the filter carrier, which can be classified into two main types based on the material: ceramic-based and metal-based. Ceramic-based carriers are made of materials such as cordierite, silicon carbide, mullite, and zirconia, while metal-based carriers are made of sintered metal, foam metal, and wire mesh. Among these, cordierite and silicon carbide are the most frequently used filter materials [62].

2.2.2.1 Partial Flow DPF and Catalyst

Partial flow DPF is the transition stage for full flow DPF. It mainly has two internal structures as show in **Figure 2.5 A.** The first layer is metal foil that guide the exhaust gas passing through the second layer metal fiber. During this process, the soot in the exhaust gas will be trapped on

metal fiber. Furthermore, partial flow DPF allow around half of emissions flow out directly owing to the structure itself, another half of exhaust gas will flow through metal fiber.

In some developing countries, there're a quantity of diesel engine vehicles which couldn't meet the Euro 3 or 4 emission standards. They couldn't afford a full flow DPF due to the electronic unit for monitor the F-DPF are expensive, therefore, a P-DPF is a preferable choice for them to improve the emissions reduction ability because it doesn't require a control unit.

In this research, Ce selected as the P-DPF catalyst due to its economic characteristic and excellent O_2 absorbing performance. Ce supplies the O_2 at lower oxygen or stoichiometric conditions. The Ce catalyst will effect on soot oxidation; the soot oxidation involves two concurrent processes: one occurring at the ceria-soot interface and the other at the surface of the soot, driven by superoxide species. The experimental observations reveal a mechanism wherein ceria is initially reduced by soot, liberating CO2 in the process. Subsequently, the reduced ceria undergoes oxidation when exposed to gaseous oxygen, producing peroxide and superoxide species. These reactive species then migrate to the surface of the soot, leading to a more efficient reaction that forms CO2 at a lower activation energy. As a consequence, a fresh contact point is established between the soot particle and the ceria surface, effectively restarting the cycle. This entire process is visually depicted in **Figure 2.5 B.**

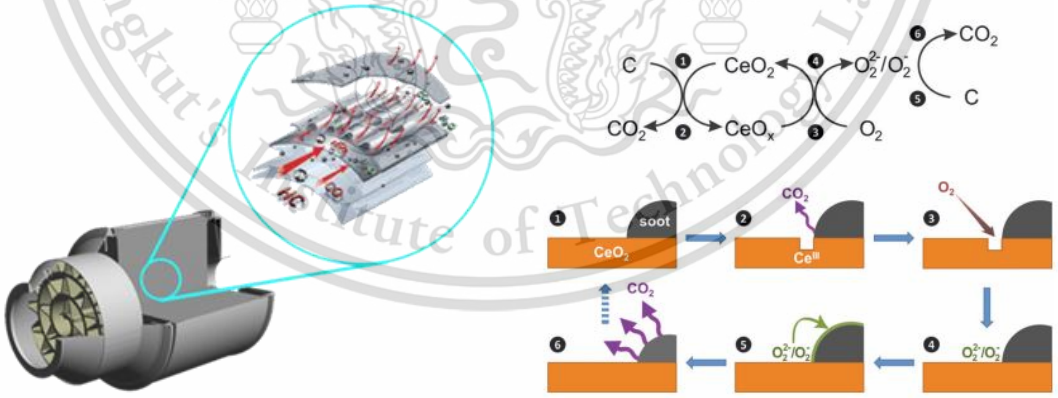

A B

Figure 2.5 Working principal diagram of partial flow DPF and Mechanism of soot oxidation over ceria [63]

2.2.2.2 Full Flow DPF

The Wall-flow diesel particulate filter (DPF) typically consists of a cylindrical ceramic structure that contains many small, parallel channels in the axial direction. Unlike typical flow-through traps, one end of the wall-flow filter is blocked at the adjacent channel to the filter layer, forcing exhaust gas to pass through the porous wall surface to capture particulate matter, as illustrated in **Figure 2.6 A**. The exhaust flow resistance of the honeycomb ceramic particle filter element is primarily determined by the thickness of the particle layer deposited on the filter's surface. A higher filtration area per unit volume results in slower growth of the particle layer thickness and less flow resistance. Thus, a higher honeycomb density and thinner channel wall are preferred. However, excessively high honeycomb density and small channels can lead to increased exhaust flow resistance and clogging. Micropores of the particle filter are typically micron-scale, much larger than the soot particles. They cannot directly purify the exhaust but facilitate the diffusion, interception, inertial collision, and gravity deposition mechanisms. The tinier particles exhibit a tendency to adhere to the filter's surface due to Brownian motion. Interception on the filter substrate is notably influenced by the superficial velocity as indicated in **Figure 2.6 B**. As the flow rate rises, so does the superficial velocity. Consequently, the efficacy of Brownian motion-driven trapping diminishes at higher flow rates. This elucidates the reason behind the deterioration in filtration efficiency for smaller particles when the flow rate is elevated. During the DPF's working process, the collection efficiency is affected by various factors, including particulate matter properties, exhaust flow rate, temperature, DPF specifications, and material characteristics [2], [64].

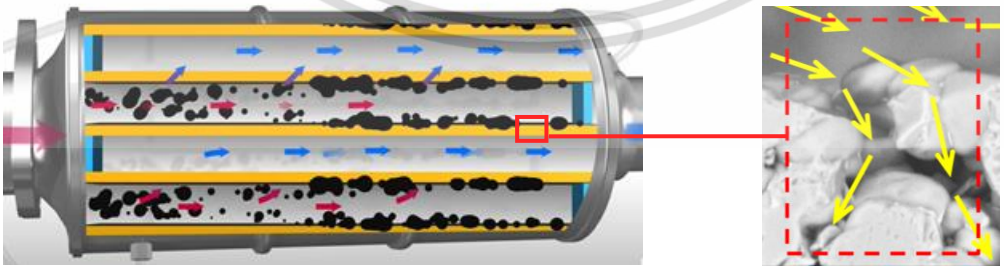

A B

Figure 2.6 Working principal diagram of full flow DPF and superficial velocity [2], [64]

2.2.2.3 DPF Regeneration

When particulate matter accumulates in a diesel particulate filter (DPF), it increases the carbon load and exhaust back pressure of the diesel engine. This can significantly reduce engine performance if the back pressure exceeds a certain limit. The DPF must undergo regeneration to remove the particulate matter from the filter element. The basic principle of regeneration is to oxidize the particles into CO2, which is discharged along with the exhaust gas. Regeneration is influenced by factors such as the total accumulated particle amount, particle storage density and distribution, exhaust flow rate, heat transfer of the trap, and activation reaction capacity of the particles. There are two types of DPF regeneration: active and passive.

Active regeneration involves providing external energy to increase the filter element's temperature to burn the particles and restore the filter's clean state. This includes various methods such as heating regeneration, fuel injection combustion regeneration, electric heating regeneration, and microwave regeneration.

Heating regeneration involves using techniques like intake and exhaust throttling or in-cylinder post-injection to quickly increase the DPF inlet temperature to around 600°C. However, this method can result in increased fuel consumption and secondary pollution [65].

Fuel injection combustion regeneration involves adding fuel injectors in front of the filter's inlet to inject a small amount of fuel, which is ignited with spark plugs or electric glow plugs. This ignites the particles with high-temperature gas, and the regeneration process is typically completed within 1-2 minutes. While this method can regenerate in most cases and has good regeneration effects, it requires an additional fuel supply device, which can be expensive, and the airflow should not accelerate rapidly to avoid blowing out the flame [65].

Electric heating regeneration utilizes electric heating methods to heat the particle filter and promote the ignition of particles. This method includes using ceramic fiber wound on a metal resistance heating tube or crystalline SiC as a filter material. However, electric heating control systems have high requirements, high cost, and high-power consumption, and uneven heating may cause uneven regeneration of the filter element, leading to local overheating that can damage it [66-67].

Microwave regeneration utilizes the unique selective and volume heating characteristics of microwave energy to heat the PM deposited on the filter and make the particles ignite and burn. The effect of microwave regeneration treatment depends on the different dielectric properties of the particle filter material and the particles deposited on its surface. Selecting the right matrix material for the filter can result in successful selective heating of the particles, while using a microwave-absorbing material can cause simultaneous heating of the trap and particles [68-69].

Passive regeneration involves using chemical catalysis to reduce the reactivity of particles, allowing them to burn under normal operating conditions of a diesel engine. This can be achieved through several methods, including regeneration using NO2, catalytic combustion regeneration filter (CDPF) regeneration, and fuel additive regeneration.

Regeneration by NO2 involves combining diesel oxidation catalyst (DOC) and diesel particulate filter (DPF). When exhaust gas passes through the DOC at a temperature of 200-600℃, CO and HC are first oxidized into CO2 and H2O, while NO is converted into NO2. The NO2 then oxidizes the particles in the DPF to generate CO2, and NO2 is reduced to NO, achieving regeneration. While this method requires little space and has a low cost, it only works for low-sulfur diesel engines with a minimum ratio of NOx to PM of 15:1. Sulfur content can generate sulfate, affecting the effectiveness of this method. Passive regeneration also requires a suitable exhaust temperature, with too high a temperature accelerating the decomposition of NO2 and too low a temperature resulting in slow oxidation of C [70].

CDPF regeneration involves coating an oxidation catalyst directly on the filter body wall, reducing the ignition temperature of soot to allow it to burn at normal diesel engine exhaust temperature, achieving complete regeneration in a specific temperature window (T>320-350℃). However, this method requires high diesel sulfur content, engine thermal management, and can lead to increased emissions at low exhaust temperatures [71].

Fuel additive regeneration involves using soluble metals or metal salts as additives, with the metal oxides generated after combustion catalyzing particles and reducing their ignition temperature, allowing the filter body to regenerate itself at lower exhaust temperatures without

external energy. However, the combustion products of fuel additives can accumulate on the filter body, blocking its pores, shortening its service life, and increasing back pressure, affecting engine power and economy. Additionally, the metal drift into the atmosphere can cause secondary pollution [72].

CHAPTER 3

DPF DESIGN

3.1 DPF Pressure Drop

Back pressure has always been a significant factor affecting the engine; therefore, reducing or eliminating back pressure is essential to improve engine power; back pressure is caused by the obstruction of exhaust gas flow, such as the air generated by DOC and DPF in the after-treatment system flow hinders back pressure.

3.1.1 DPF Pressure Drop calculation

Empirical solutions have been proposed to account for the pressure drop that occurs through honeycomb structures. The pressure-loss coefficient **Kh**, is one such solution, and it can be predicted using the Eckert Equation as presented by Barlow et al. [73], is given by:

$$Kh = \lambda h \left[\frac{Lh}{Dh} + 3\right] \cdot \left[\frac{1}{\beta h}\right]^2 + \left[\frac{1}{\beta h} - 1\right]^2 \quad (3.1)$$

$$\lambda h = \begin{cases} 0.375 \left[\frac{\Delta}{Dh}\right]^{0.4} \cdot R_{e\Delta}{}^{-0.1}, & R_{e\Delta} \leq 275 \\ 0.214 \left[\frac{\Delta}{Dh}\right]^{0.4}, & R_{e\Delta} > 275 \end{cases} \quad (3.2)$$

In this equation, **Dh** represents the hydraulic diameter of the honeycomb cell, βh represents the honeycomb porosity, and **Lh** represents the thickness of the honeycomb in the direction of flow. The coefficient of Reynolds number, λh, is another important factor that determines the pressure-loss coefficient. This coefficient is based on the material roughness and incoming flow speed, and it is related to the surface roughness Δ of the honeycomb cells. The Idelchik Eckert Equation provides a useful means of estimating λh; $R_{e\Delta}$ is Reynolds number.

Minor losses can also be expressed as a ratio of the head loss to the velocity head and are typically determined using a pressure loss coefficient **Kh**. The following equation relates minor losses to velocity head and loss coefficient, as presented in [74]:

$$Kh = \frac{hm}{v^2/2g} = \frac{\Delta p}{\rho v^2/2} \quad (3.3)$$

In this equation, **g** represents the gravitational constant, **v** represents the exhaust gas velocity, **hm** is minor head loss, **ρ** represents air density, and **Δp** represents the pressure drop.

3.1.3 DPF Pressure Drop Simulation

To begin, the DOC and DPF models need to be established through Solidworks. These models should have the same geometric dimensions as the laboratory samples. Next, import the models into the Fluent software for model simplification and finite element division as shown in **Figure 3.1**. Assign a porosity of 0.9 to DOC and 0.85 to DPF, as measured by the laboratory sample drainage method. The geometric parameters of DOC and DPF should be input into the software as shown in **Table 3-1**. Then, the mass flow rates obtained in the engine test should be input into the Fluent program as boundary conditions, as shown in **Table 3-2**. The program should be solved until convergence. Soot simulation is difficult, so this experiment will use GT Power for the simulation alone.

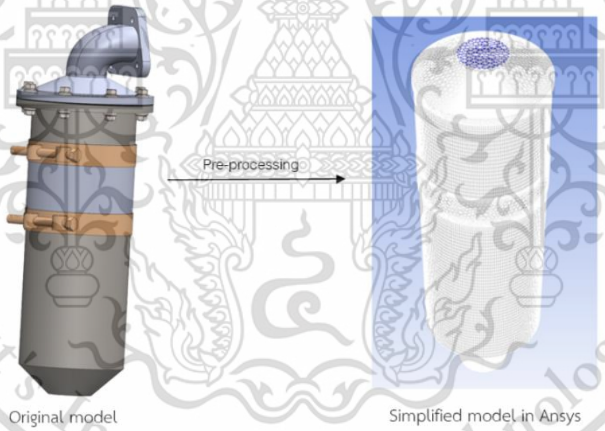

Figure 3.1 Geometry model and simplified mesh model of DOF and DPF

Table 3-1 DOC and DPF specification in simulation

Parameter	DOC	DPF
Porosity	0.90	0.85
Channel length / mm	100	200
Hydraulic diameter / mm	141	141

Table 3-2 Boundary condition in simulation

RPM	Mass flow rate (g/s)	Soot loading (g/s)
1000	0.90	0.85
1500	100	200
2000	141	141

3.2 Effective Attributes on DPF

There are many factors that affect DPF pressure drop and filtration efficiency, which can be divided into physical and chemical factors. This article will only focus on the physical factors, such as CPSI, DPF length, and diameter, which can have a significant impact on DPF pressure drop. Typically, the porosity of F-DPF is around 0.5, while P-DPF is around 0.89 measured by a real P-DPF; In this simulation the porosity has substituted with a P-DPF as a fixed condition.

To conduct related research on physical factors, this experiment used GT Power software to conduct quantitative analysis on DPF pressure drop and filtration efficiency. The mass flow rate at the DOC inlet was 90.6 g/s (at 2000 rpm) and the soot concentration was 0.0005 g/s (based on empirical data). The operating temperature was 708K (average temperature). The experiment ran for 3 hours, and the model established in GT Power is shown in **Figure 3.2**. Pressure drop sensors were added at both ends of the DOC and DPF.

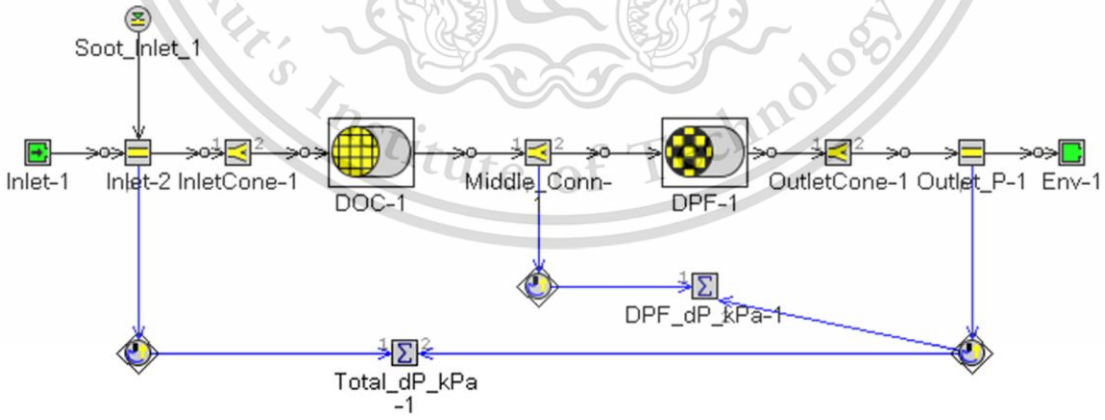

Figure 3.2 DPF simulation pressure drop

3.2.1 Cell Density (CPSI)

CPSI means cells per square inch, it's the primary parameter for DPF. **Figure 3.3** shows that as the CPSI value increases for filters with the same diameter and length, the filtration efficiency also increases. This is because a higher number of channels per unit area results in a larger effective filter wall area, and hence, a higher filter collection efficiency. However, **Fig. 3.4** indicates that the pressure drop also increases with CPSI due to the greater passage resistance created by a higher number of channels. But for CPSI values of 50 or 100, the situation is different. Even though the initial pressure drop is less than that of 200 CPSI, with particle deposition on the filter body, the pressure drop rises faster and exceeds that of 200 CPSI, especially for 50 CPSI. This is because at the same particle deposition rate, the thickness of the particle layer deposited on the 50 CPSI filter wall is relatively large, causing a rapid increase in the pressure drop. Therefore, a cell density that is too low is not appropriate. Considering all factors, the DPF CPSI for a 3L diesel engine should be set between 200-300 CPSI.

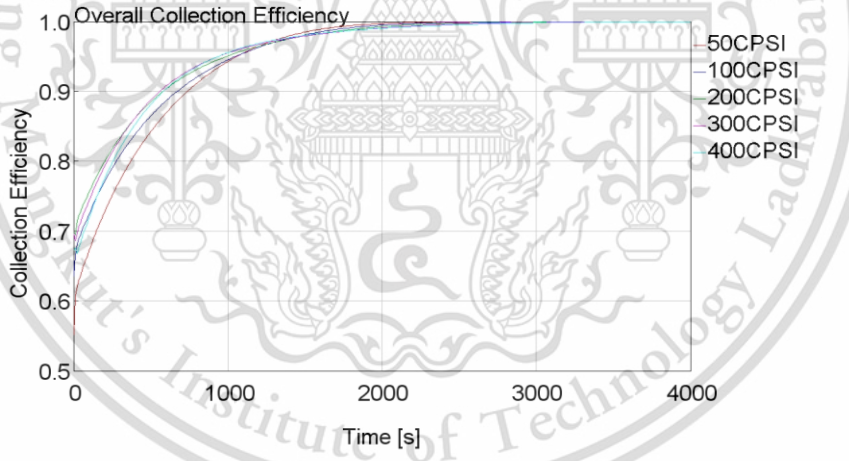

Figure 3.3 DPF filtration efficiency with different CPSI

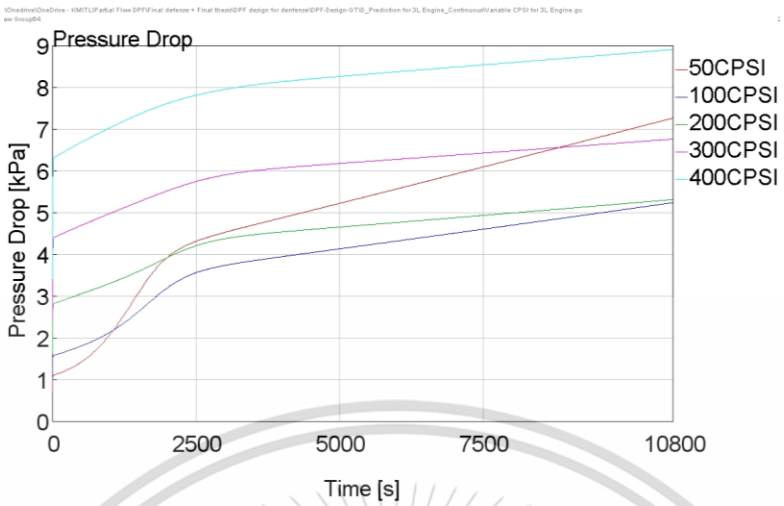

Figure 3.4 DPF pressure drop with different CPSI

3.2.2 Channel Length

Figures 3.5 and 3.6 demonstrate that the initial filtration efficiency gradually increases as the filter length increases with the same DPF CPSI and hydraulic diameter, but it no longer affects the filtration efficiency once it reaches 150mm. When the filter diameter is 50mm, the initial filtration efficiency is the lowest at 0.53 in the simulation, and the pressure drop also increases with the length of the DPF. Although the overall impact is not significant, a DPF with a length of only 50mm will lead to a rapid increase in pressure drop. Meanwhile, the installation space of the car should be considered, and the size of the DPF should not be too large. Generally, the diameter of the filter should be selected between 150mm and 230mm.

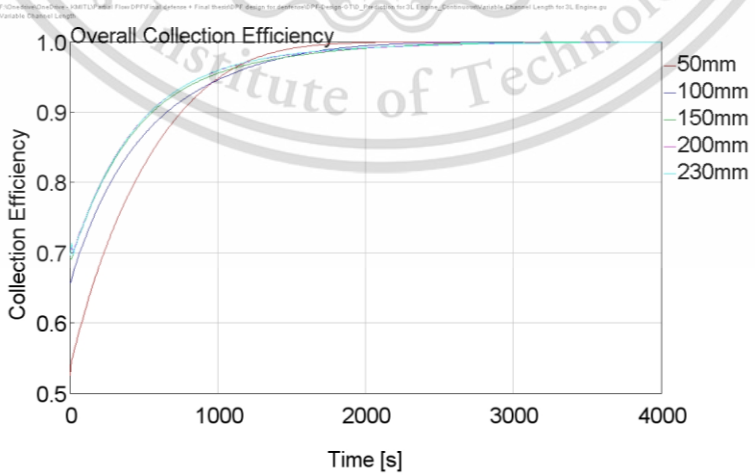

Figure 3.5 DPF filtration efficiency with different channel length

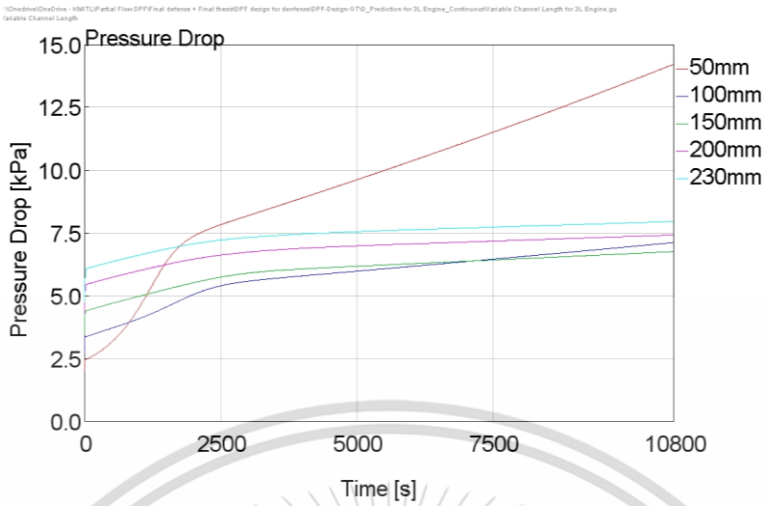

Figure 3.6 DPF pressure drop with different channel length

3.2.3 Hydraulic Diameter

Finally, regarding hydraulic diameter, **Figures 3.7 and 3.8** show that, for a constant CPSI and DPF length, increasing filter diameter gradually enhances the initial filtration efficiency, and reduces pressure drop. However, the initial filtration efficiency is relatively low (0.62) when the filter diameter is 120mm, and pressure drop rises sharply. All DPFs with varying diameters attain maximum collection efficiency at around 3000s. At the same time, for space-saving considerations, the size of the DPF should not be too large, and in general, the filter diameter should range from 120mm to 240mm.

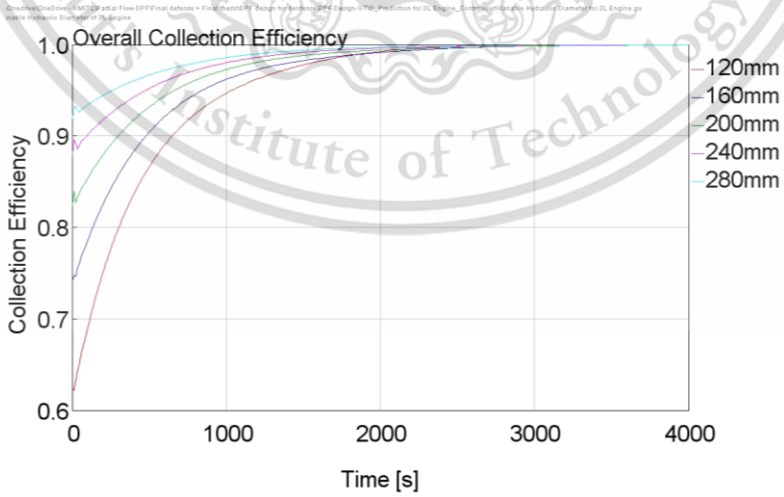

Figure 3.7 DPF filtration efficiency with different hydraulic diameter

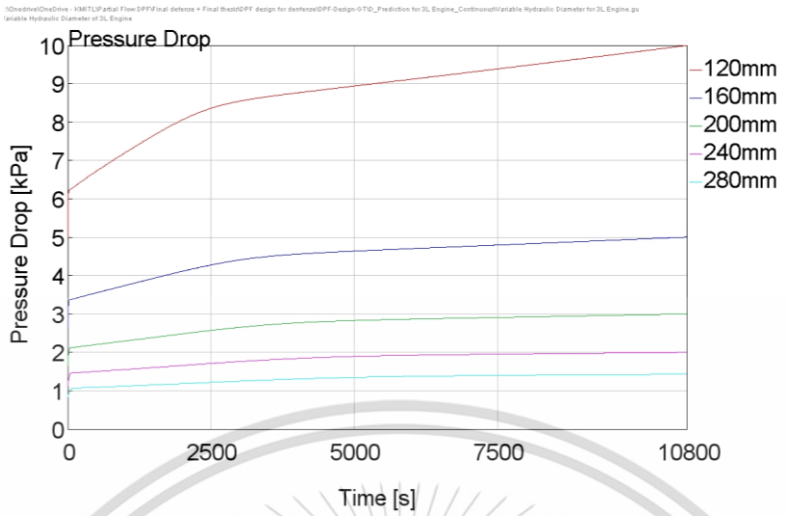

Figure 3.8 DPF pressure drop with different hydraulic diameter

3.2.4 Other Attributes

There are several physical parameters that affect DPF filtration efficiency, including filter wall thickness, particle diameter, filter pore diameter, and porosity. Additionally, filter wall thickness, particle diameter, porosity, and filter wall permeability are among the other parameters that affect pressure drop. Furthermore, different types of catalysts used on DPFs can also impact pressure drop and filtration efficiency chemically.

CHAPTER 4

EXPERIMENTAL METHODOLOGY

There are two experiments in this study. The first one is a transient test based on a 3-liter diesel engine; the purpose is to investigate and compare the engine performances, combustion characteristics, and the emissions with and without DOC and DPF system; Operating conditions are performed on various engine loads (56, 84, 112, and 140Nm) at constant engine speeds (1000, 1500, and 2000rpm). The second experiment is real-time test for Euro 2, 3 or Euro 4 diesel vehicles at Pollution Control Department of Thailand; the objective is to evaluate the effect of DOC and DPF system on vehicle exhausts with a NEDC driving cycle and meet the Euro 5 emission standard.

4.1 Experimental Samples

To evaluate the impact of DOC and DPF system, experimental samples are sending for two types of testing: Engine test and chassis test. The testing samples was selected based on the simulation result and experience as below:

1. No DOC and DPF
2. CeO2 DOC and Non-Cat DPF
3. CeO2 DOC and CeO2 DPF

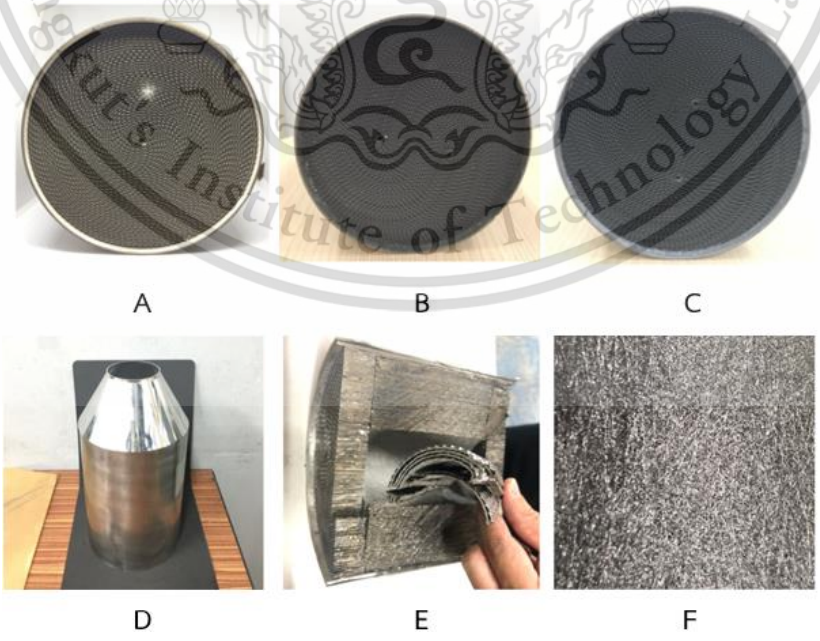

Figure 4.1 Samples of CeO2 DOC, Non-Cat DPF, and CeO2 DPF

The testing group consists of 3 samples. As shown in **Figure 4.1**, **A** is CeO2 DOC 300 CPSI; **B** indicates non-Cat DPF 300 CPSI; **C** represents CeO2 DPF 300 CPSI. When we change the samples, we need a connector for DOC and engine with a frustum as show in **Figure 4.1 D, E** and **F** are the section image after cutting the DPF, which P-DPF was consist by metal foil and metal fiber layers. The assembling method of vehicle aftertreatment as show in **Figure 4.2**. All DOC and DPF specifications are listed in **Table 4-1**.

Figure 4.2 DOC & DPF systems' assembling method

Table 4-1 All DOC and DPF specification

		Element	Cell Density (CPSI)	Diameter (mm)	Length (mm)
Testing samples	DOC	CeO2	300	144	100
	DPF	Non-Cat	300	144	200
		CeO2	300	144	200

4.2 Engine Dyno Testing

The process of engine dyno testing involves analyzing the effect of DOC and DPF system on the performance of an unaltered direct injection diesel engine by examining metrics thermal

efficiency, specific fuel consumption, specific energy consumption, and combustion characteristics including heat release rate. This is accomplished by subjecting the engine to varying loads of 20-50% at consistent engine speeds of 1000, 1500, and 2000 RPM.

4.2.1 Schematic Diagram

The schematic diagram of engine test has shown in **Figure 4.3**. Prior to the start of the experiment, the diesel fuel will be prepared using a fuel supply system controlled by a three-way valve and a weight meter to measure fuel consumption. The engine's torque and speed will be regulated by a load cell incorporated in the dynamometer and ECU. In addition, the exhaust gases will pass through a DOC and DPF before entering the exhaust gas analyzer. The exhaust temperature at P1, P2, and P3 will differ due to exothermic reactions in the DOC, heat flux, and diffusion after the exhaust gases pass through the catalytic converter. During engine operation, the exhaust gas analyzer will automatically measure carbon dioxide, carbon monoxide, hydrocarbon, oxygen, lambda, nitrogen oxide, and exhaust temperature. The quantity of PMs will be measured simultaneously by the smoke intensity meter and exhaust gas analyzer.

Table 4-2 shows the units for the exhaust results, where PPM denotes parts per million and indicates the amount of each exhaust gas. 1 ppm = 1 mg/L = 1mg/kg = 1mg/km, 1 ppb = 1 µg/L, and 1%Vol = 100000ppm. **Table 4-3** represents the accuracy of each exhaust gas, and the error increases with the quantity of exhaust gas.

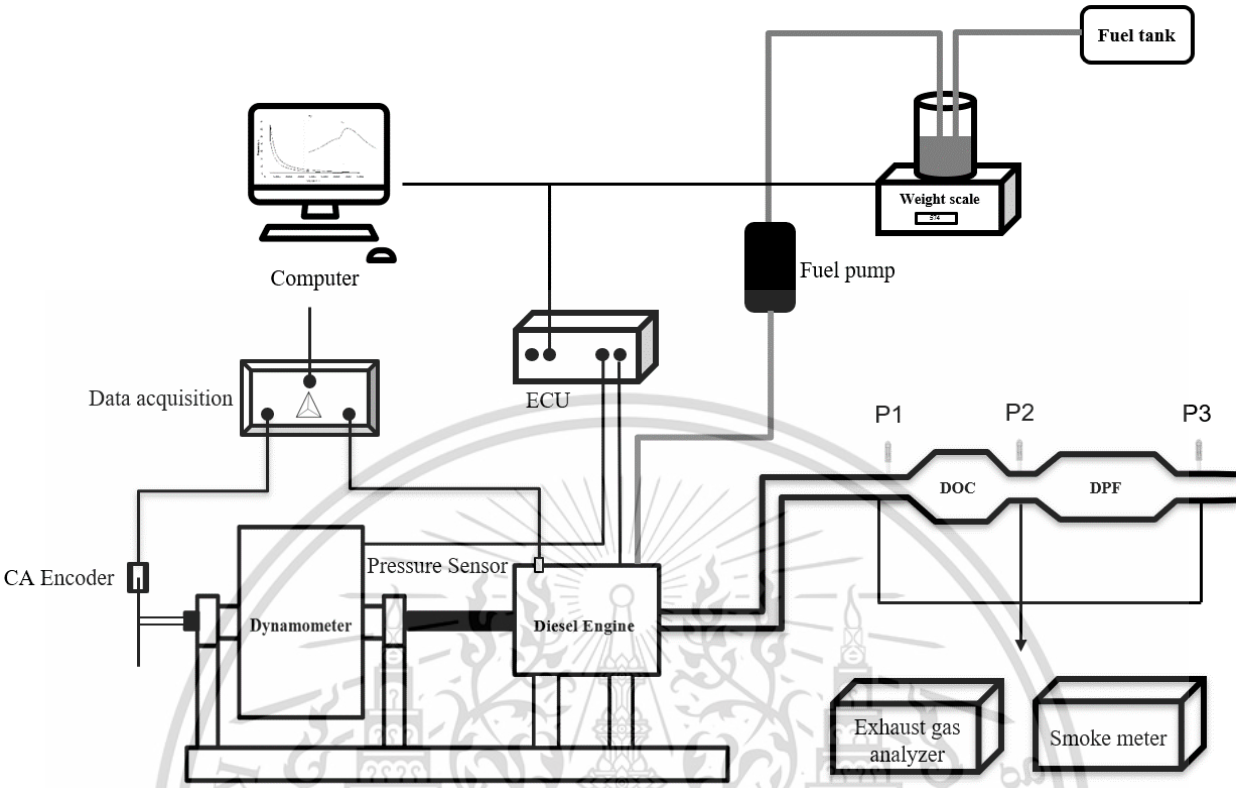

Figure 4.3 Engine test schematic diagram

Table 4-2 Unit of exhaust parameters

Test results	Unit
CO	% Vol
CO_2	% Vol
O_2	% Vol
NOx	ppm
HC	ppm
Opacity	%
Smoke intensity	%

Table 4-3 Exhaust gas accuracy

Factors	Accuracy

CO	<10.0%.: ± 0.02% vol., ±3% o.M. ≥10.0%.: ± 5% o.M.
CO2	<16.0%.: ± 0.3% vol., ±3% o.M. ≥16.0%.: ± 5% o.M.
HC	<2000ppm vol.: ± 4% ppm vol., ±3% o.M. ≥5000% ppm vol.: ± 5% o.M. <10000% ppm vol.: ± 10% o.M.
O2	± 0.02 % vol., ±1% o.M.
NOx	± 5ppm vol., ±1% o.M.
Lambda	Calculated from CO, CO2, HC, O2

4.2.2 Engine Specification

An engine specification of direct injection diesel engine which used in this research is shown in **Figure 4.4**. **Table 4-4** displays the specifications of the diesel engine used in the bench test, which can generate a power output of up to 170 kW. **Table 4-5** presents three different testing conditions, and it is recommended to perform multiple tests at high engine load and speed due to the unstable experimental data.

Table 4-4 Engine's specification

Items	Details
Engine Model	Isuzu 4JJ1-TC
Engine Type	Diesel
Injection Type	Direct Injection
Displacement Volume	2,999 cc
Compression Ratio	18.3: 1
Bore x Stroke	95.4 mm x 104.9 mm
Maximum Power	170kW

Table 4-5 Boundary conditions

Conditions	rpm	Load / Nm

Condition 1-4	1000	56/84/112/140
Condition 2-8	1500	56/84/112/140
Condition 9-12	2000	56/84/112/140

Figure 4.4 Direct injection diesel engine (Isuzu 4JJ-TC)

4.2.3 Eddy Current Dynamometer's Specification

The ED-150-LC eddy current dynamometer is connected to the engine and utilizes the engine flywheel to impose a load, all while measuring both torque and power. The eddy current dynamometer's cooling system incorporates external water cooling. **Table 4-6** and **Figure 4.5** illustrate the specifications of the eddy current dynamometer.

Table 4-6 Eddy current dynamometer's specification

Items	Details
Model	Tokyo Plant ED-150-LC
Maximum Brake Horsepower	150 PS / 3000rpm
Maximum Brake Torque	35.81 kgm
Maximum Speed	3000rpm

Figure 4.5 Eddy current dynamometer (Tokyo Plant ED-150-LC)

4.2.4 DPF Pressure Drop Testing

In this experiment, pressure values were measured before DOC, between DOC and DPF, and after DPF as indicate in **Figure 4.6**; subtract them to obtain the pressure drop, which is the scheduling back pressure caused by DOC and DPF. In this experiment, the average value was calculated for multiple measurement at each point.

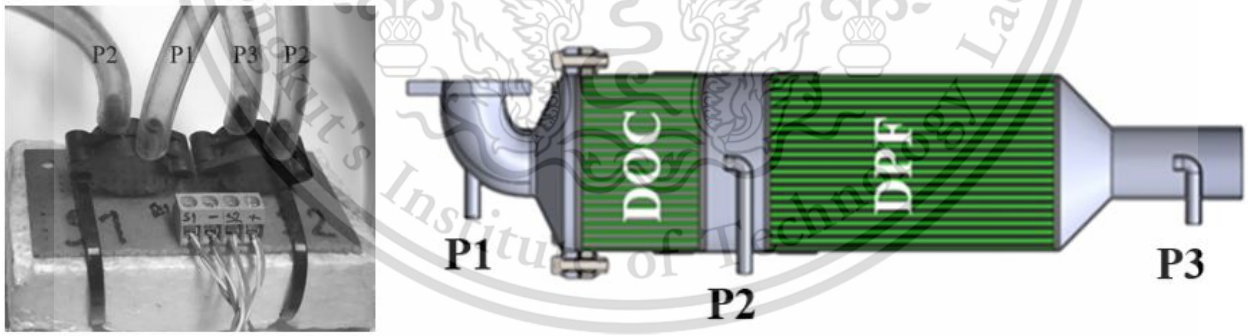

Figure 4.6 Pressure drop measurement with and without DOC and DPF systems

4.3 Chassis Dyno Testing

To observe the impact of CeO2 DOC and DPF on emissions from unaltered diesel vehicles, chassis dynamometer tests were conducted. And the testing was conducted based on Euro 4 standards.

4.3.1 Schematic Diagram

The diesel vehicle is placed on the chassis dynamometer as indicates in **Figure 4.7**. In order to prevent the engine from overheating, a high-power fan is placed in front to simulate actual driving; the surrounding environment will be closed during the test to ensure stable test results; Into the AVL exhaust gas measuring instrument because the exhaust gas just coming out of the engine is very humid and the temperature is very high, the proportion of each exhaust gas molecule at this time is unstable. AVL will measure PM, PN, NOx, CO, and HC. The diesel vehicle testing layout in pollution control department as shown in **Figure 4.8**.

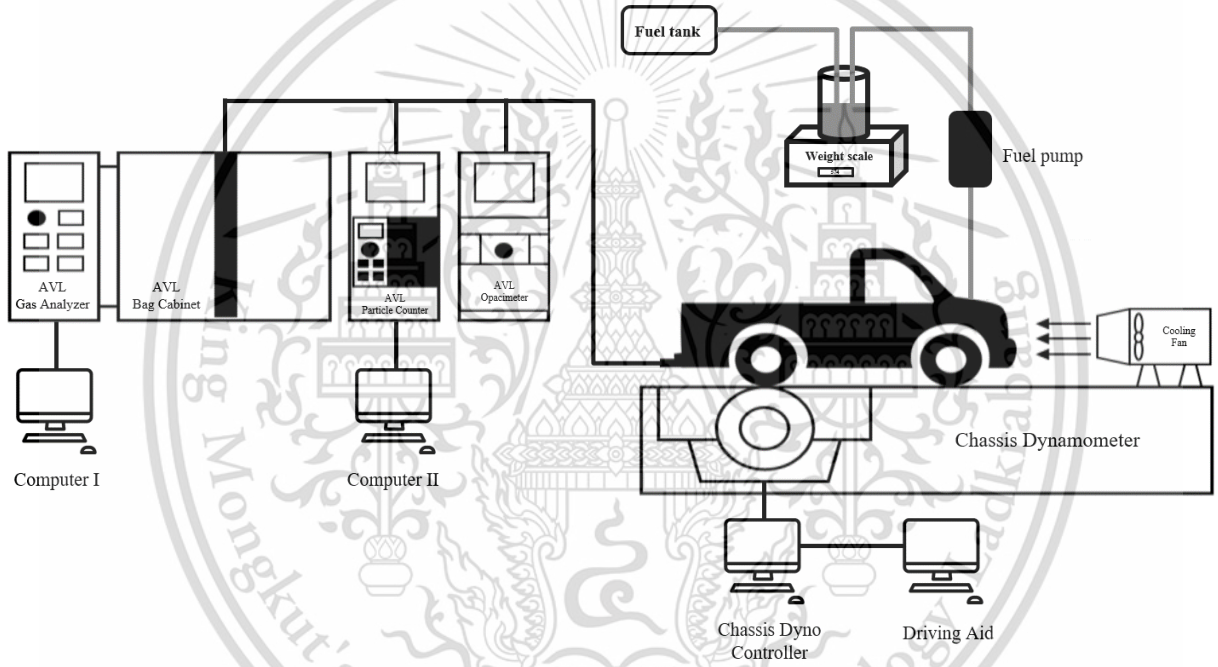

Figure 4.7 Schematic diagram of chassis test

Figure 4.8 Chassis dyno testing in PCD

4.3.2 Vehicle Specification

The Toyota Hilux Tiger 2.5 L diesel vehicle with the maximum power of 75kW was selected for chassis testing as shown in **Figure 4.9**, the vehicle specifications can be found in **Table 4-7.**

Table 4-7 Vehicle's specification

Items	Details
Vehicle	Toyota Hilux Tiger
Engine type	Diesel, 4 Cylinder, In-line
Injection type	Direct Injection
Displacement volume	2,500 cc
Compression ratio	18.5: 1
Bore x Stroke	92.0 mm x 93.8 mm
Maximum Power	75 kW @3600 rpm
Maximum Torque	260 N.m. @1600-2400 rpm

Figure 4.9 Toyota Hilux Tiger diesel vehicle

4.3.3 MVEG_H Testing Cycle

The Motor Vehicle Emissions Group-MVEG also refer as NEDC, which has become a standard driving mode adopted by many countries, comprises four urban driving sequences (ECE) and one suburban driving sequence (EUDC). The EUDC segment is added to the end of the fourth ECE cycle to account for more aggressive and high-speed driving modes, as illustrated in **Figure 4.10**. The driving cycle lasted, on average, 1180 seconds (19.67 minutes) with an average speed of 33.4 km/h. While the duration and average speed of the two driving cycles were similar, the NEDC test mode is simpler because it includes straight-line acceleration, constant speed, and deceleration curve driving behaviors that do not reflect real-world driving. In contrast, the BDC features more transient speed variations that better reflect real-world driving. Another notable observation is that during the first three minutes of the NEDC test, an ECE sequence is completed, whereas during the same time window, the BDC test involves more idling and low vehicle speed conditions.

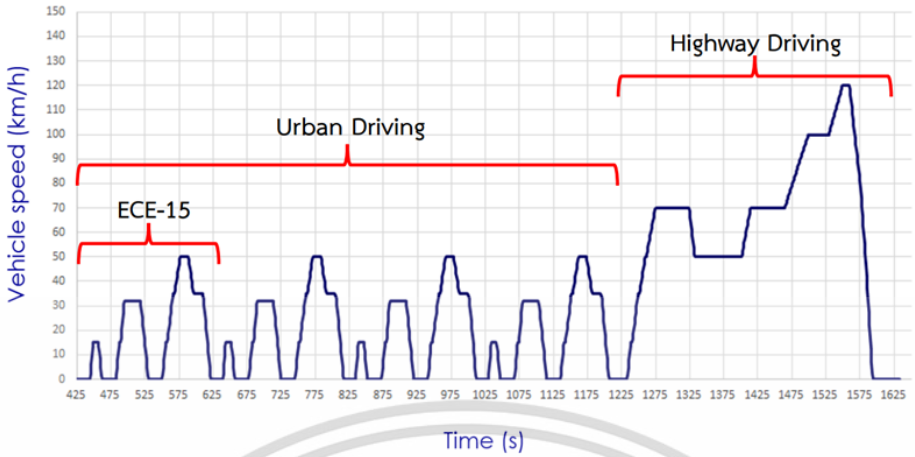

Figure 4.10 MVEG_H testing cycle

4.4 Data Collection System

4.4.1 In-cylinder pressure and Crank Angle

In order to observe the phenomenon taking place within the tested engine, a piezoelectric crystal sensor called "Kistler 6052C31" is utilized. This sensor is capable of measuring pressures of up to 250 bar and is highly sensitive with an accuracy of ±0.7%. It is mounted at the cylinder head, as depicted in **Figure 4.11**. Additionally, to accurately determine the timing of the crank angle position and calculate the volume of the combustion chamber, an optical crankshaft encoder known as "CA-RIE-360" is installed between the sensors gate at the end of the dynamometer shaft. This encoder comprises of a customized disc containing 720 slits, and it has a resolution of 0.5 degrees. The encoder sensor operates on the principle of transmission light, where an infrared beam is emitted and received at the sensor, as shown in **Figure 4.12**.

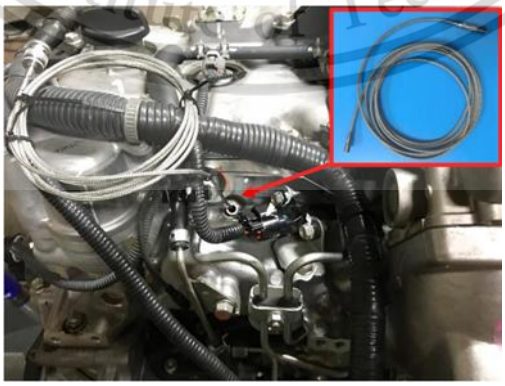

Figure 4.11 Pressure sensor

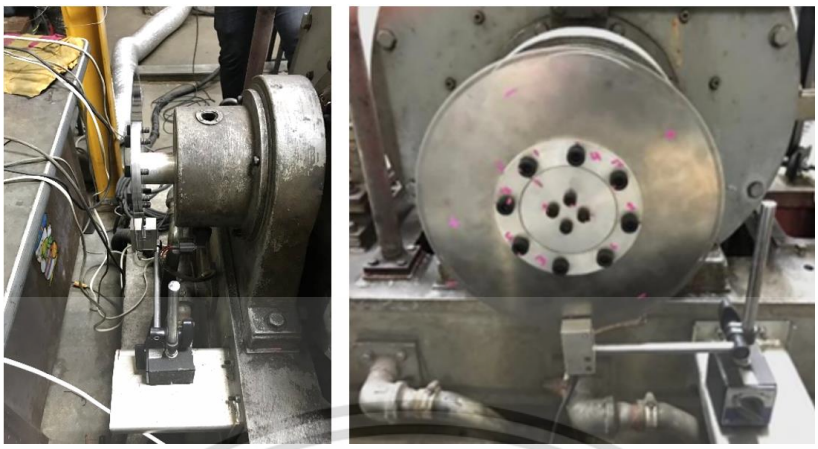

Figure 4.12 Crank encoder

4.4.2 Emissions

The smoke intensity meter was utilized to measure exhaust emissions by optically evaluating the soot on the paper filter using the light reflectance method. The smoke meter was employed to determine the concentration of particulate matter in the exhaust gas. The smoke meter indicated 0% intensity when no particles were detected on the filter, and 100% intensity when particles covered all areas. **Figure 4.13** displays the smoke meter, "Okuda DSM-240," along with the filter paper. Additionally, the AVL exhaust gas analyzer "DITEST GAS 1000" was employed to measure other gases discharged from the engine, such as carbon dioxide (CO2) and nitrogen oxides (NO), as shown in **Fig. 4.14**.

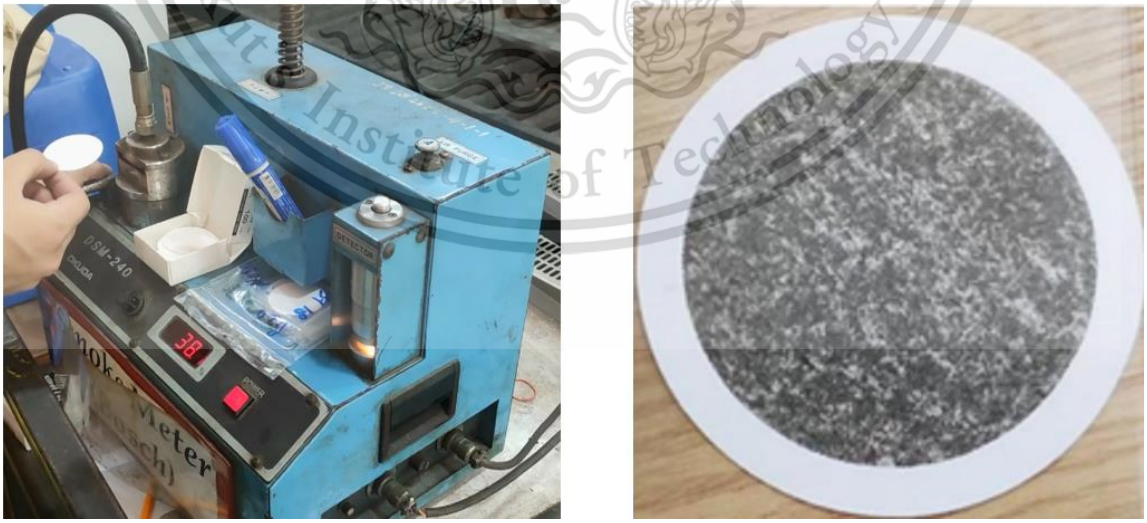

Figure 4.13 Smoke intensity meter

Figure 4.14 AVL gas analyzer

4.4.3 Data Acquisition System

A DEWESOFT DAQ system is employed to store data from the pressure and crank angle sensors for monitoring and collecting combustion characteristics in the combustion chamber, **Figure 4.15** illustrates this process. Real-time data analysis is performed by the DewesoftX software, which calculates parameters such as pressure-crank angle diagrams and pressure-volume diagrams. The DAQ system collects data for a total of 1000 cycles during stable engine conditions at each set condition.

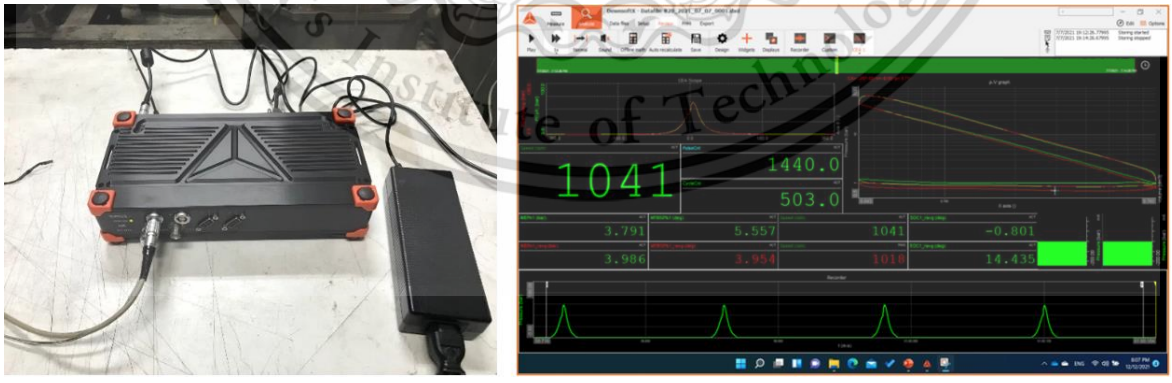

Figure 4.15 Dewesoft DAQ data acquisition system

4.5 Calculation method

The combustion data parameters were utilized to compute and examine the quantitative combustion information. This analysis encompasses two types of combustion characteristics, namely, cumulative heat release and heat release rate, which help elucidate the relationship between compression and expansion pressure with crank angle in the combustion chamber. Additionally, engine performance is evaluated through factors such as fuel consumption, energy consumption, and thermal efficiency to gauge fuel efficacy.

4.5.1 Engine performance

he determination of engine performance is based on several metrics including specific fuel consumption, specific energy consumption, and thermal efficiency. These metrics are quantified through indicated values and brake values, which can be calculated using the equations provided below.

1) Specific Fuel Consumption

ISFC and BSFC are acronyms that refer to the rate of fuel consumption in kilograms per kilowatt-hour, which is the amount of power generated by an engine.

$$\mathrm{ISFC} = \frac{\text{Fuel Consumption Rate}}{\text{Indicated Power}} = \frac{\dot{m}_f}{\mathrm{PdV}} \tag{4.1}$$

$$\mathrm{BSFC} = \frac{\text{Fuel Consumption Rate}}{\text{Brake Power}} = \frac{\dot{m}_f}{4\pi\tau \cdot \frac{N}{60} \cdot \frac{1}{2}} \tag{4.2}$$

2) Specific Energy Consumption

ISEC and BSEC are terms used to refer to the rate of energy consumption to power produced by an engine, which is measured in kJ/kWh.

$$\mathrm{ISEC} = \mathrm{ISFC} \cdot \mathrm{LHV} \tag{4.3}$$

$$\mathrm{BSEC} = \mathrm{BSFC} \cdot \mathrm{LHV} \tag{4.4}$$

3) Thermal Efficiency

The thermal efficiency of a system is the quantity of power output that is derived from the heat energy supplied to it. Normally ITE is 5-10% higher than BTE due to the friction loss.

$$\text{ITE} = \frac{\text{Indicated Power}}{\text{Heat Energy Input Rate}} = \frac{\text{PdV} \cdot \frac{\text{N}}{60} \cdot \frac{1}{2}}{\dot{m}_f \cdot Q_{LHV}} \quad (4.5)$$

$$\text{BTE} = \frac{\text{Brake Power}}{\text{Heat Energy Input Rate}} = \frac{4\pi\tau \cdot \frac{\text{N}}{60} \cdot \frac{1}{2}}{\dot{m}_f \cdot Q_{LHV}} \quad (4.6)$$

$$\text{Friction Loss} = \text{ITE-BTE} \quad (4.7)$$

Where P is cylinder pressure, V is combustion chamber volume, N is engine speed, $\dot{m}_f$ is mass of fuel consumption rate, LHV is low heating value, Q_{LHV} is Energy input, k is specific heat ratio, and θ is crank angle.

CHAPTER 5

RESULTS AND DISCUSSION

5.1 Engine Dyno Testing

5.1.1 Combustion Characteristic

The study investigated the combustion profile of the samples, including in-cylinder pressure data plotted with respect to volumetric and crank angle. **Figure 5.1-5.4** show the in-cylinder pressure plot with respect to volumetric in logarithmic scale. At 1000 RPM, the pressure during intake, compression stroke increases due to DPF cause a back pressure. Indicated work is higher with engine load increasing due to inject more fuel to achieve more power. From overall, DPF system has no significant influence in P-V diagram at 1000rpm. The DPF cause the combustion pressure increase 0.3 bar due to less cooling loss and exhaust loss resulting in a higher indicated work; meanwhile as illustrate in **Figure 5.5**. Meanwhile, the ignition delay 2 degrees owing to the DPF back pressure as shown in **Figure 5.6**. During intake and exhaust stroke the pressure increase due to DPF back pressure block the gas flow. The peak pressure of combustion increases with an increase in engine load as more fuel is burnt at higher loads. At 1500rpm and 2000rpm, the combustion pressure even higher due to higher engine load as indicated in **Figure 5.7-5.14**. Especially at 2000 rpm, the combustion pressure increases 2 bar due to the cooling loss and exhaust loss are reduced by DPF as shown in **Figure 5.15-5.16**. In such cases, the energy remaining

larger quantity in the molecule, which results in a higher combustion pressure and exhaust temperature. At higher engine rpm, the pressure during intake and exhaust stroke system becomes stable compare with low rpm. Additionally, the air-fuel mixing duration decreases with an increase in engine speed due to faster combustion cycles. Therefore, less fuel is burnt in the premixed combustion phase at higher engine speeds, resulting in a lower peak pressure. When the ignition delay time is longer, more fuel is combusted in the premixed combustion phase due to increased mixing time. Based on the results of the in-cylinder pressure data plot, pressure versus crank angle diagrams, it can be concluded that DOC and DPF do not significantly influence on engine combustion characteristics at lower rpm, while at higher rpm, engine combustion is better due to more heating energy and kinetic energy blocked by DPF systems.

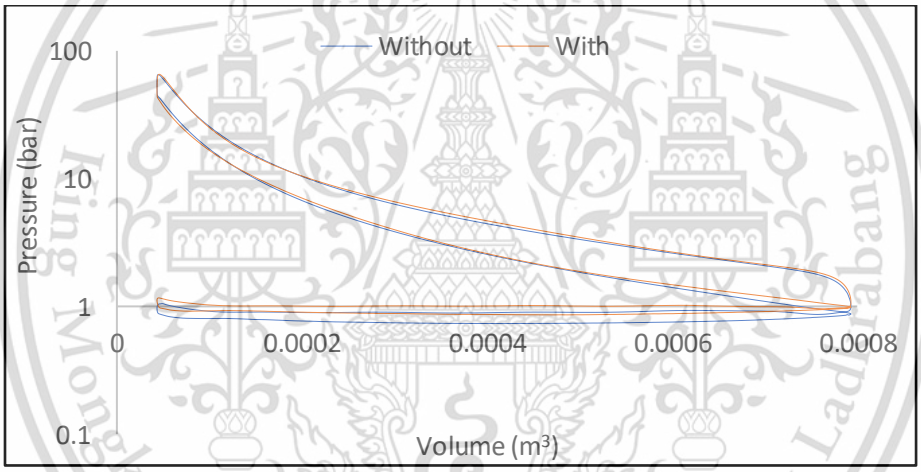

Figure 5.1 Log-PV diagram with and without DOC and DPF 56Nm at 1000rpm

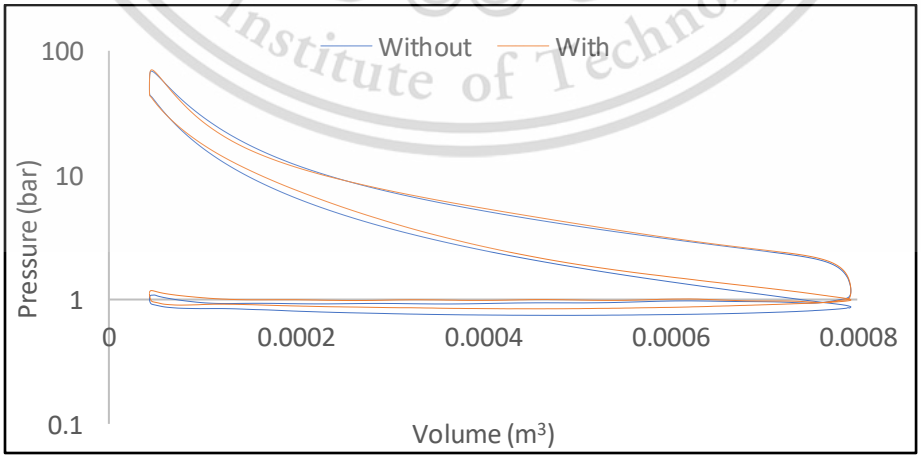

Figure 5.2 Log-PV diagram with and without DOC and DPF 84Nm at 1000rpm

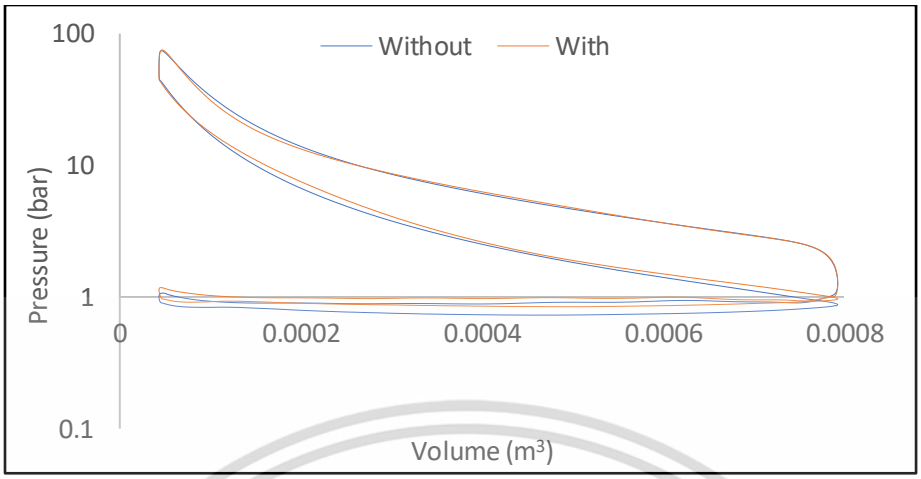

Figure 5.3 Log-PV diagram with and without DOC and DPF 112Nm at 1000rpm

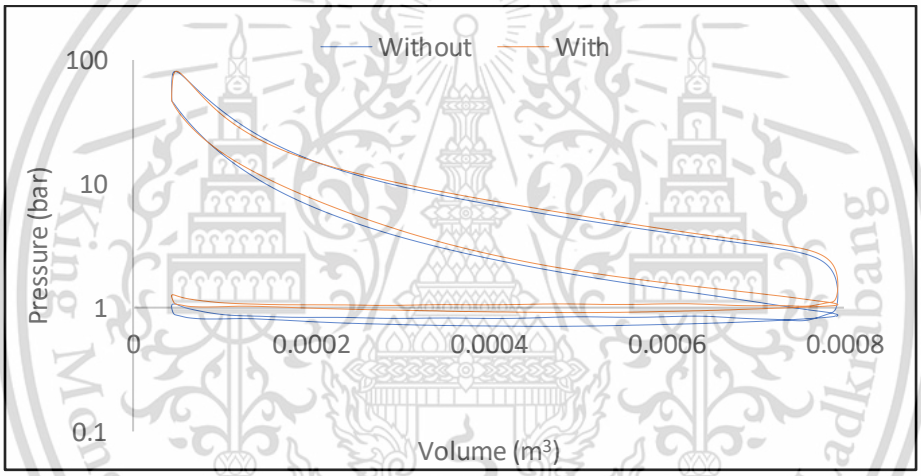

Figure 5.4 Log-PV diagram with and without DOC and DPF 140Nm at 1000rpm

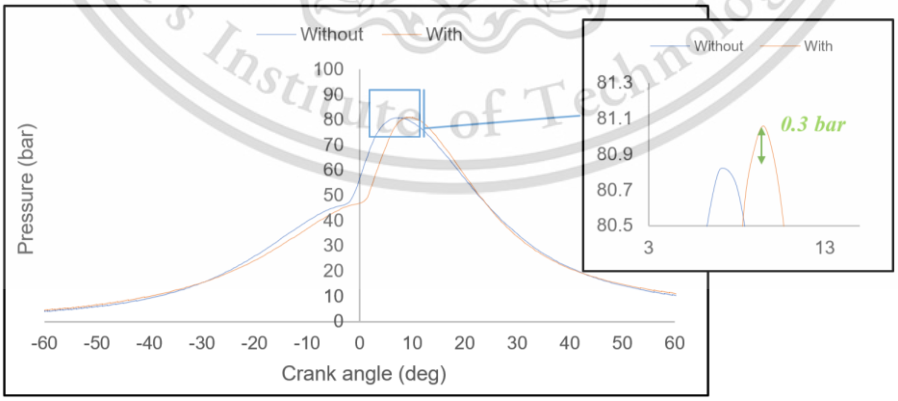

Figure 5.5 P-CA diagram with and without DOC and DPF 140Nm at 1000rpm

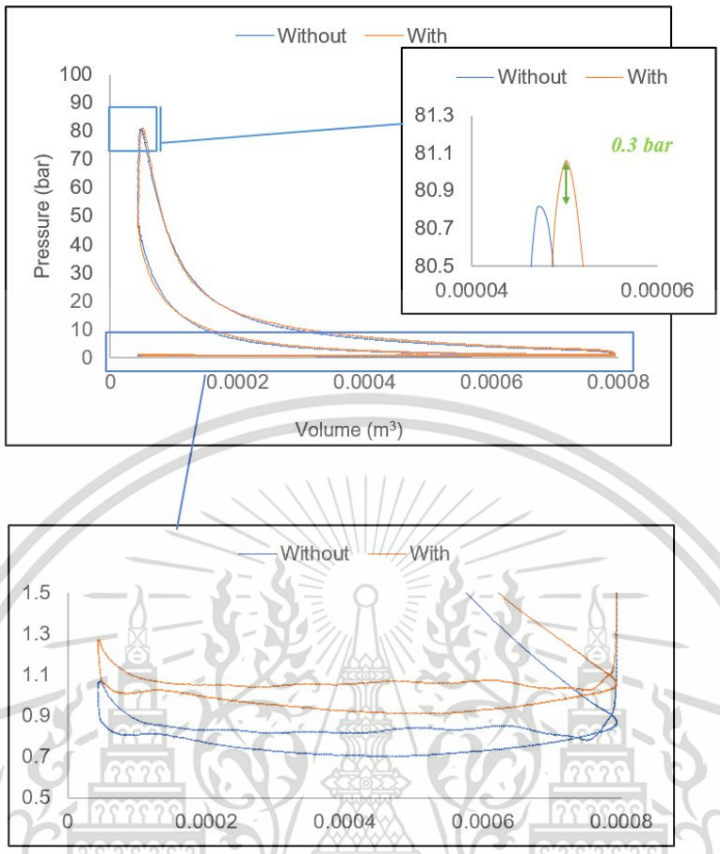

Figure 5.6 PV diagram with and without DOC and DPF 140Nm at 1000rpm

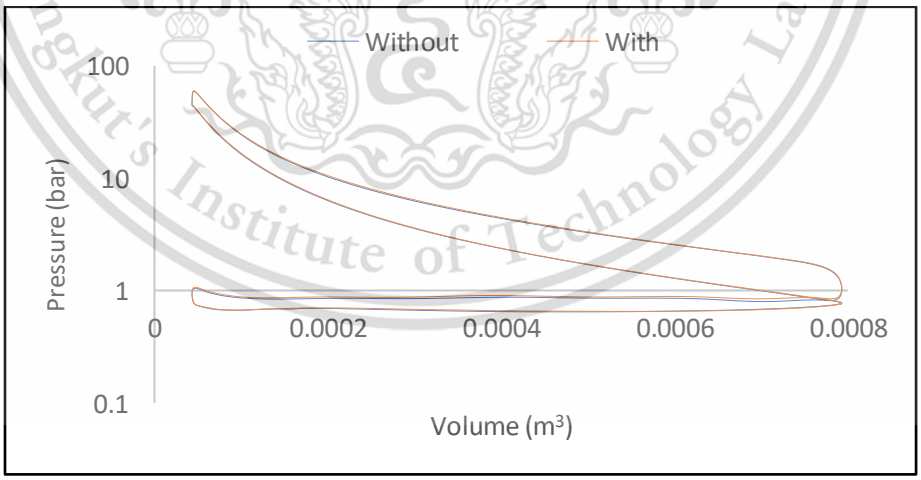

Figure 5.7 Log-PV diagram with and without DOC and DPF 56Nm at 1500rpm

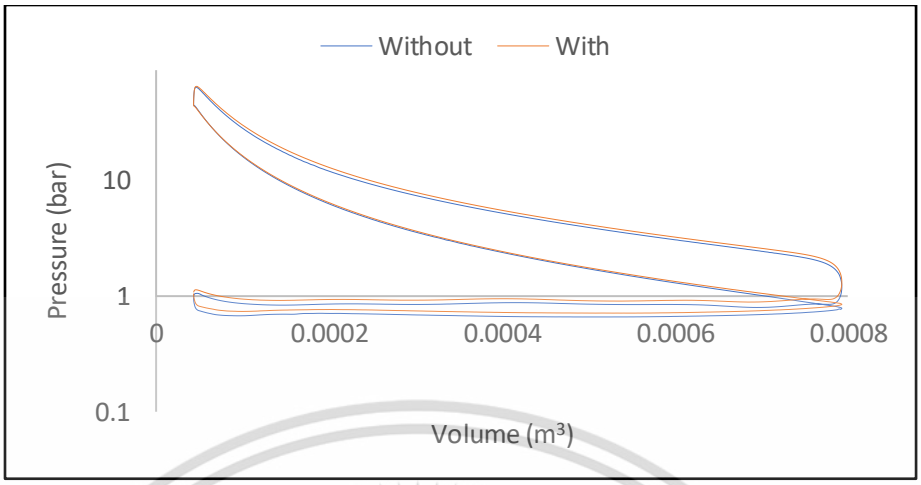

Figure 5.8 Log-PV diagram with and without DOC and DPF 84Nm at 1500rpm

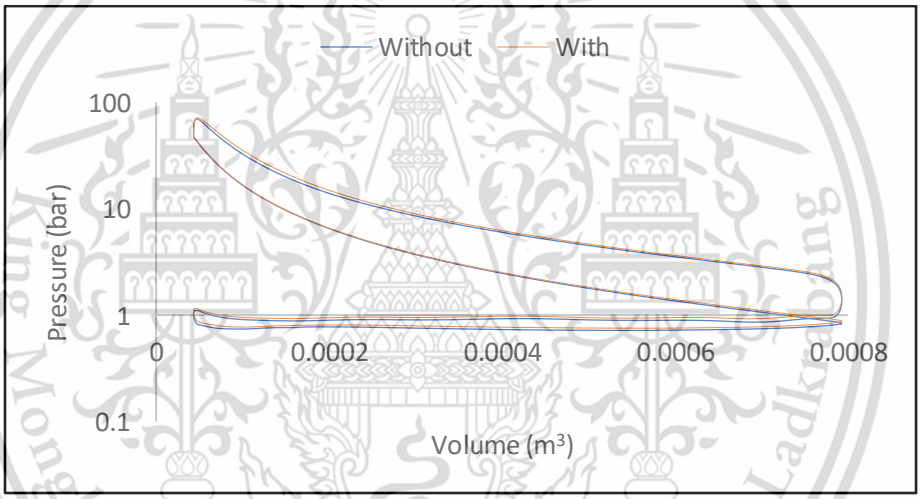

Figure 5.9 Log-PV diagram with and without DOC and DPF 112Nm at 1500rpm

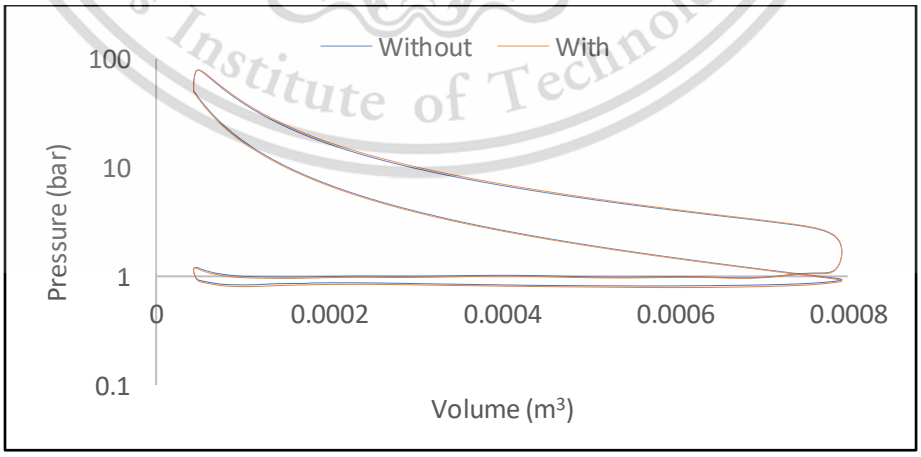

Figure 5.10 Log-PV diagram with and without DOC and DPF 140Nm at 1500rpm

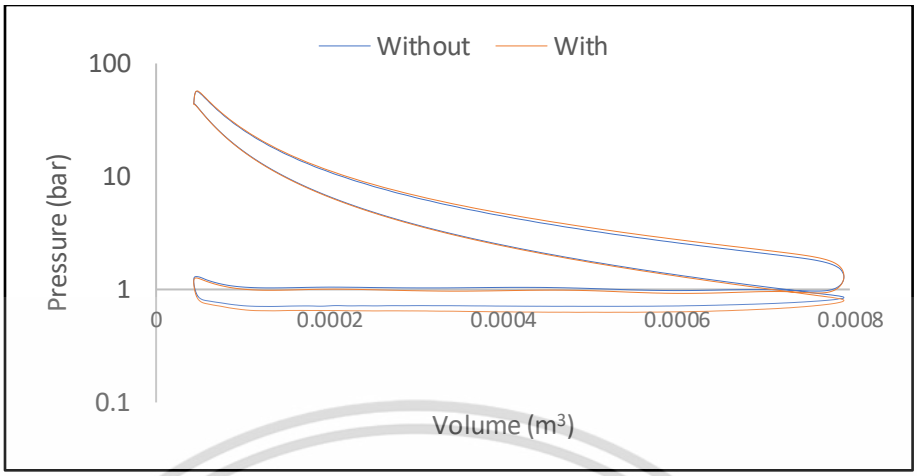

Figure 5.11 Log-PV diagram with and without DOC and DPF 56Nm at 2000rpm

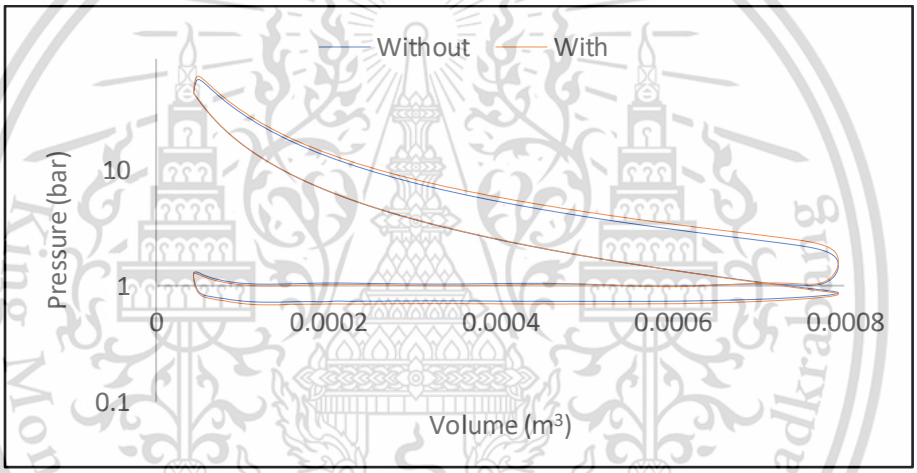

Figure 5.12 Log-PV diagram with and without DOC and DPF 84Nm at 2000rpm

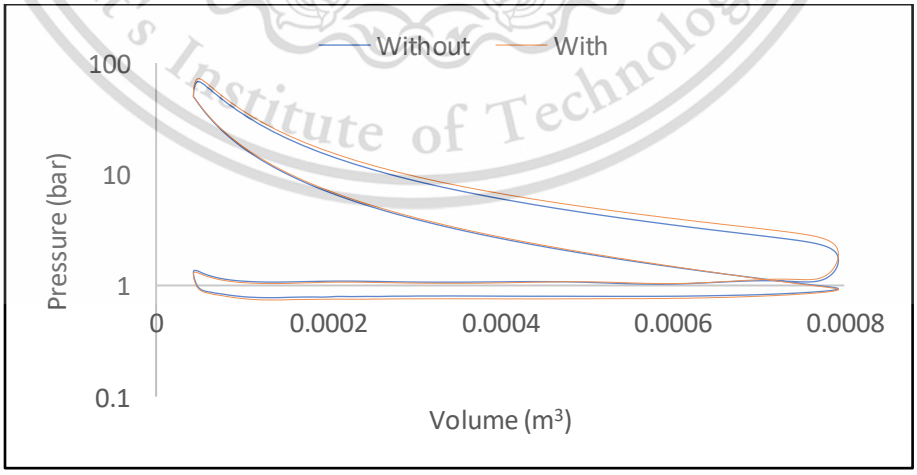

Figure 5.13 Log-PV diagram with and without DOC and DPF 112Nm at 2000rpm

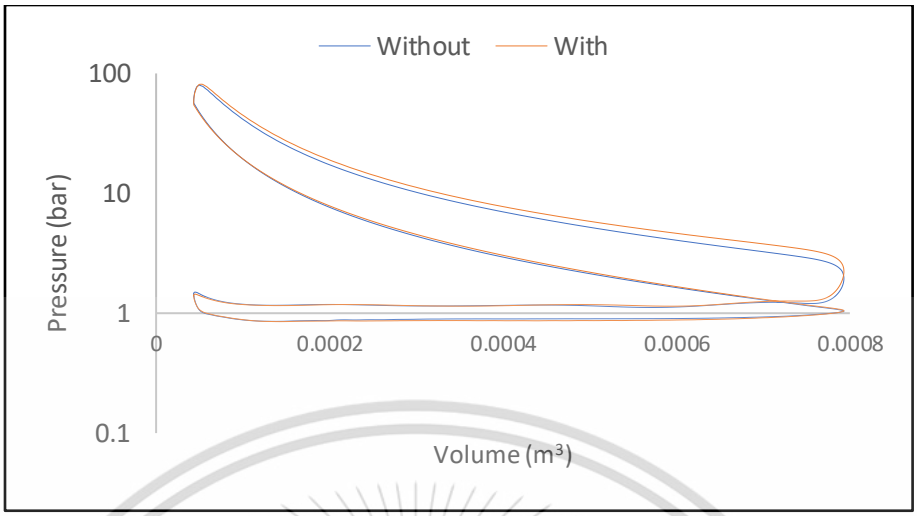

Figure 5.14 Log-PV diagram with and without DOC and DPF 140Nm at 2000rpm

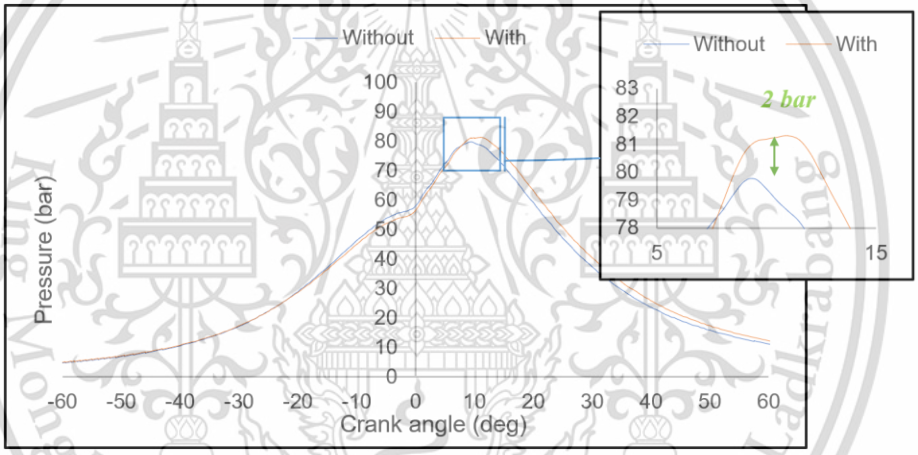

Figure 5.15 P-CA diagram with and without DOC and DPF 140Nm at 2000rpm

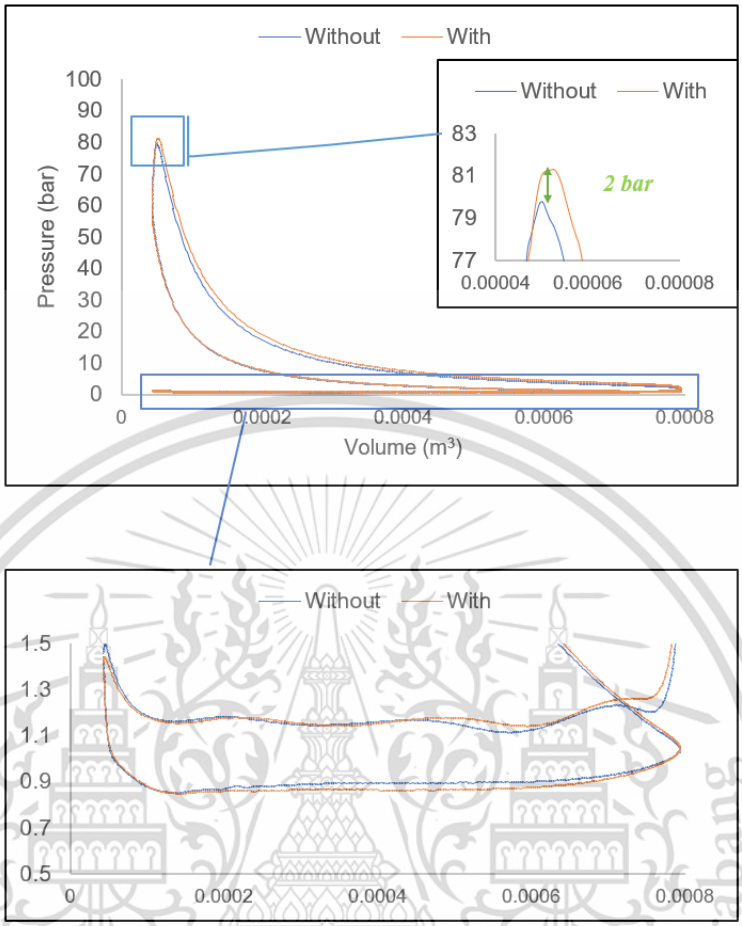

Figure 5.16 PV diagram with and without DOC and DPF 140Nm at 2000rpm

5.1.2 Engine Performance

In-cylinder pressure and fuel consumption rate are used to estimate Indicated Specific Fuel Consumption (ISFC), Indicate Specific Energy Consumption (ISEC), and Indicated Thermal Efficiency (ITE). On the other hand, engine speed, torque, and fuel flow rate are measured to calculate Brake Specific Fuel Consumption (BSFC), Brake Specific Energy Consumption (BSEC), and Brake Thermal Efficiency (BTE).

As engine load increases, fuel flow rate also increases due to the injection of more fuel, as depicted in **Figure 5.17**. Indicated power increase with DPF system due to less heating loss and exhaust loss as show in **Figure 5.18**. Specific fuel consumption refers to fuel consumption per unit power, with ISFC and BSFC representing fuel consumption values with the unit of brake power output and indicated power, respectively, as illustrated in **Figures 5.19** and **Figures 5.21**.

ISEC and BSEC are shown in **Figures 5.20** and **Figure 5.22**, respectively. Both BSFC and ISFC decrease with increasing engine load due to higher engine operation. Higher engine revs result in a faster combustion cycle, which reduces energy loss from heat radiation to the cylinder wall and cooling system, compared to lower engine speeds.

Thermal efficiency describes the efficiency of converting thermal energy input to mechanical energy output. At the same engine speed, both thermal efficiencies increase with increasing load due to a higher burning rate, as shown in **Figures 5.23** and **Figure 5.24**. Thermal efficiencies increase with increasing engine load while the engine speed remains constant. Additionally, all cases have a similar brake thermal efficiency of around 30%. Meanwhile, without DPF system, the IET is 4-6% higher than BTE; While with DPF system, ITE is 5-11% higher than BTE owing to the DPF system cause the friction loss increase between 1-6% as indicated in **Figure 5.25**; the friction loss increases with engine rpm increasing due to more revolution cause more friction work; and friction loss increase with DPF system due to the DPF cause a backpressure impede the piston and crank angle movement.

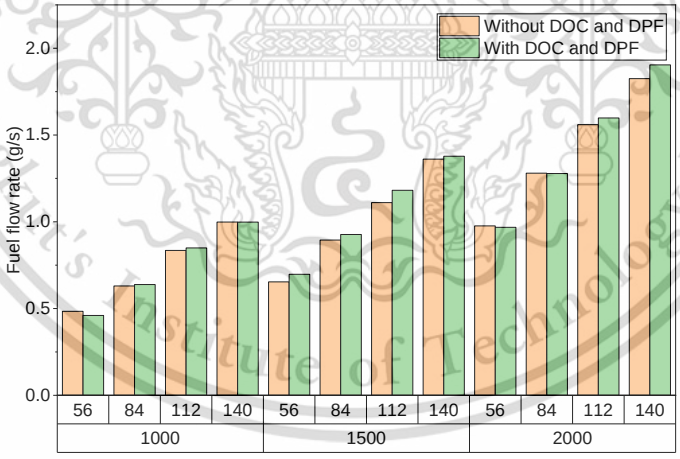

Figure 5.17 Fuel consumption with and without DOC and DPF

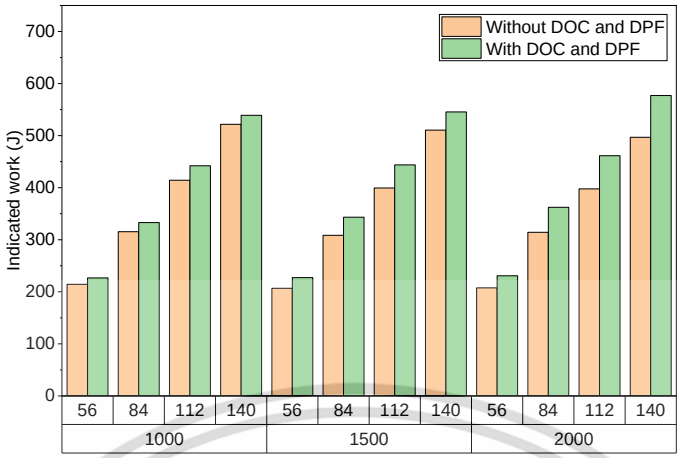

Figure 5.18 Indicated work with and without DOC and DPF

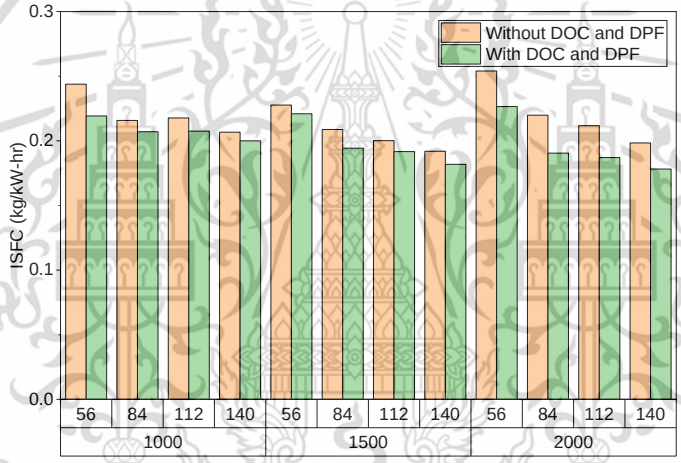

Figure 5.19 ISFC with and without DOC and DPF

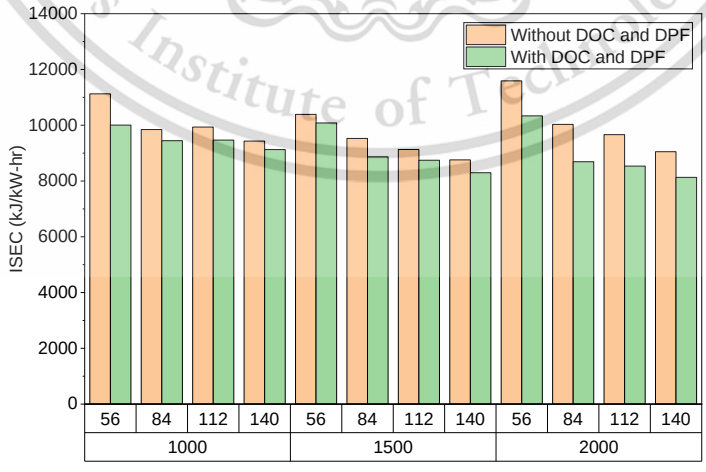

Figure 5.20 ISEC with and without DOC and DPF

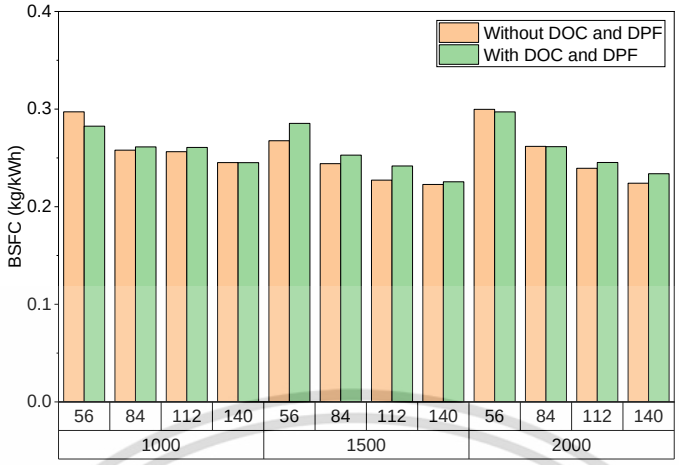

Figure 5.21 BSFC with and without DOC and DPF

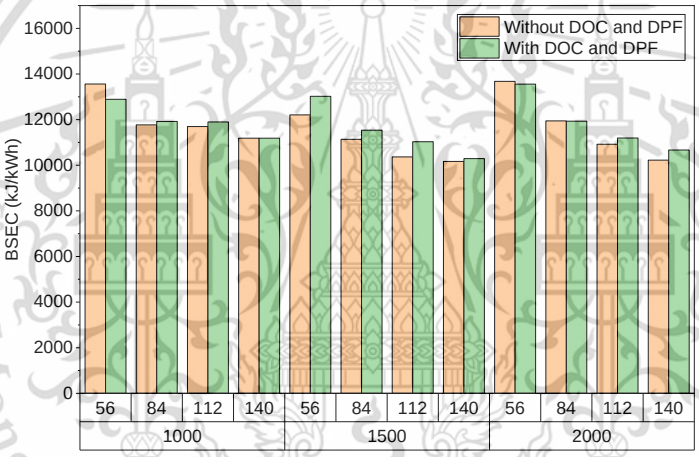

Figure 5.22 BSEC with and without DOC and DPF

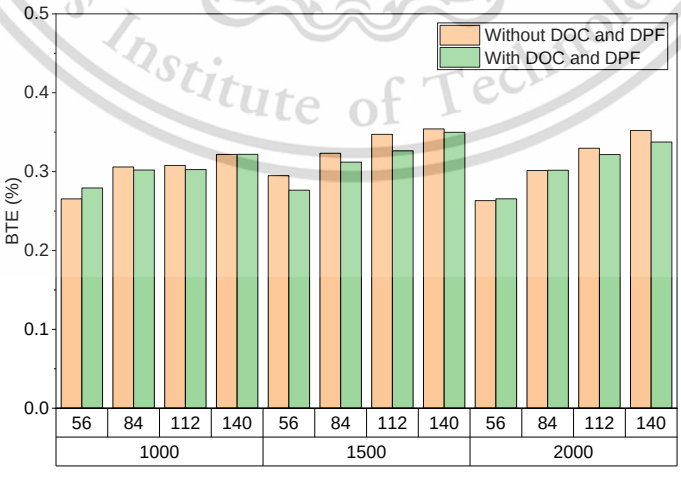

Figure 5.23 BTE with and without DOC and DPF

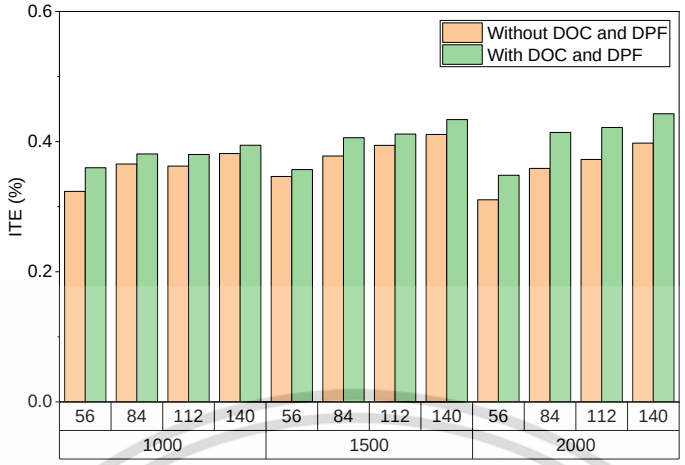

Figure 5.24 ITE with and without DOC and DPF

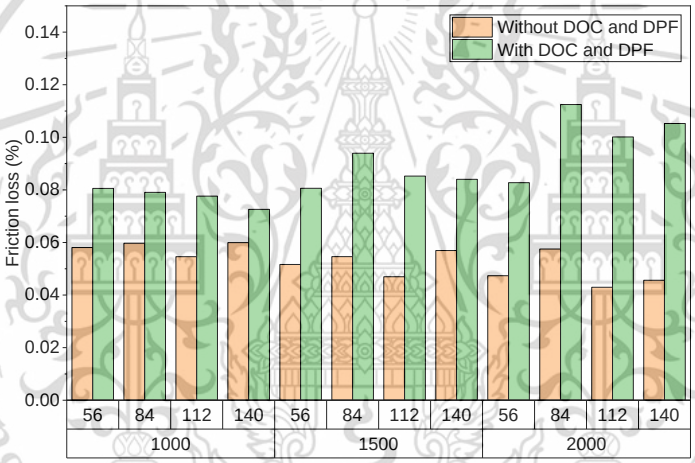

Figure 5.25 Friction loss with and without DOC and DPF

5.1.3 DPF Pressure Drop Comparison

The comparison results as present in **Figure 5.26** indicate the pressure drop between the calculated, simulated, and tested results of the 300 CPSI DOC and 300 CPSI DPF. The results demonstrate that the simulation and calculation results are highly consistent, and the deviation from the experimental results is only 5-10%, primarily due to operational and instrumental precision errors. From the results, it is apparent that the pressure drop of a clean DPF increases with engine speed, as the engine operates better. At 2000rpm, the transient pressure drop of a clean DPF is approximately 1.4kPa.

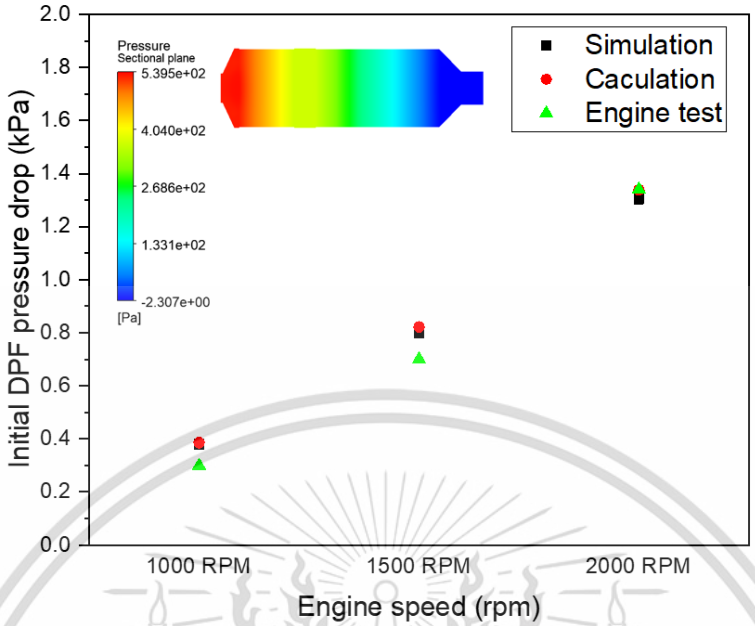

Figure 5.26 Comparison of transient pressure drop between calculation, simulation, and test

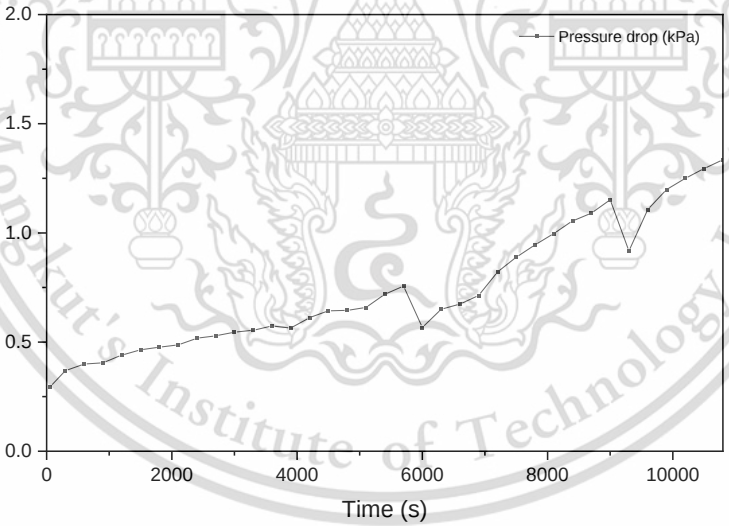

Figure 5.27 Partial flow DPF continuous pressure drop

The continuous pressure drop across the diesel particulate filter (DPF) was tested under steady-state loading conditions for the diesel oxidation catalyst (DOC)-DPF system, as depicted in **Figure 5.27**. A steady rise in pressure drop was observed with increasing load across the DPF system, attributed to soot accumulation. The initial pressure drop was 0.3 kPa, and it increased

to 1.3 kPa after three hours of engine running. The pressure drop of P-DPF is relatively lower than F-DPF due to the physical structure, it's a strong point of P-DPF. Pressure drops were also observed around 6000s and 9000s due to the engine stopping due to the temperature is too high.

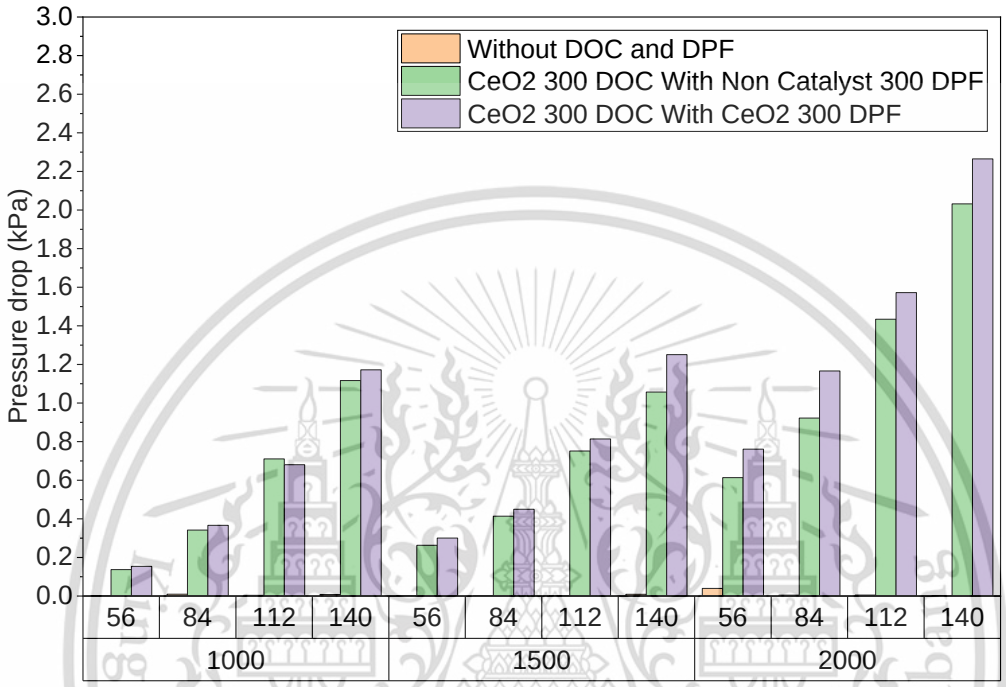

Figure 5.28 Testing DPF pressure drop

Figure 5.28 represents the pressure drop of DOC and DPF system, from the result, we found pressure drop increase with engine load increasing due to faster engine operation and more soot trapped in DPF. CeO2 catalyst DPF has lower pressure drop than non-Cat DPF owing to CeO2 promotes the soot regeneration. The pressure drop is varied from new DPF to cleaned DPF depending on how much soot oxidize, the catalyst does not influence much if the temperature is not higher enough. From the experimental results that pressure drop of DOC and P-DPF has no significant impact on engine performance.

5.1.4 Emissions

Soot, NOx, CO, HC, CO2 etc, were generated during diesel engine combustion. The diesel fuels exhibit their highest smoke intensity at an engine speed of 1000 rpm and an engine load of 140 Nm. This engine speed is associated with a higher fuel-air equivalent ratio, indicating a richer

combustion compared to other speeds. Moreover, the engine load of 140 Nm at 1000 rpm is considered heavy, leading to incomplete combustion due to the higher equivalent ratio and engine load. Consequently, the smoke intensity is higher under such conditions. To address this issue, the CeO2 DOC and P-DPF systems can be employed to reduce smoke emission. In comparison to not using these systems, their use can result in a reduction of approximately 65% in smoke emission as a result from **Figure 5.29 and Figure 5.30**.

The most concerning of diesel engine emission is NOx emissions. NOx emissions are increased with the engine speeds, engine loads as shown in **Figure 5.31**. The nitrogen oxide content increases as the temperature increasing in the combustion chamber. This corresponds to a higher exhaust temperature. According to the testing result, NOx reduced by around 30% with after-treatment system due to back pressure increases, so higher density exhaust gas goes to EGR, NOx decreases with temperature decreasing.

The exhaust temperature of no DOC and DPF system has a higher temperature due to DOC and DPF absorbing the heat, but no significant influence at high exhaust temperature due to a considerable heat flux rate. As engine speed and loads increases, the exhaust temperature measured by a thermocouple in the exhaust pipe also increasing. This is illustrated in **Figure 5.32**. The reason for this is that the increased in-cylinder pressure leads to higher combustion temperatures. Moreover, as engine load and speed increase, combustion operates at a faster rate, leaving less time for heat loss to the cooling system and heat radiation.

HC and CO were generated at low engine rpm and higher engine torque due to incomplete combustion. As presented in **Fig. 5.34**. at 1000rpm and 140Nm, CO %vol was reduced up to 82% by using a CeO2 catalyst converter. Meanwhile, HC was notably reduced when we applied a CeO2 DOC, as indicated in **Fig. 5.33**. In the test, we use a new non-catalyst 300 DPF. So, it has a better soot-trapping ability. Furthermore, part of liquid hydrocarbon trapped by metal fiber as a species of soot due to HC in the liquid phase will be easily trapping.

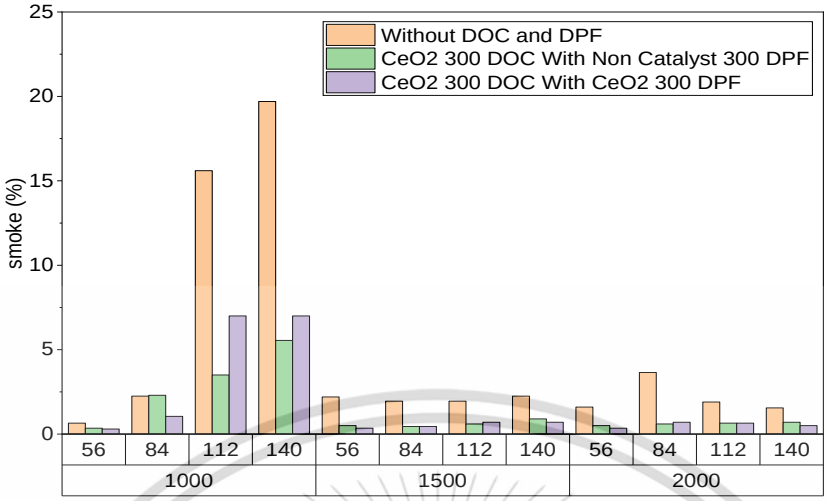

Figure 5.29 Smoke intensity of diesel engine

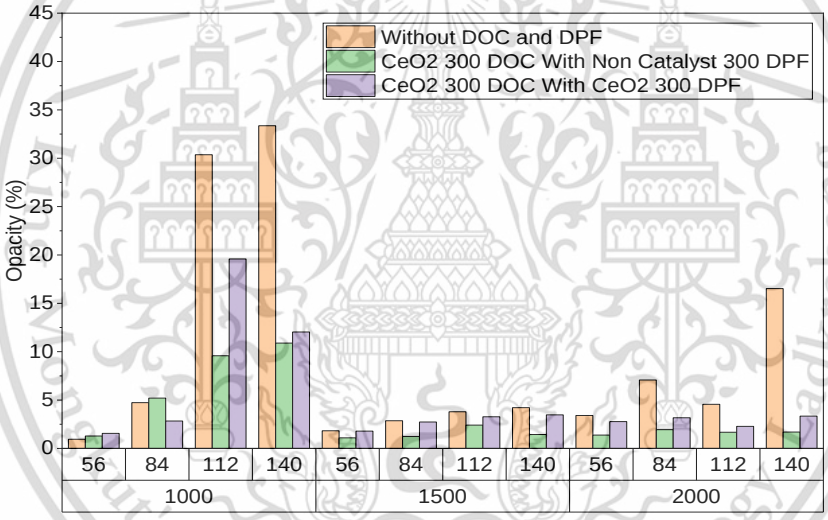

Figure 5.30 Opacity of diesel engine

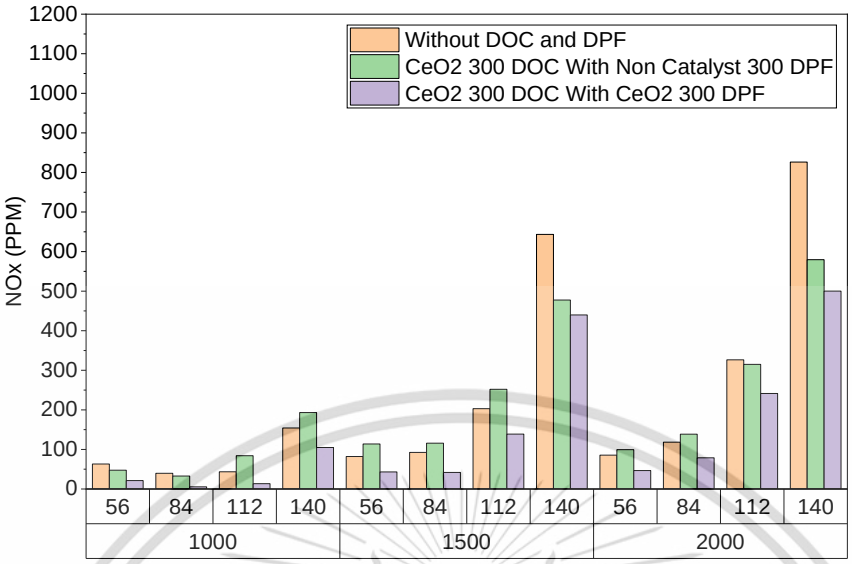

Figure 5.31 NOx of diesel engine

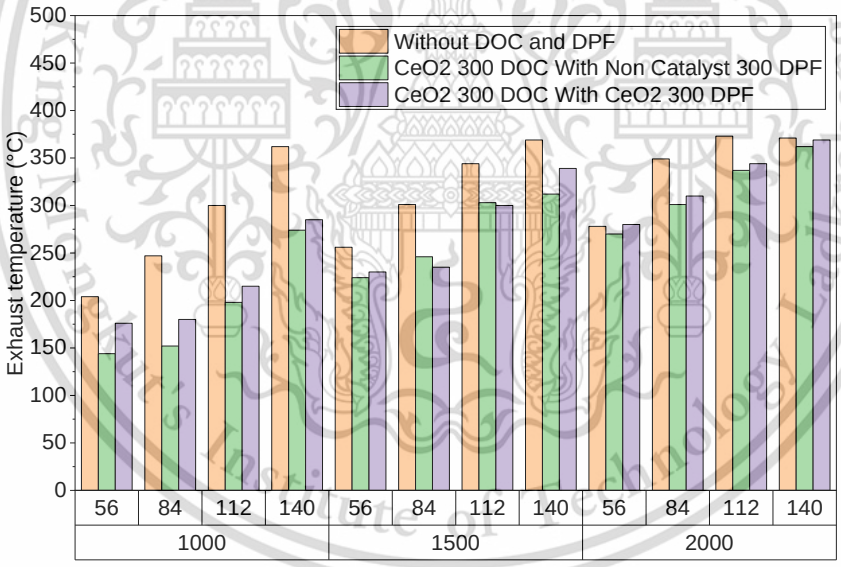

Figure 5.32 Exhaust temperature of diesel engine

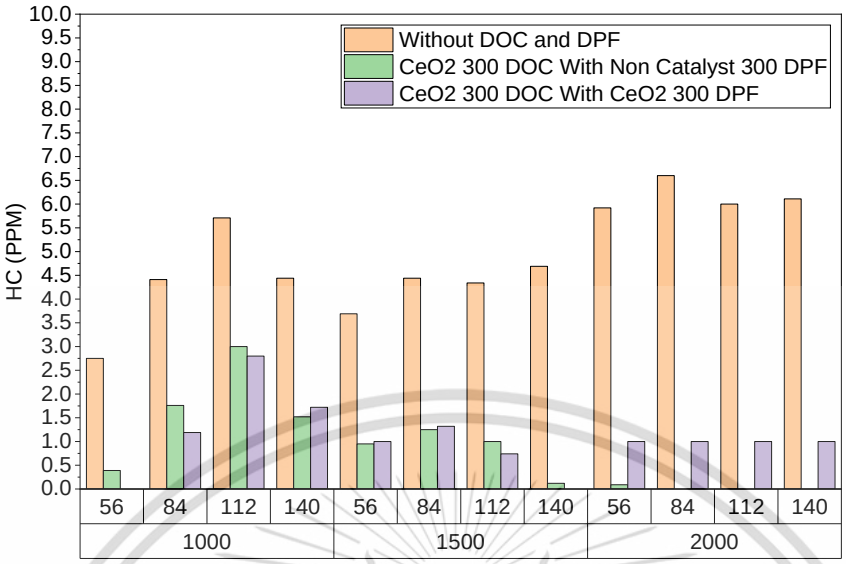

Figure 5.33 HC of diesel engine

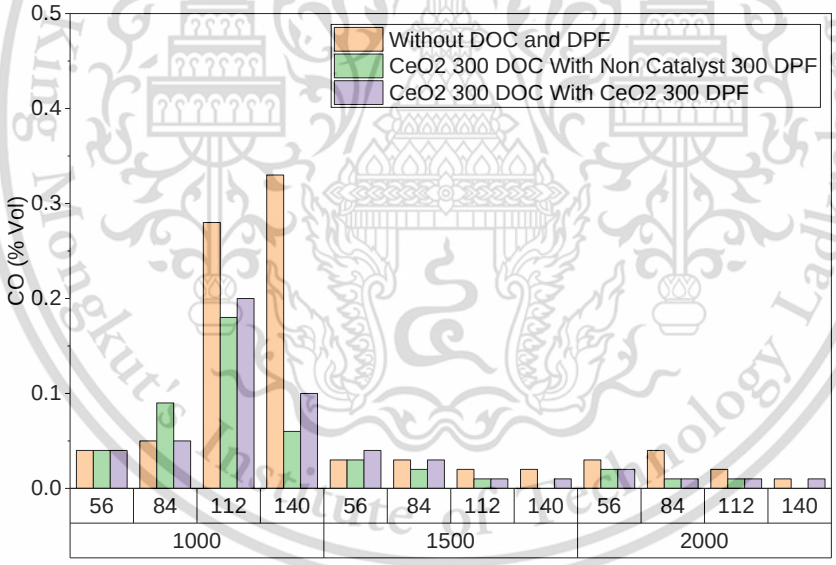

Figure 5.34 CO of diesel engine

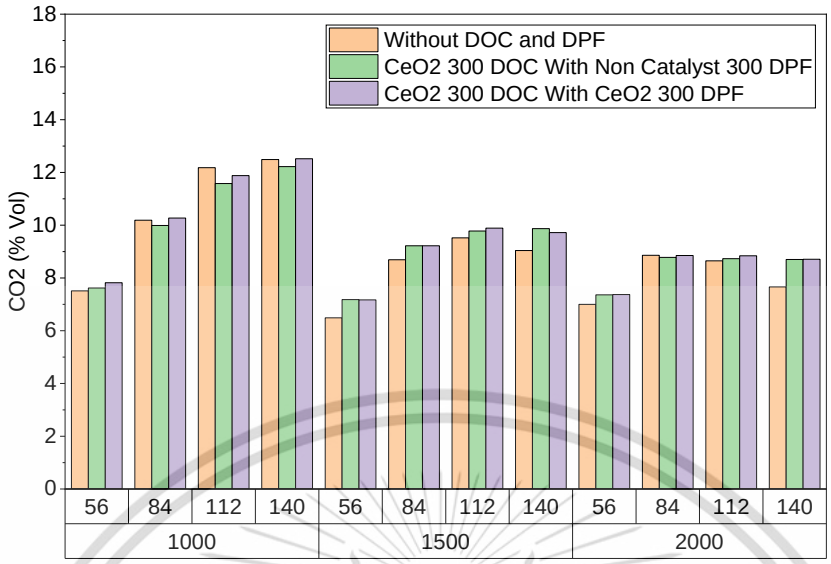

Figure 5.35 CO2 of diesel engine

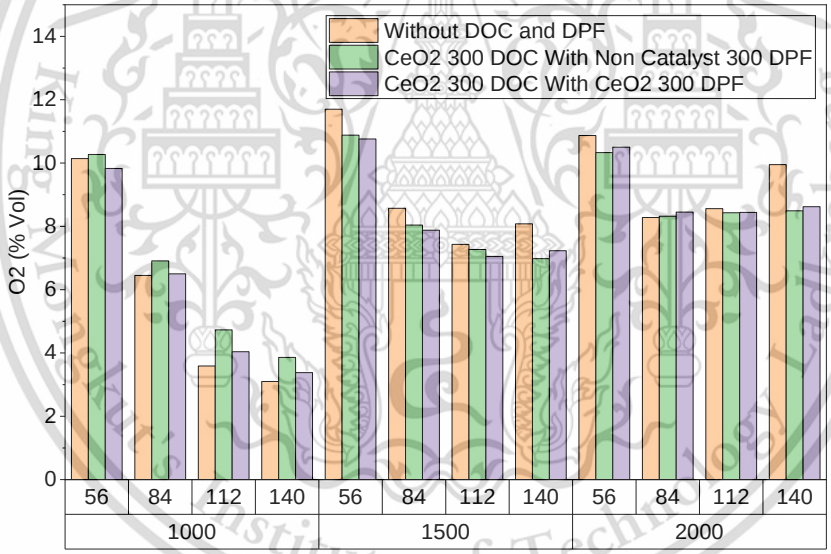

Figure 5.36 O2 of diesel engine

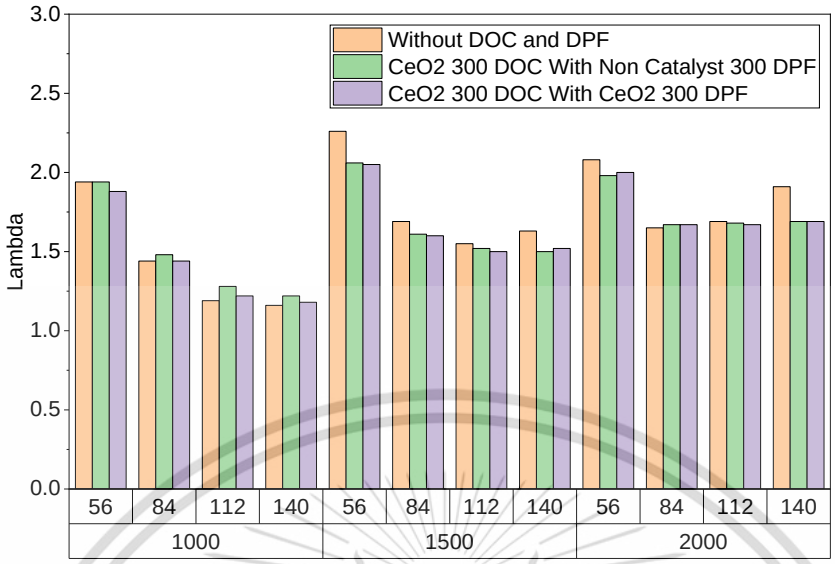

Figure 5.37 Lambda of diesel engine

The amount of CO2 emissions represents in **Figures 5.35** in vol% unit. The CO2 increase with the engine load increasing due to inject more fuel. During the oxidation process, CO2 was generated at the same time. In CeO2 DOC and P-DPF cases at high load conditions, CO2 is increased while O2 reduced, this is because partial of NO2 passive regenerate the soot at a normal engine operation.

The oxygen in the exhaust reduces as the engine load increasing due to more fuel injected into the combustion chamber as indicates in **Figure 5.36**, a greater amount of oxygen in the air is chemically reacted with the fuel. Typically, after diesel combustion, around 10% of oxygen remains in the exhaust. The remaining oxygen will react with hydrocarbons (HC), nitrogen oxides (NO), and carbon monoxide (CO) in the CeO2 catalyst before proceeding to the next stage. In the next stage, the remaining oxygen will react with soot in the partial flow diesel particulate filter (DPF) at a high temperature. The amount of carbon dioxide is opposite with O2 quantity.

Lambda λ indicates air-fuel equivalent ratio that equals to stoichiometric air-fuel ratio divided by the actual air-fuel ratio. From the testing result as show in **Figure 5.37**, all of the testing condition are lean combustion because the test conditions conduct at 20-50% engine load. Lambda decreases with the engine load increasing due to more complete combustion. The lambda is lower with DOC and DPF system due to the back pressure.

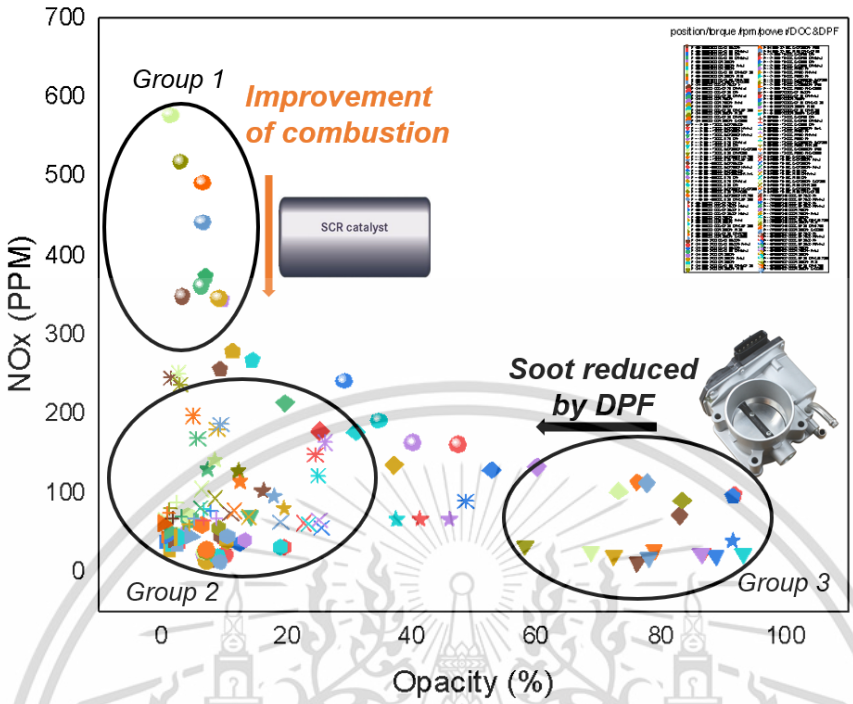

Figure 5.38 NOx and soot analysis

It shows a trade-off between NOx and soot by gathering all testing cases illustrated in **Figure 5.38**. It approximately separate into three groups:

Group 1: Low PMs and high NOx with low torque; 14.66kW-29.32kW (high torque)

Group 2: Low PMs and low NOx; 5.86kW-17.6kW

Group 3: High PMs and low NOx; 11.73kW-22kW (higher torque).

Based on the results of nitrogen and carbon particle tests, higher torque conditions generate a significant amount of thermal-NOx through Zeldovich's Mechanism, but better engine combustion results in less soot. In contrast, incomplete combustion at low engine power conditions results in fewer NOx emissions but more soot. To address these issues, we can design a strategy for the after-treatment system. For example, gasoline engine fuels are premixed to improve combustion, but high temperatures generate NOx emissions, which can be reduced by applying SCR. For diesel engines, incomplete combustion leads to soot production, and we can use the EGR system to lower combustion temperature and the DPF system to trap particulate

matter. Both of these strategies have been successfully applied in commercial vehicles. NOx increases with exhaust temperature up to 375 degree Celsius than goes down as in **Figure 5.39**.

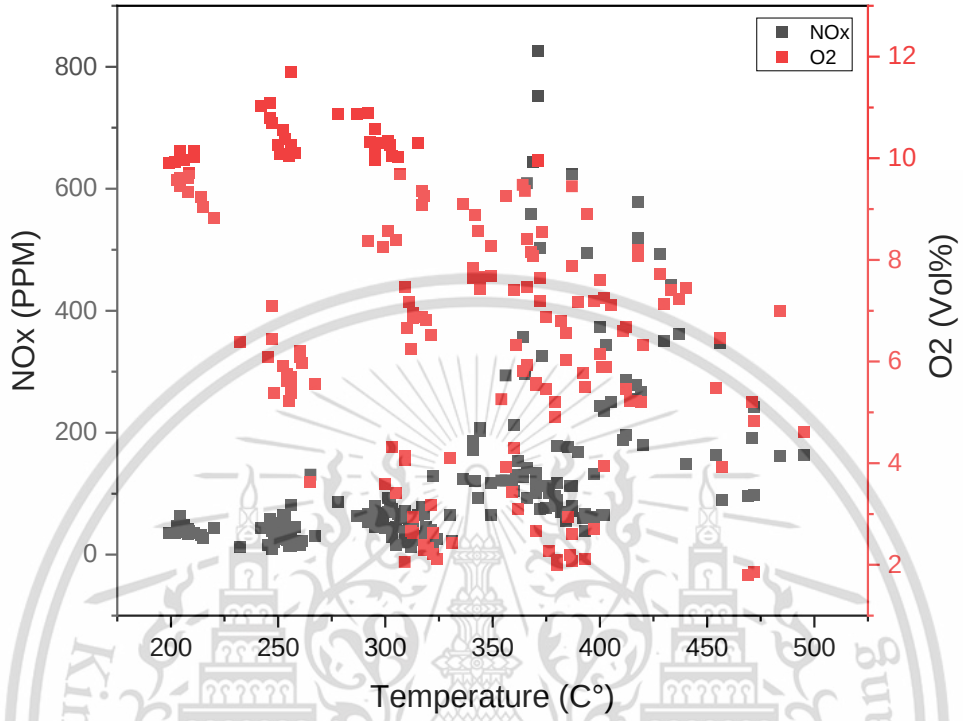

Figure 5.39 NOx and O2 analysis

5.2 Chassis dyno testing

The Pollution Control Department conducted chassis dyno testing on the Toyota Tiger with and without DOC and DPF systems. To replicate actual driving conditions, the test used European standards, with urban driving (Phase 1) limited to a maximum speed of 50km/h and highway driving (Phase 2) limited to a maximum speed of 120km/h. The results showed that the use of DOC and DPF systems led to a 40% reduction in PN, as demonstrated in **Figures 5.41** and **Figure 5.40**, CeO2 DOC with CeO2 DPF proved to be the best case for PN reduction in this experiment.

Figure 5.42 illustrates the average weight of particulate matter, which is the total weight of all sizes of black soot based on Euro standard 4 to 5. The use of DOC and DPF systems reduced the weight of particulate matter by approximately 50%, with CeO2 DPF achieving up to 70%

reduction. This is due to the CeO2 catalyst's ability to reduce the soot regeneration temperature. However, the original DOC only reduced PM by 20%.

HC levels were reduced by around 30% with the after-treatment system, as shown in **Figure 5.43**. However, only the original DOC achieved the best HC reduction rate, as DPF's pressure drop can impact engine performance.

NOx levels decreased by 20% with the use of DOC and DPF systems, as demonstrated in **Figure 5.44**. With a CeO2 catalyst, NO2 can regenerate soot more efficiently at a normal engine operating temperature.

CO levels decreased with the original DOC, as the catalyst promotes the HC reaction with O2. However, DPF may cause a slight increase in CO due to the back pressure, as shown in **Figure 5.45**. The use of DOC and DPF systems had little impact on CO2 levels, as seen in **Figure 5.46**.

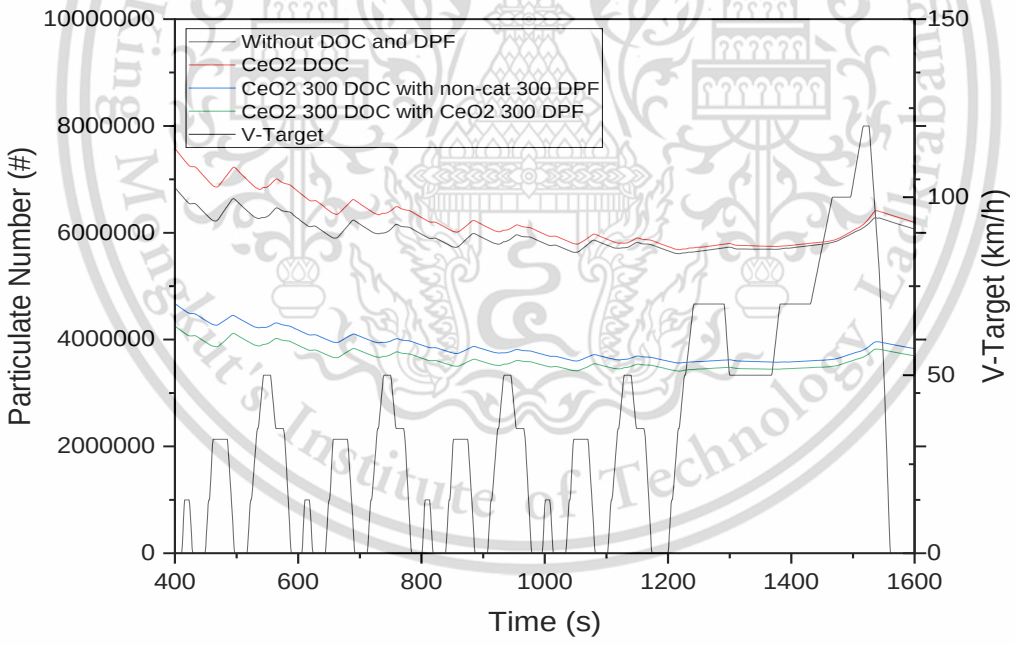

Figure 5.40 Real time particulate number of diesel vehicle

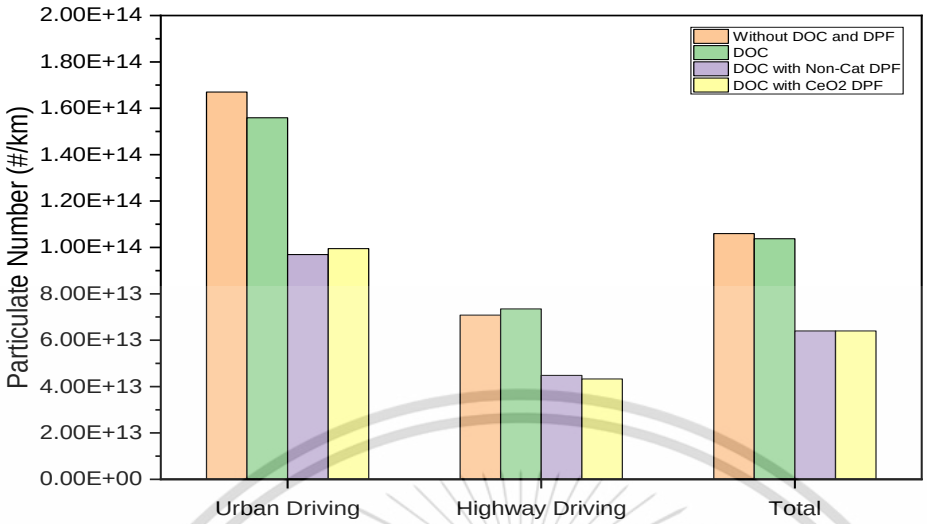

Figure 5.41 Particulate number of diesel vehicle

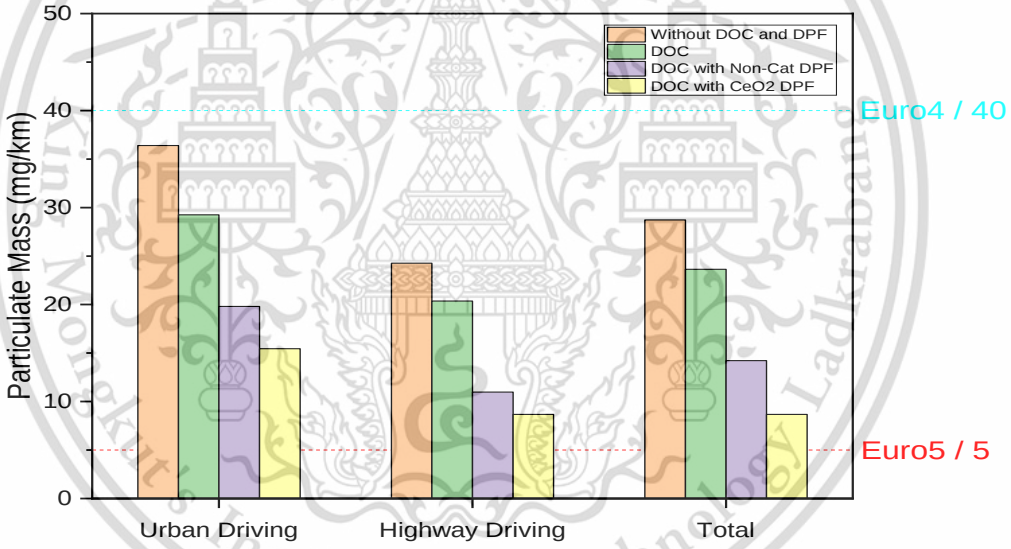

Figure 5.42 Particulate mass of diesel vehicle

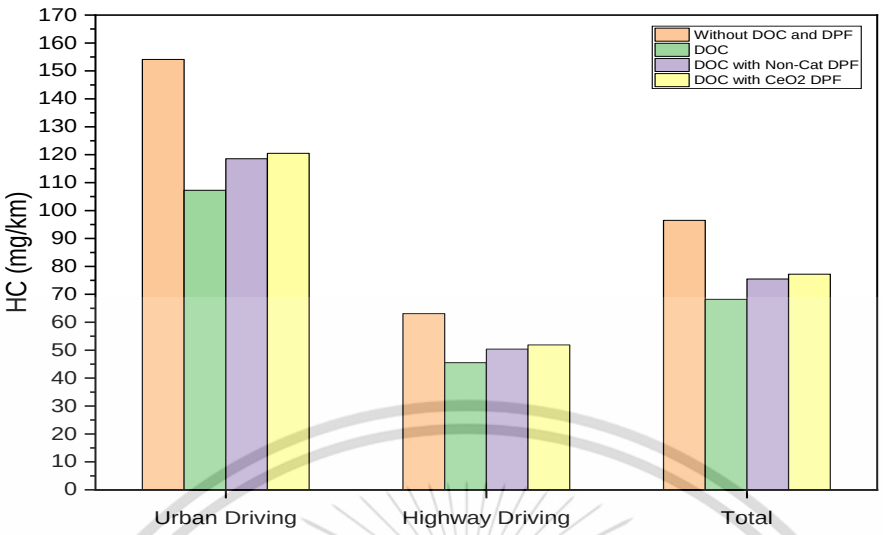

Figure 5.43 Hydrocarbon of diesel vehicle

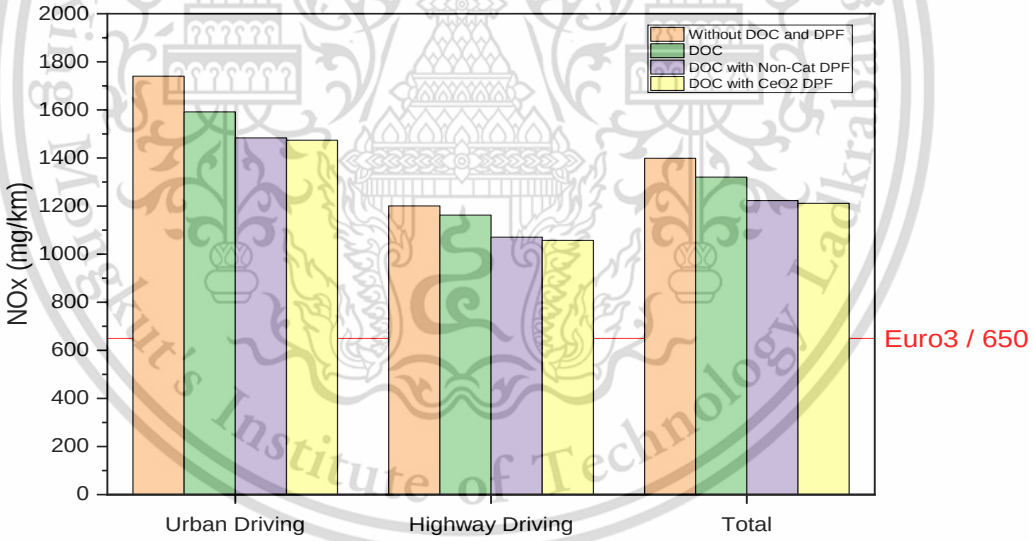

Figure 5.44 NOx of diesel vehicle

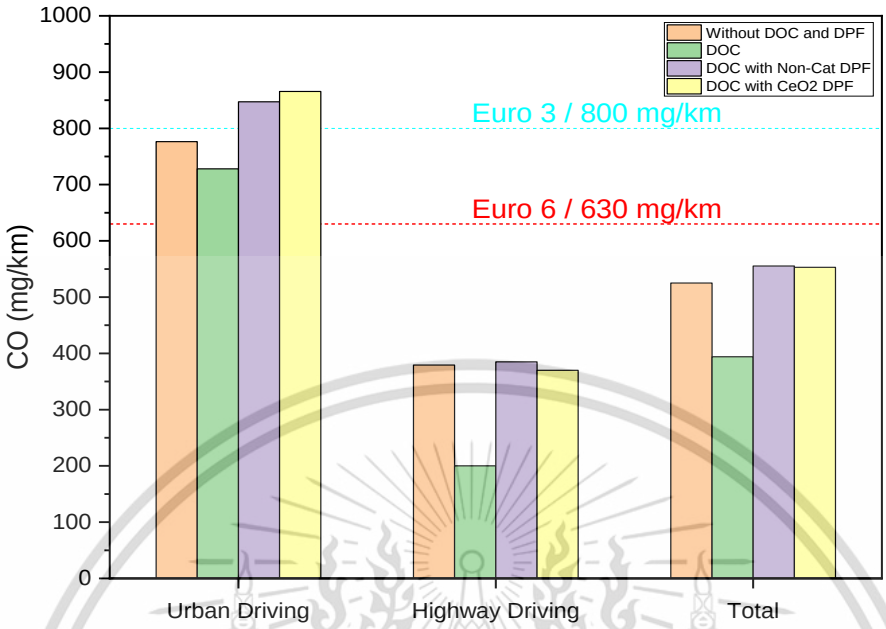

Figure 5.45 Carbon monoxide of diesel vehicle

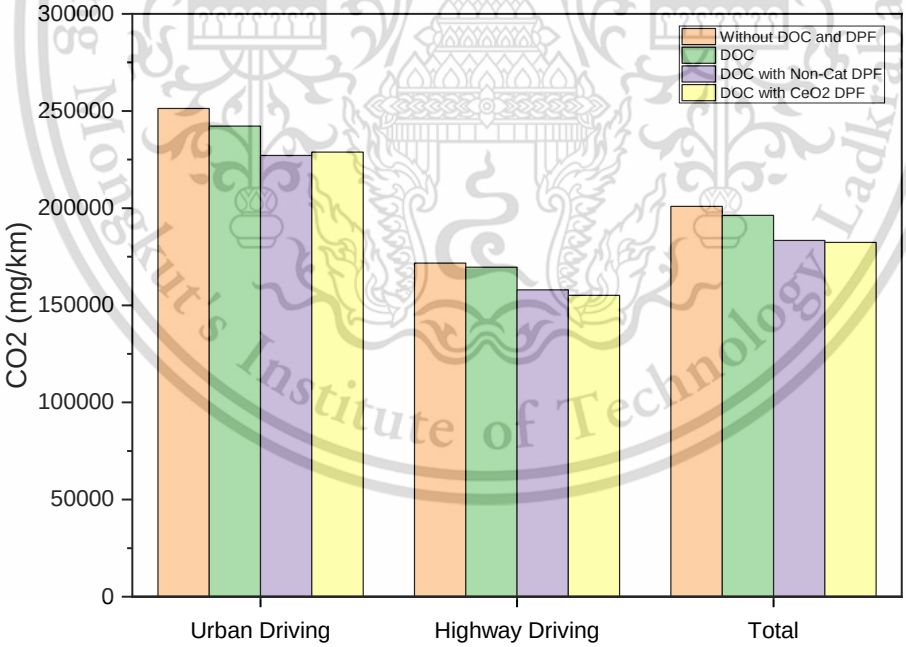

Figure 5.46 Carbon dioxide of diesel vehicle

CONCLUSION

In this study, the effects of catalytic DOC and partial flow DPF systems on combustion characteristics, performance, and emissions were examined. The experiment was conducted on a diesel engine with a three-liter and four-cylinder common rail system using an engine dynamometer. The engine was tested at various loads of 56, 84, 112, and 140 Nm and constant engine speeds of 1000, 1500, and 2000 rpm. The results of the combustion analysis revealed that the maximum pressure and heat release rate increased with increasing engine load but decreased with decreasing engine speed. Furthermore, fuel consumption rate and thermal efficiency increased with increasing engine load and engine speed, whereas specific fuel consumption decreased.

Due to increased back pressure, the CeO2 DOC and DPF systems could reduce NOx by approximately 300 ppm at higher engine loads — the combustion temperature decrease when high-density exhaust gas goes to EGR. Therefore, the NOx decreases, particularly at 140Nm, where there is an increase in CO2 quantity. This suggests that some of the NO2 was passively regenerating the soot that was trapped in the partial-flow DPF. In addition, the CeO2 DOC and DPF systems were able to decrease particulate matters by about 65%. Moreover, after applying the after-treatment systems, there was a substantial reduction in CO and HC. Combustion pressure and crank angle were detected by an in-cylinder pressure sensor and crank angle encoder. From the results, without DPF system, the IET is 4-6% higher than BTE; While with DPF system, ITE is 5-11% higher than BTE owing to the DPF system cause the friction loss increase between 1-6%; the friction loss increases with engine rpm increasing due to more revolution cause more friction work.

The chassis dyno testing of diesel vehicle is the simulation of an actual driving cycle of urban and highway driving. As a result, from the vehicle test at the pollution control department indicate that with DOC and DPF systems, PN was reduced by 4.8E+13/km, PM was reduced by 20.9mg/km, NOx reduces by 182mg/km, and HC decreased by 20mg/km. Comparing a catalytic DPF with a Non-Cat DPF, the PM is 3mg/km lower when applying CeO2 DPF. It has emerged that DOC has a better HC reduction rate of around 5mg/km compared with DPF because DPF leads to more significant back pressure. CO decreased by around 140mg/km with only a DOC system; it could reduce by 200mg/km in highway driving mode.

This study focuses on the pressure drop and filtration efficiency of a 3-litre diesel engine. It was investigated that partial-flow DPF has around 50% lower back pressure than full-flow DPF at the exact geometric condition; meanwhile, the average filtration efficiency is around 30% less. For the 3L engine, the ideal cell density should be set between 200-300 CPSI; the channel length should be 150-230mm; the hydraulic diameter should be designed between 120-240mm.

REFERENCES

[1] Karin, P., Borhanipour, M., Songsaengchan, Y., Laosuwan, S., Charoenphonphanich, C., Chollacoop, N., & Hanamura, K. (2015). Oxidation kinetics of small CI engine's biodiesel particulate matter. International Journal of Automotive Technology, 16(2), 211–219.

[2] SRILOMSAK, M., & HANAMURA, K. (2020). Time‐lapse visualization of shrinking soot in diesel particulate filter during active – regeneration using field emission scanning electron microscopy. Journal of Microscopy, 279(2), 85—97.

[3] Mayer, A., Czerwinski, J., Comte, P., & Jaussi, F. (2009). Properties of Partial-Flow and Coarse Pore Deep Bed Filters Proposed to Reduce Particle Emission of Vehicle Engines. SAE International Journal of Fuels and Lubricants, 2(1), 497–511.

[4] J.P.A. Neeft, M Makkee, J.A. Moulijn, Diesel particulate emission control, Fuel Process. Technol., 47 (1996) 1.

[5] Strzelec A., Vander Wal R.L., Thompson T., Toops T. and Daw C., "NO2 oxidation reactivity and burning mode of diesel particulates," Top Catal 2016; 59: 686–694.

[6] Kim, J. K., Kim, W. G., & Kim, Y. K. (2011). A Study of HDD Performance Improvement through Filter Driver & NAND FLASH Memory. The Journal of the Korean Institute of Information and Communication Engineering, 15(8), 1635–1641.

[7] TOYAMA, S., MORI, H., & SUZUKI, M. (1987). FLOW PATTERNS THROUGH TUBE BUNDLES AND PARTICULATE FOULING ONTO CYLINDERS. Particulate Science and Technology, 5(4), 397–408.

[8] Karin, P., & Hanamura, K. (2010). Particulate Matter Trapping and Oxidation on a Catalyst Membrane. SAE International Journal of Fuels and Lubricants, 3(1), 368–379.

[9] Das, R., Madhusoodana, C., Purushothama, M., Paramesh, S. et al., "Development and Field Test of Ceramic-based Diesel Particulate Filter (DPF) for Urban Transport Vehicle," SAE Technical Paper 2003-26-0004, 2003.

[10] Lehmann, F., Torres, R., and Park, S., "EMISSION STUDY OF AN EURO 5 DIESEL ENGINE OPERATING ON BIODIESEL BLENDS," SAE Technical Paper 2012-36-0168, 2012.

[11] Amanatidis, S., Ntziachristos, L., Samaras, Z., Kouridis, C. et al., "Use of a PPS Sensor in Evaluating the Impact of Fuel Efficiency Improvement Technologies on the Particle Emissions of a Euro 5 Diesel Car," SAE Technical Paper 2014-01-1601, 2014.

[12] Key world energy statistics. Int. Eng. Agency (IEA), 2020, https://www.iea.org/reports/key-world-energy-statistics-2020.

[13] Key energy statistics, Thailand. Int. Eng. Agency (IEA), 2019.

[14] Energy Balance of Thailand Report, 2020.

[15] C. ChooChuay, S. Pongpiachan, D. Tipmanee, O. Suttinun, W. Deelaman, Q. Wang, L. Xing, G. Li, Y. Han, J. Palakun and J. Cao, "Impacts of PM2.5 sources on variations in particulate chemical compounds in ambient air of Bangkok, Thailand.", Atmospheric Pollution Research, Vol. 11(9), pp. 1657-1667, 2020.

[16] Zielinska, B., Sagebiel, J., Arnott, W. P., Rogers, C. F., Kelly, K. E., Wagner, D. A., ... & Palmer, G. (2004). Phase and size distribution of polycyclic aromatic hydrocarbons in diesel and gasoline vehicle emissions. Environmental Science & Technology, 38(9), 2557-2567.

[17] May, A. A., Nguyen, N. T., Presto, A. A., Gordon, T. D., Lipsky, E. M., Karve, M., ... & Robinson, A. L. (2014). Gas-and particle-phase primary emissions from in-use, on-road gasoline, and diesel vehicles. Atmospheric Environment, 88, 247-260.

[18] R. Zhu, C. S. Cheung, Z. Huang and X. Wang, "Regulated and unregulated emissions from a diesel engine fueled with diesel fuel blended with diethyl adipate," Atmospheric Environment, vol. 45, p. 2174–2181, April 2011.

[19] 龚金科. 汽车排放及控制技术. 北京: 人民交通出版社, 2007, 23-29.

[20] 王桂华, 陆家祥, 陆辰, 等. WD615.67 型柴油机常态排气微粒成分试验测定及分析, 内燃机学报, 2000, 18(4):161-164.

[21] 谭丕强, 胡志远, 楼狄明, 柴油机捕集器结构参数对不同粒径微粒过滤特性的影响, 机械工程学报, 2008, 44(2):175-181.

[22] 刘巽俊, 内燃机的排放与控制. 北京:机械工业出版社, 2005, 6-10.

[23] Walsh, M. (1989). Worldwide Developments in Motor Vehicle Diesel Particulate Control. SAE International Congress and Exposition.

[24] Höök, M., Fantazzini, D., Angelantoni, A., & Snowden, S. (2014). Hydrocarbon liquefaction: viability as a peak oil mitigation strategy. Philosophical Transactions of the Royal Society A, 372(2006), 20120319.

[25] Kaneko, T., Derbyshire, F., Makino, E., Gray, D., & Tamura, M. (2001). Coal Liquefaction. Ullmann's Encyclopedia of Industrial Chemistry.

[26] Alternative Fuels Data Center Fuel Properties Comparison. United States: N. p., 2021. Web.

[27] Bhadra, B.N.; Song, J.Y.; Uddin, N.; Khan, N.A.; Kim, S.; Choi, C.H.; Jhung, S.H. Oxidative denitrogenation with TiO2@porous carbon catalyst for purification of fuel: Chemical aspects. Appl. Catal. B Environ. 2019, 240, 215–224.

[28] Mirante, F.; Mendes, R.F.; Paz, F.A.A.; Balula, S.S. High Catalytic Efficiency of a Layered Coordination Polymer to Remove Simultaneous Sulfur and Nitrogen Compounds from Fuels. Catalysts 2020, 10, 731.

[29] Prado, G.H.C.; Rao, Y.; de Klerk, A. Nitrogen Removal from Oil: A Review. Energy Fuels 2016, 31, 14–36.

[30] Wang, B.; Zheng, P.; Fan, H.; Meng, Q.; Duan, A.; Chen, Z.; Xu, C. Insights into the effect of solvent on dibenzothiophene hydrodesulfurization. Fuel 2021, 287, 119459.

[31] Paucar, N.E.; Kiggins, P.; Blad, B.; De Jesus, K.; Afrin, F.; Pashikanti, S.; Sharma, K. Ionic liquids for the removal of sulfur and nitrogen compounds in fuels: A review. Environ. Chem. Lett. 2021, 19, 1205–1228.

[32] Angelici, R.J. Hydrodesulfurization & Hydrodenitrogenation. In Encyclopedia of Inorganic Chemistry; John Wiley & Sons, Inc.: Hoboken, NJ, USA, 2005.

[33] Li, H.; Jiang, X.; Zhu, W.; Lu, J.; Shu, H.; Yan, Y. Deep Oxidative Desulfurization of Fuel Oils Catalyzed by Decatungstates in the Ionic Liquid of [BMIM]PF6. Ind. Eng. Chem. Res. 2009, 48, 9034–9039.

[34] Shiraishi, Y.; Tachibana, K.; Hirai, T.; Komasawa, I. Desulfurization and Denitrogenation Process for Light Oils Based on Chemical Oxidation followed by Liquid-Liquid Extraction. Ind. Eng. Chem. Res. 2002, 41, 4362–4375.

[35] Yao, Z.; Miras, H.N.; Song, Y.-F. Efficient concurrent removal of sulfur and nitrogen contents from complex oil mixtures by using polyoxometalate-based composite materials. Inorg. Chem. Front. 2016, 3, 1007–1013.

[36] Julião, D.; Gomes, A.C.; Pillinger, M.; Gonçalves, I.S.; Balula, S.S. Desulfurization and Denitrogenation Processes to Treat Diesel Using Mo(VI)-Bipyridine Catalysts. Chem. Eng. Technol. 2020, 43, 1774–1783.

[37] Gao, Y.; Mirante, F.; de Castro, B.; Zhao, J.; Cunha-Silva, L.; Balula, S.S. An Effective Hybrid Heterogeneous Catalyst to Desulfurize Diesel: Peroxotungstate@Metal-Organic Framework. Molecules 2020, 25, 5494.

[38] 王天友, 林漫群, 等. 燃油催化微粒捕集器微粒捕集与强制再生特性的研究. 内燃机学报, 2007,25(6): 527-531.

[39] 刘明安, 潘克煜, 含氧燃料添加剂对柴油机微粒排放的影响. 空军工程大学学报 (自然科学版), 2006, 5 (3): 71-74.

[40] 孙跃东, 周萍, 邹敏, 等. 含氧添加剂对单缸柴油机性能影响的研究. 武汉理工大学学报, 2007, 29 (2): 33-36.

[41] 闫淑芳, 宫长明, 刘巽俊. 喷油压力对直喷式柴油机性能和排放的影响. 吉林大学学报 (工学版), 2002, 32 (7): 53-56.

[42] 汪洋, 苏万华, 谢辉, 等. 共轨蓄压式电控喷射系统的喷油规律对发动机燃烧特性及排放性能的影响. 内燃机学报, 2002, 20 (3): 200-204.

[43] 张艳. 高压共轨柴油机电控系统的研究. [北京交通大学硕士学位论文], 北京: 北京交通大学机械与电子控制工程学院, 2006, 5-9.

[44] 胡朝阳. 电控共轨喷射系统降低柴油机排放的试验研究. [大连理工大学硕士学位论文], 大连: 大连理工大学能源与动力学院, 2008,50-54.

[45] 李金武. 4102BZLQ 型增压中冷柴油机颗粒排放的研究. [天津大学硕士学位论文], 天津: 天津大学机械工程学院, 2003, 26-53.

[46] 赵昌普, 宋崇林, 李晓娟, 等. 喷油定时和燃烧室形状对柴油机燃烧及排放的影响. 燃烧科学与技术, 2009, 15 (5): 393-398.

[47] 焦运景, 张惠明, 田远, 等. 直喷式柴油机燃烧室几何形状对排放影响的多维数值模拟研究. 内燃机工程, 2007, 28 (4): 11-15..

[48] 郑乃金. 汽车排放控制发展趋势, 汽车技术, 1996, (4): 47-49.
[49] 裘金科. 汽车排放污染及控制. 北京: 人民交通出版社, 2005: 80-81.
[50] Gharahbaghi S, Wilson T S, Xu H， et al. Modelling and experimental investigations of supercharged HCCI Engines, SAE Paper 2006-10-0634.
[51] Shi L, Cui Y, Deng K, et al. Study of low emission homogeneous charge compression ignition (HCCI) engine using combined internal and external exhaust gas recirculation (EGR). Energy, 2006, 31(14): 2665-2676.
[52] Kim D S， Lee C S. Improved emission characteristics of HCCI engine by various premixed fuels and cooled EGR Fuel, 2006, 85(5-6): 695-704.
[53] 尧命发, 张波, 郑尊清, 等. 废气再循环与燃料辛烷值对均质压燃发动机性能和排放影响的试验研究. 2006, 24 (1): 15-21.
[54] 侯玉春. 燃料设计控制 HCCI 燃烧与排放的试验研究. [上海交通大学博士学位论文], 上海: 上海交通大学机械与动力工程学院, 2007, 50-86.
[55] 曾文, 解茂昭, 贾明. 催化燃烧对均质压燃发动机排放影响的数值模拟. 燃烧科学与技术, 2007, 13 (1): 55-62.
[56] Kalghatgi G T, Risberg P, Angstrom H E. Partially premixed auto-ignition of gasoline to attain low smoke and low NOx at high load in compression ignition engine and comparison with a diesel fuel. SAE Paper 2007-01-0006.
[57] 刘永志. 柴油燃烧微粒形成、演化及物理特性研究，天津大学硕士学位论文，天津: 天津大学机械工程学院, 2009, 31-41.
[58] Khajepour, A., Fallah, M. S., & Goodarzi, A. (2014). Electric and hybrid vehicles: technologies, modeling, and control: a mechatronic approach. Choice Reviews Online, 52(04), 52–2009.
[59] EnggStaff. (2020, February 3). 4 Stages of combustion in CI engine. EnggStudy. https://www.enggstudy.com/stages-of-combustion-in-ci-engine/#Final_Words.
[60] J. Heywood, Internal Combustion Engine Fundamentals 2E, McGraw Hill Professional, 2018.
[61] What Is a Diesel Oxidation Catalyst? | Nett Technologies. (2020, June 9). Nett Technologies.
[62] Khair, M. K. (2003). A Review of Diesel Particulate Filter Technologies. SAE Technical Paper Series.

[63] L. Soler, A. Casanovas, C. Escudero, V. Pérez-Dieste, E. Aneggi, A. Trovarelli and J. Llorca, "Ambient pressure photoemission spectroscopy reveals the mechanism of carbon soot oxidation in ceria-based catalysts," Chemcatchem, vol. 8, no. 17, pp. 2748-2751, 2016.

[64] Siedlecki M, Szymlet N, Sokolnicka B. Influence of the Particulate Filter Use in the Spark Ignition Engine Vehicle on the Exhaust Emission in Real Driving Emission Test. Journal of Ecological Engineering. 2020;21(1):120-127.

[65] Zelenka, P., Telford, C., Pye, D., & Birkby, N. (2002b). Development of a Full-Flow Burner DPF System for Heavy Duty Diesel Engines.

[66] 段家修, 龚晓辉, 许斯都, 等. 柴油机微粒过滤器电加热再生技术的实验研究, 内燃机学报, 1999, 17 (1): 22-26.

[67] Arai, M., Saito, M., & Mitsuyama, Y. (2007). Continuous regeneration of an electrically heated diesel particulate trap. International Journal of Engine Research, 8(6), 477–486.

[68] Nixdorf, R. W., Green, J. B., Story, J., & Wagner, R. (2001). Microwave-Regenerated Diesel Exhaust Particulate Filter. SAE Technical Paper Series.

[69] Zhang-Steenwinkel, Y., Van Der Zande, L. M., Castricum, H. L., Bliek, A., Van Den Brink, R., & Elzinga, G. (2005). Microwave-assisted in-situ regeneration of a perovskite coated diesel soot filter. Chemical Engineering Science, 60(3), 797–804.

[70] Smayda, T. J. (2008). Complexity in the eutrophication–harmful algal bloom relationship, with comment on the importance of grazing. Harmful Algae, 8(1), 140–151.

[71] Harle, V., Pitois, C., Rocher, L., & Garcia, F. (2008). Latest Development and Registration of Fuel Borne Catalyst for DPF Regeneration. SAE World Congress & Exhibition.

[72] Simon, G., & Stark, T. L. (1985). Diesel Particulate Trap Regeneration Using Ceramic Wall-Flow Traps, Fuel Additives, and Supplemental Electrical Igniters. SAE Transactions.

[73] Barlow, J.B., W.H. Rae, and A. Pope, Low-Speed Wind Tunnel Testing. Third ed. 1999: John Wiley & Sons.

[74] White, F.M., Fluid Mechanics. Fourth ed. 2010: McGraw-Hill.

APPENDIX A

TEST RESULTS

FOCUSLAB Fluid & Oil Analysis Technology

ISO 9001 : 2015 Certified

Focuslab Ltd

Customer Code : 20010
Customer Name : KMITL
Address : 3 Moo 2, Chalongkrung Road
Ladkrabang
Bangkok 10520

Test Code : 811A

Sample Information

Unit ID /
Sample Information Identification : **B10**
Unit type : FUEL
Oil type : DIESEL B10
Sampling Date : 22-Jun-21
Recieved Date : 22-Jun-21

Test Report Sample No 21063747

Test Description	Test Method	Test Result	Limit (a)
Apperance			
Color	Visual Inspection	Bright and Clear	Bright and Clear
Diesel Fuel			
Density at 15 C , g/cm^3	ASTM D4052	0.835	0.81 - 0.87
Cetane Index	ASTM D976	54.9	Min 50
Distillation , C	ASTM D86		
Initial Boiling Point		180.0	-
90%vol. Recovered		344.2	Max 357
Flash Point	ASTM D93	66.0	Min 52
Fatty Acid Methyl Ester, %vol	EN 14078	10.2	9 - 10
Pour Point , °C	ASTM D97	0.0	Max 10
Flow Properties			
Viscosity at 40 C , cSt	ASTM D445	3.0	1.8 - 4.1
Cleanliness			
Total Contamination , mg/kg	EN 12662	6.2	Max 24.0
Micro Carbon Residue (MCR) , %mass	ASTM D4530	<0.01	Max 0.3
Ash , %wt	ASTM D482	<0.001	Max 0.010
Total Sulfur Content , mg/kg	ASTM D5453	24.4	Max 50
Water Content , mg/kg	ASTM D6304	691	Max 200
Water and Sediment , %Vol.	ASTM D2709	<0.01	Max 0.05

Interpretation of the Test Result
- Test results are based on received fuel sample , submitted and identified by client.
- Data is provided above.

Recommendation
- No recommendation for R&D.

Remark
(a) Diesel fuel is from Thailand Diesel Specification - MOE - 2563

Tested and Issued By

Kanjana K.
Lab Technologist

Approved and Authorised by

Somchai J.
Machine Lubricant Analyst

2/57 Bangna Complex Office Tower, 12 th Fl , Soi Bangna- Trad 25, North Bangna, Bangna, Bangkok 10260, Thailand
http://www.focuslab.co.th
Tel : (66 2) 3618600-3 Fax : (66 2) 3618567

FL-6.7

Customer Code	: 20010	Sample Information		
Customer Name	: KMITL	Unit ID /		
Address	: 3 Moo 2, Chalongkrung Road Ladkrabang Bangkok 10520	Sample Information Identification	:	**B10**
		Unit type	:	FUEL
		Oil type	:	not given
		Sampling Date	:	22-Jun-21
		Recieved Date	:	22-Jun-21
Test Code	: 811A			

B10

Good and Qualified Diesel Fuel

FOCUSLAB™ Fluid & Oil Analysis Technology

ISO9001:2015 Certified

FocusLab Ltd.

CUSTOMER

Code : **20010**
Name : **KMITL**
Address : 3 Moo 2, Chalongkrung Road
Ladkrabang
Bangkok 10520
Site :
Location :
Test code : 601.200 60400 611.4

EQUIPMENT

Unit ID : **DIESEL B10**
Unit Type : FUEL
Unit Make : (not given)
Unit Model : (not given)

OIL

Oil type / Viscosity : DIESEL B10
Oil System Capacity :

Notes (Finding, Evaluation, Interpretation, Suggestion and Recommendation)

Data is provided below.

Somchai J.

Condition History	Test Method	Result	Current Sample Wear Oil Cont.	Previous Sample	Baseline and Alarm Limit
					BASELINE: Alarm Limit — Alarm Limit Matrix -Set Name (Equipment type / oil type) — No Interpretation Required
Lab ID			20091079		
Bottle ID			701419		
Date Sampled			03-Sep-20		
Oil Hours (Kms)			Not Given		
Unit Hours (Kms)			Not Given		
Oil Change					
Oil Added (Liters)					
Filters Hours (Kms)					
Wear Condition					Reference Oil (RO) / Fine Wear (ICP) U-Caution U-Warning / Coarse Wear (RFS) U-Caution U-Warning
Wear Element	Method	Unit	Fine Wear (ICP-AES) / Coarse Wear (RFS-AES)		
Iron	D-5185	PPM	0.0		
Chromium	D-5185	PPM	0.0		
Lead	D-5185	PPM	0.1		
Copper	D-5185	PPM	0.0		
Tin	D-5185	PPM	0.1		
Aluminum	D-5185	PPM	0.4		
Nickel	D-5185	PPM	0.0		
Silver	D-5185	PPM	0.0		
Molybdenum	D-5185	PPM	0.0		
Titanium	D-5185	PPM	0.0		
PQ Index	D-8184	Index			
Oil Condition					RO L-Warning L-Caution U-Caution U-Warning
Viscosity @ 40°C	D-445	cSt	2.7		
Viscosity @ 100°C	D-445	cSt			
Oxidation	D-7414	Abs			
Nitration	D-7624	Abs/cm			
Acid Number	D-974	mg KOH/g			
Contamination					RO U-Caution U-Warning
Water	D-6304	% (Wt.)			
Sodium	D-5185	PPM	0		
Silicon	D-5185	PPM	0.2		
Additive Element					RO
Boron	D-5185	PPM	0		
Magnesium	D-5185	PPM	0		
Calcium	D-5185	PPM	0		
Barium	D-5185	PPM	0		
Phosphorus	D-5185	PPM	1		
Zinc	D-5185	PPM	0		
Additional Test					RO L-Caution L-Warning U-Caution U-Warning
Flash Point	D-3828	°C			
Viscosity Index	D-2270				
Flash Point	D-93	°C	65		

Note: Alarm Limits are variable and dependent upon dataset size and to be used as general guideline.
No Sign or N : NORMAL , C or C : CAUTION (first level warning limit) , W or W : Warning (second level warning limit)
Accuracy of interpretation and recommendation are based on representatives sample and information supplied. No warranty is expressed or implied for this report.

Analysis Report

Sample	Biodiesel
Sample owner	King Mongkut's Institute of Technology Ladkrabang
Objective	To analyse heating value of combustion
Instrument	Automatic Bomb Calorimeter ; Leco model AC - 500
Job ID	640707-9246
Analysis Date	July 28, 2021

Results

Sample name	Heating value of combustion (MJ/kg)		
	#1	#2	Average
Biodiesel B7	45.26	45.24	45.25
Biodiesel B10	45.80	45.46	45.63
Biodiesel B20	44.89	45.01	44.95
Biodiesel B100	39.84	40.03	39.94
Biodiesel B20E5	43.90	43.99	43.95
Biodiesel B20E10	42.66	42.78	42.72
Biodiesel B20E20	40.61	40.45	40.53

(Mrs. Aree Limnirandorn)

Analyst

EagerSmart Summarize Results

Date : 11/08/2021 at 15:52:41
Method Name : CHNS
Method Filename : CHNS.mth

Group No : 1 Sample Name	Element % Nitrogen	Carbon	Hydrogen	Sulphur
B100_1	0	76.40828705	12.38687801	0
B100_4	0	77.04006958	12.53007603	0
B20_2	0	82.24542999	13.38155937	0
B20_3	0	82.98455048	13.52551937	0
B10_1	0	84.58450317	13.53221703	0
B10_2	0	84.74507141	13.58557034	0

6 Sample(s) in Group No : 1

Component Name	Average	Std. Dev.	% Rel. S. D.	Variance
Nitrogen	0	0.00000	0.0000	0.0000
Carbon	81.33465195	3.70018	4.5493	13.6913
Hydrogen	13.15697002	0.54714	4.1586	0.2994
Sulphur	0	0.00000	0.0000	0.0000

APPENDIX B

PUBLICATION

ICERE 2022

School of Environmental Science and Technology
(Hanoi University of Science and Technology) Vietnam

February 25-27, 2022

CONTACT

Tel: +86-(0)28-88220101
Mobile: +86-15908122414

Conference Secretary: Ms. Alice Lin
icere@ieet.ac.cn

http://www.icere.org/

SUBMISSION METHOD

★ Online Submission System:
http://confsys.iconf.org/submission/icere2022

★ Email:icere@ieet.ac.cn

CALL FOR PAPER

Topics of interest for submission include, but are not limited to:

Session A: Energy Science and Technology

- (01) Development and Utilization of Solar Energy
- (02) Development and Utilization of Biomass Energy
- (03) Development and Utilization of Wind Energy

Session B: Environmental Science and Engineering

- (1) Environmental Chemistry and Biology
- (2) Environmental Materials
- (3) Environmental Safety and Health

Session C: Motivation, Electrical Engineering and Automation

- (1) Engineering Thermophysics
- (2) Thermal Engineering
- (3) Power Machinery and Engineering

Session D: The Development and Utilization of Resources

- (1) Mineral Prospecting and Exploration
- (2) Mining Engineering
- (3) Mining Machinery Engineering

CONFERENCE INTRODUCTION

ICERE 2022 is supported by School of Environmental Science and Technology (Hanoi University of Science and Technology), Vietnam, VNU-University of science and Beijing CAS Industrial Energy and Environment Technology Institute. As a leader in the global trend of scientific and technological innovation, China is creating an increasingly open environment for scientific and technological innovation, expanding the depth and breadth of academic cooperation, and building an innovation community. These efforts have made new contributions to advancing globalization and building a community with a shared future for mankind. In order to adapt to the changes of the world and the rapid development of China in the new era, the 2022 8th International Conference on Environment and Renewable Energy (ICERE 2022) will be held during February 25-27, 2022 in School of Environmental Science and Technology (Hanoi University of Science and Technology), Vietnam. The conference aims to facilitate the exchange of the latest and advanced information among scientists and engineers in a wide range of fields such as "environment" and "renewable energy". In particular, the Forum aims to promote exchanges and cooperation between basic researchers and those engaged in the development of practical technologies in related fields such as environment and renewable energy.

PAPER PUBLICATION

For papers submitted to ICERE 2022, after the peer reviewing process by at least 2-3 experts, the accepted papers will be published into International Conference Proceeding, which is indexed by **EI Compendex**, **Scopus**, Thomson Reuters (WoS), Inspec,et al.

IMPORTANT DATE

Paper Submission	Before January 31, 2022
Notification of Acceptance	Before February 15, 2022
Authors' Registration	Before February 25, 2022
Conference Dates	February 25-27, 2022

Reduction of Diesel Engine's Particulate Matters using Retrofit CeO_2 Diesel Oxidative Catalyst and Partial Flow Diesel Particulate Filter System

Reduction of Diesel Engine's Particulate Matters using Retrofit CeO_2 Diesel Oxidative Catalyst and Partial Flow Diesel Particulate Filter System

Hai Liu*[1], Chinda Charoenphonphanich[1], Preechar Karin[1], Mek Srilomsak[1], Sompong Srimanosaowapak[2], Katsunori Hanamura[3].

1 School of Engineering, King Mongkut's Institute of Technology Ladkrabang, Bangkok, 10520, Thailand
2 National Metal and Materials Technology Center, National Science and Technology Development Agency, Pathum Thani 12120, Thailand
3 School of Engineering, Tokyo Institute of Technology, Tokyo, 152-8552, Japan
E-mail: 63601186@kmitl.ac.th

Abstract. In this research, CeO2 was chosen for the DOC catalyst. Moreover, a partial-flow DPF was installed after DOC. The exhaust gas experiment was conducted at 20% - 50% engine load varying 1000,1500, and 2000 rpm of engine speed. The research results show that NOx reduced around 25% with CeO2 DOC and DPF systems at higher engine load. On the other hand, particulate matters decrease around 65% after CeO2 DOC and DPF systems. Furthermore, CO and HC amount were substantially reduced after applying after-treatment systems. According to fuel consumption, BSFC, and BTE results, the after-treatment system has no significant impact on engine performance.

1. Introduction

In recent years, the diesel engine has developed widely in passenger cars, trucks, buses, heavy equipment in construction generators in buildings and industrial plants due to thermal efficiency, engine performance, and lifetime in different purposes. The diesel engine is in a non-homogeneous combustion processing because diesel fuel is directly injected into the combustion chamber. There are high quantities of emission particles called soot or PMs coming from non-homogenous combustion. Incomplete combustion is the beginning of pollutants, particles of soot that consist mainly of carbon in solid phase mixed with other components such as minor ash of metals from the additive lubricants and unburned hydrocarbon fuels condensed on the surface of carbon soot in a liquid phase. We should remove the particulate matter from the exhaust gas emitted from diesel engines to protect the environment and human health. Therefore, regulation of vehicle emissions has become increasingly strict [1,2,3]. During the non-homogeneous combustion NOx, HC, CO, SOF are generated simultaneously. Thus, the diesel engine after-treatment system adopts a variety of purification technology integrated systems, of which the diesel vehicle oxidation catalytic DOC technology is an important part [4]. The traditional three-way catalytic technology cannot effectively play the role of purification. DOC with catalyst can oxidize the toxic exhaust gas to eco-friendly gas. Pt, Pd, and Ce are typically chosen for DOC. In this article, CeO_2 was selected for DOC, the catalyst requires a low-temperature performance and sulphur resistance. Another essential issue with removing carbon particulate matter from the diesel exhaust gas is a challenging and relevant topic in automotive catalysis and engineering. The emission standards are tightened worldwide, whereas the intensive engine development and optimization programmer will

probably not result in the required reduction of emissions [5]. The particle filter DPF is used to capture and oxidize exhaust particles. Diesel particulate filters are used in vehicles to decrease the amount of particulate matter emitted by diesel engines. An efficiently working DPF is subjected to soot accumulation and periodic filter regeneration by soot oxidation [6,7,8].

After-treatment technology is designed to trap and disperse polluting soot particles into CO_2, automatically coupled with an electronic engine control system. This technology is used in developed countries where enforced pollution control laws: Euro 5 and above, such as European countries, Japan and America. Nevertheless, there is a standard equivalent to Euro 3 for trucks and large buses and Euro 4 for passenger cars in some Asian countries. Personally, it is not necessary to install the post-combustion technology at the time. However, it is expected that a more stringent pollution control law equivalent to Euro 5 is expected soon to address pollution problems in large cities. Must start from diesel engine exhaust gas to protect the environment and human health. Therefore, the regulation of automobile exhaust emissions is becoming stricter and stricter [9,10,11].

2. Experiment

2.1. Structure of DOC and Partial Flow DPF Mechanism

The investigated DOC and DPF mechanism with a honeycomb structure are shown in the section view of Fig. (1, D). Partial-flow diesel particulate filters have a double internal structure presented in Fig. (1, A). The first layer is a metal foil shown in Fig. (1, B), like the DOC metal flow guide that allows the exhaust gas to pass through and leads partial of the soot to be trapped in the second layer, which is metal fiber as Fig. (1, C).

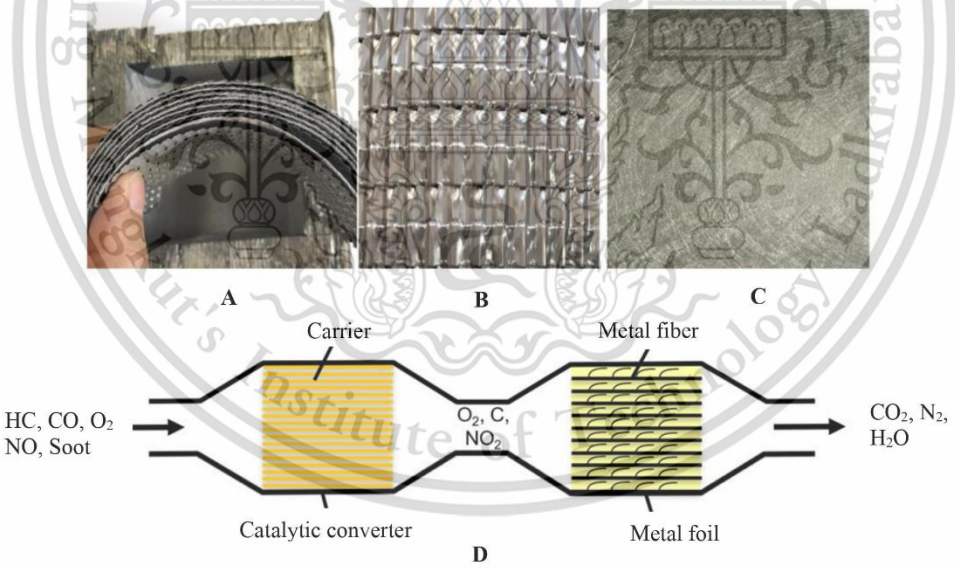

Fig. 1. Physical mechanism of DOC and DPF.

Diesel oxidative catalyst has an internal structure as metal fins or metal foil. It is uniformly coated with CeO_2 catalyst on its surface to convert nitrogen oxides (NO) from the exhaust gas to nitrogen dioxide (NO_2). Carbon soot reacts with nitrogen dioxide previously prepared by catalytic converters, where carbon soot becomes carbon dioxide (CO_2). Furthermore, partial flow DPF allow around half of

emissions flow out directly owing to the structure itself, another half of exhaust gas will flow through metal fibre. Therefore, soot, HC in solid phase, and ash will be trapped in metal fibre. The exhaust gas come from combustion chambers, including hydrocarbon, carbon monoxide, NOx, and particulate matter. HC and CO are eliminated due to catalyst. During the process, NO will be oxidized to NO_2, and it plays an essential role in soot regeneration in particulate filters [12,13,14,15].

2.2. Experimental setup

The diesel engine with a common-rail and direct-injection system is connected to a dynamometer, as shown in Fig. (2). The engine is tested with B10 fuel at 1000, 1500, and 2000 rpm under 20%-50% engine load. The exhaust ingredients have been measured by an exhaust gas analyzer. The analyzer measures the ingredients quantity based on the proportion of each gas species at a certain exhaust volume. At the same time, smoke intensity was gauged by a smoke meter. The smoke intensity determines the amount of soot based on the light reflection. In this experiment, we measure the exhausts, temperature, and pressure at 3 locations as shown in Fig. (2), P1 indicates position 1, which exhausts gas flow out from the engine; P2 means position 2 with DOC effecting; P3 represents position 3 after DOC and partial-flow DPF system. The whole system was controlled by electronic control unit that operates in another room for safety.

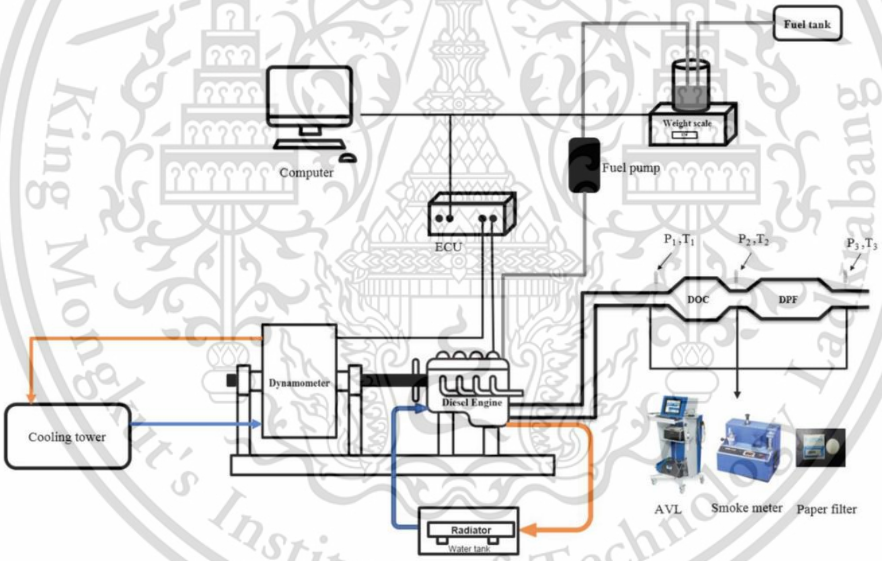

Fig. 2. Experimental equipment set up

Tab. (1) provides the engine specification of the diesel engine, which the engine power for this bench test is approximately up to 100 kW. There are three conditions shown in Tab. (2) with 1000rpm, 1500rpm, and 2000rpm testing under 10%-40% engine load, respectively are 56Nm, 84Nm, 112Nm, and 140Nm. Multi-testing should be considered under high engine load and high engine speed due to unstable experimental data.

Before the experimental start, the diesel fuel will be prepared by the fuel supply system controlled by a three-way valve and a weight meter to measure the fuel consumption. The vehicle's engine speed was settled at 1,000, 1,500, and 2,000 rpm at 20-50% of engine load. The engine torque and speed were controlled by a load cell settled in the dynamometer and ECU. Furthermore, exhausts get through DOC and DPF then arrive in the exhaust gas analyzer. After exhausts pass through the catalyst converter, the

exhaust temperature is different at P1, P2, and P3 because of exothermic reactions in DOC, heat flux, and diffusion. The exhaust gas analyzer automatically measures carbon dioxide, carbon monoxide, hydrocarbon, oxygen, lambda, nitrogen oxide, and exhaust temperature during the engine operation. The PMs quantity was measured by the smoke intensity meter and exhaust gas analyzer at a meantime.
Tab. (3) shows the units of exhausting results. PPM means parts per million which indicate the amount of each exhaust gas. (1 ppm = 1 mg/L = 1mg/kg = 1mg/km, 1 ppb = 1 µg/L, %Vol = 100ppm). Tab. (4) represents the accuracy of each exhaust gas, and the error increases with the quantity of exhaust gas goes up.

Table 1. Engine specification

Items	Details
Engine Model	4JJ1-TC
Engine Type	Diesel, 4 Cycles
Layout	Inline - 4
Bore x Stroke (mm)	95.4 x 104.9
Total Displacement (cc)	2,999
Compression Ratio	18.3
Compression Pressure	>3 MPa
Combustion Chamber	Direct Injection
Cylinder Liner	Liner Less
Engine Idle Speed (rpm)	700 ± 25
Maximum Engine Speed	4,400 ± 50
Fuel System	Common Rail
Maximum Torque (Nm)	108
Maximum Power (kW)	170

Table 2. Boundary conditions

Conditions	rpm	Load / Nm
Condition 1-4	1000	56/84/112/140
Condition 2-8	1500	56/84/112/140
Condition 9-12	2000	56/84/112/140

Table 3. Investigated factors units

Test results	Unit
CO	% Vol
CO_2	% Vol
O_2	% Vol
NOx	ppm
HC	ppm
Opacity	%
Smoke intensity	%

Table 4. Accuracy of measured factors

Factors	Accuracy
CO	<10.0%.: ± 0.02% vol ≥10.0%.: ± 5% o.M
CO_2	<16.0%.: ± 0.3% vol ≥16.0%.: ± 5% o.M
HC	<2000ppm ≥5000% ppm <10000% ppm
O_2	± 0.02 % vol
NOx	± 5ppm vol

3. Results and discussion

3.1. Engine performance analysis
Fuel flow rate increases with the engine load go up, as represented in Fig. (3). Brake specific fuel consumption and brake specific energy consumption of different DOC and DPF systems are shown in Fig. (4) and Fig. (5). Specific fuel consumption can be described as fuel consumption per power unit, which fuels have higher or lower specific fuel consumption at the same power unit. BSFC are reduced at higher engine loads due to better combustion. Moreover, the fuel and air are mixed well cause a complete combustion. From the results, it was found that BTE in Fig. (6) is higher when the engine load increases which corresponds to BSFC and fuel flow rate. Thermal efficiency can describe the efficiency of the mechanical energy generated by the thermal energy input. At the same engine speed, both thermal efficiencies are increased following the load increase because of the higher burning rate. Moreover, all

cases are nearly the same brake thermal efficiency at around 30%. According to the results, the aftertreatment system has no great impact on the engine performance.

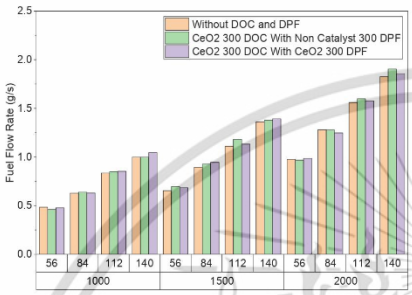

Fig. 3. Fuel flow rate.

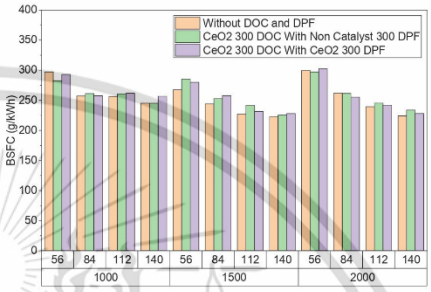

Fig. 4. Brake specific fuel consumption.

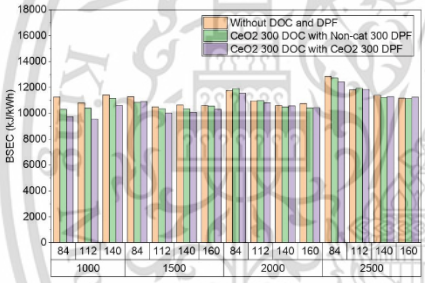

Fig. 5. Brake specific energy consumption.

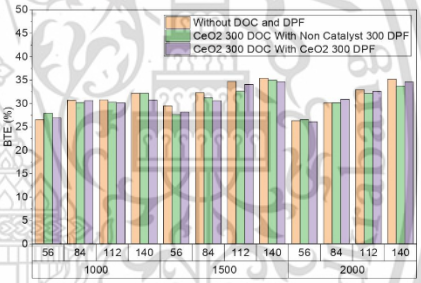

Fig. 6. Brake thermal efficiency.

3.2. Emission analysis

Fig. (7) shows oxygen in the exhaust gas. The oxygen in the exhaust is reduced as the engine load increases due to a higher proportion of fuel injected into the combustion chamber. Therefore, oxygen in the air is chemically reacted with a higher proportion of fuel. After diesel combustion, there is approximately 10% of oxygen left. Moreover, oxygen will react with HC, NO, CO in CeO_2 catalyst firstly. After that, O_2 oxidizes the soot in partial flow DPF at a high temperature. During the oxidation process, CO_2 was generated at the same time. Fig. (8) indicates carbon dioxide in %vol in the exhaust gas. Carbon dioxide rises with the quantity of fuel injected into the combustion chamber, opposite to oxygen. The CO_2 amount is lower while using a partial-flow DPF due to the soot reacting with O_2 at a relatively higher temperature. CO was generated as a result of incomplete combustion as presented in Fig. (9). At 1000rpm and 140Nm, CO %vol was reduced up to 82% by using a CeO_2 catalyst converter. Meanwhile, HC was notably reduced when we applied a CeO_2 DOC as indicated in Fig. (10). In the test, we use a new non-catalyst 300 DPF. So, it has a better soot trapping ability; HC in the liquid phase will be easily trapped in the metal fibre. The exhaust temperature of no DOC and DPF system has a higher temperature due to DOC and DPF absorbing the heat, but no significant influence at high exhaust temperature due to a considerable heat flux rate. The nitrogen oxide content increases as the temperature increases in the combustion chamber as shown in Fig. (11); this corresponds to a higher exhaust temperature in Fig. (12). NO_x was reduced with the DPF system at high load due to NO_2 being easy to

react with soot in terms of passive regeneration. Fig. (13) indicates the opacity of exhaust gas measured from the exhaust gas analyzer. This graph shows much soot particle generated at high load with a lower engine rpm condition due to incomplete combustion. The soot was reduced by more than 50% with DOC and DPF systems. With a DPF system, higher density exhaust gas goes to EGR because back pressure increases; the temperature reduces owing to CO_2's vast heat capacity; thus, NO_x decreases in the meantime.

Fig. (14) represents the smoke intensity of exhaust gas measured from the smoke meter. The result is like opacity percentage from exhaust gas analyzer; both are shown over 50% soot reduction with an after-treatment system. From nitrogen and carbon particles results, there is a trade-off between NO_x and soot measured from tested cases. Under higher torque conditions, much amount of thermal-NO_x is generated by Zeldovich's Mechanism; but little soot is due to better engine combustion. On the other hand, there are few NO_x but more soot due to incomplete combustion at low engine power conditions. Therefore, we could make a strategy to design the after-treatment system. For instance, most gasoline engine fuels are premixed to better combustion, but NO_x is generated due to high temperature; therefore, we can apply SCR to reduce NO_x. Go further to the diesel engine; soot is produced due to incomplete combustion. In this case, we could use EGR system to reduce the combustion temperature and add the DPF system to trap the particulate matter. These two strategies are successfully applied in commercial vehicles.

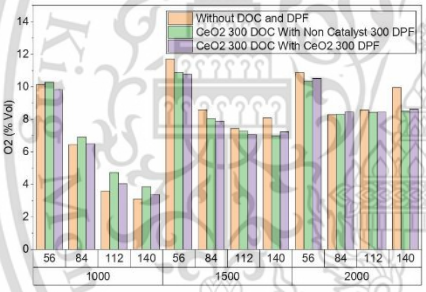

Fig. 7. Oxygen.

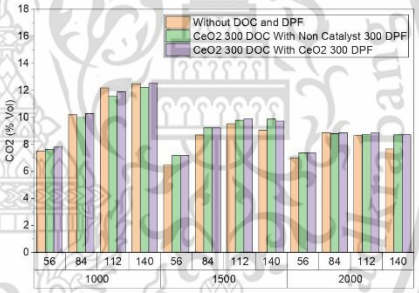

Fig. 8. Carbon dioxide.

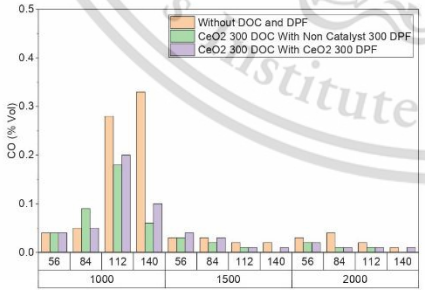

Fig. 9. Carbon monoxide.

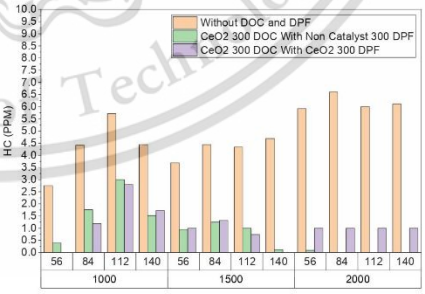

Fig. 10. Hydrocarbon.

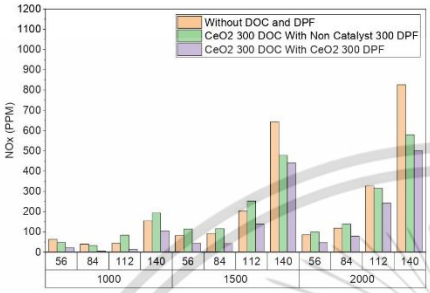

Fig. 11. NOx quantity.

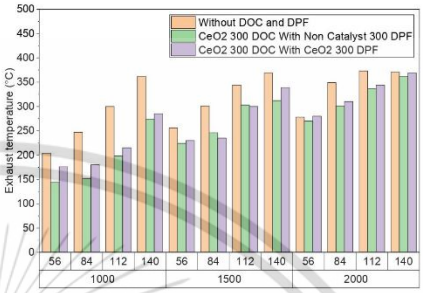

Fig. 12. Exhaust temperature.

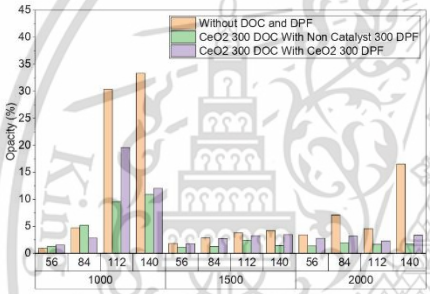

Fig. 13. Opacity.

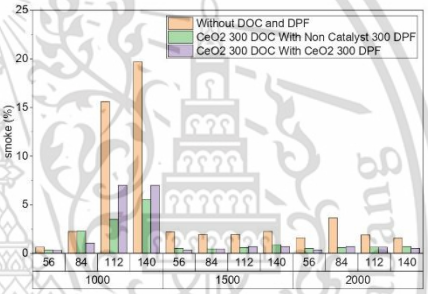

Fig. 14. Smoke intensity.

4. Conclusion

According to the testing results that NOx ppm reduced around 25% with CeO_2 DOC and partial flow DPF systems at 140Nm corresponding to CO_2 quantity increasing owing to NO_2 passive regenerating the soot trapped in the filter. On the other hand, particulate matters decrease around 65% due to metal fibre trapping process. Furthermore, CO %vol and HC ppm were substantially reduced after applying after-treatment systems. As the results of fuel consumption, BSFC, and BTE that after-treatment system has no significant impact on engine performance.

5. References

[1] Karin, P., Borhanipour, M., Songsaengchan, Y., Laosuwan, S., Charoenphonphanich, C., Chollacoop, N., & Hanamura, K. (2015). Oxidation kinetics of small CI engine's biodiesel particulate matter. International Journal of Automotive Technology, 16(2), 211–219.

[2] SRILOMSAK, M., & HANAMURA, K. (2020). Time-lapse visualization of shrinking soot in diesel particulate filter during active - regeneration using field emission scanning electron microscopy. *Journal of Microscopy*, *279*(2), 85–97.

[3] Mayer, A., Czerwinski, J., Comte, P., & Jaussi, F. (2009). Properties of Partial-Flow and Coarse Pore Deep Bed Filters Proposed to Reduce Particle Emission of Vehicle Engines. *SAE International Journal of Fuels and Lubricants*, *2*(1), 497–511.

[4] J.P.A. Neeft, M Makkee, J.A. Moulijn, Diesel particulate emission control, Fuel Process. Technol., 47 (1996) 1.

[5] Strzelec A., Vander Wal R.L., Thompson T., Toops T. and Daw C., "NO2 oxidation reactivity and burning mode of diesel particulates," Top Catal 2016; 59: 686–694.

[6] Kim, J. K., Kim, W. G., & Kim, Y. K. (2011). A Study of HDD Performance Improvement through Filter Driver & NAND FLASH Memory. The Journal of the Korean Institute of Information and Communication Engineering, 15(8), 1635–1641.
[7] TOYAMA, S., MORI, H., & SUZUKI, M. (1987). FLOW PATTERNS THROUGH TUBE BUNDLES AND PARTICULATE FOULING ONTO CYLINDERS. Particulate Science and Technology, 5(4), 397–408.
[8] Karin, P., & Hanamura, K. (2010). Particulate Matter Trapping and Oxidation on a Catalyst Membrane. SAE International Journal of Fuels and Lubricants, 3(1), 368–379.
[9] Das, R., Madhusoodana, C., Purushothama, M., Paramesh, S. et al., "Development and Field Test of Ceramic-based Diesel Particulate Filter (DPF) for Urban Transport Vehicle," SAE Technical Paper 2003-26-0004, 2003.
[10] Lehmann, F., Torres, R., and Park, S., "EMISSION STUDY OF AN EURO 5 DIESEL ENGINE OPERATING ON BIODIESEL BLENDS," SAE Technical Paper 2012-36-0168, 2012.
[11] Amanatidis, S., Ntziachristos, L., Samaras, Z., Kouridis, C. et al., "Use of a PPS Sensor in Evaluating the Impact of Fuel Efficiency Improvement Technologies on the Particle Emissions of a Euro 5 Diesel Car," SAE Technical Paper 2014-01-1601, 2014.
[12] M. Srilomsak and K. Hanamura, "A Role of NO 2 on Soot Oxidation in DPFs and Effect of Soot Cake Thickness in Catalyzed DPFs Using Temperature-Programmed Oxidation and Electron Microscopic Visualization," *SAE Technical Paper,* 2020.
[13] Z. Li, W. Zhang, Z. Chen and Q. Jiang, "Mechanism of accelerating soot oxidation by NO2 from diesel engine exhaust," *Environmental Pollution,* vol. 264, 2020.
[14] M. Singh, M. Srilomsak, Y. Wang, K. Hanamura and R. Vander Wal, "Nanostructure changes in diesel soot during NO2--O2 oxidation under diesel particulate filter-like conditions toward filter regeneration," *International Journal of Engine Research,* vol. 20, no. 8, pp. 953-966, 2019.
[15] H. Seong and S. Choi, "Oxidation-derived maturing process of soot, dependent on O2--NO2 mixtures and temperatures," *Carbon,* vol. 93, pp. 1068-1076, 2015.

Acknowledgments
The authors would like to express their sincere appreciation for financial and technical support from the National Research Council of Thailand (Diesel Engine's Particulate Matters Reduction using Ethanol-Diesel Blends and Particulate Filter 398/2563).

AUTHOR BIOGRAPHY

Author: Mr. Hai Liu

Degree: Master of Engineering

Date of Graduation:

Date of Birth: 07th May 1997

Place of Birth: AnHui, China

Undergraduate and Graduate Education

Master of Engineering in Automotive Engineering,
King Mongkut's Institute of Technology Ladkrabang, Bangkok, 2022
Bachelor degree in automotive engineering,
Nanjing Tech University Pujiang Institute, China, 2016

Major: Automotive Engineering

Patents and Publications:

[1] H Liu, W Cao, S Ding, Z Shu; Chengdu Mingtao Zhichuang Patent Agency Co., Ltd. "Pipeline Robot with Ratcheting System". China Utility Model Patent, CN 210372535 U. 2020 April 21

[2] S. Ding, H. Liu, Y. Xu, B. Lu, M. Wang, "Research on Hydrogen Electric Hybrid Power Supply System Based on UAVs", Journal of China Academic Electronic Technology & Software Engineering, 2019

[3] W. Cao, H. Liu, Y. Wen, S. Ding, Z. Su, H. Li, "Intelligent Tracking Car of Gray Sensor Based on Single Chip Microcomputer", Journal of Henan Science and Technology, 2019

[4] H. Liu, C. Charoenphonphanich, P. Karin, M. Srilomsak, S. Srimanosaowapak, K. Hanamura, “Reduction of Diesel Engine’s Particulate Matters using Retrofit CeO2 Diesel Oxidative Catalyst and Partial Flow Diesel Particulate Filter System”, 8th International Conference on Environment and Renewable Energy, 2022